

$ee \in MC$: Monte Carlo Simulations of

$e^+e^- \rightarrow \mu^+\mu^-(\gamma)$, $e^+e^- \rightarrow \text{hadrons}(\gamma)$, $e^+e^- \rightarrow \tau^+\tau^-(\gamma)$ Interactions

Seminar (January 23, 2024)

Outline:

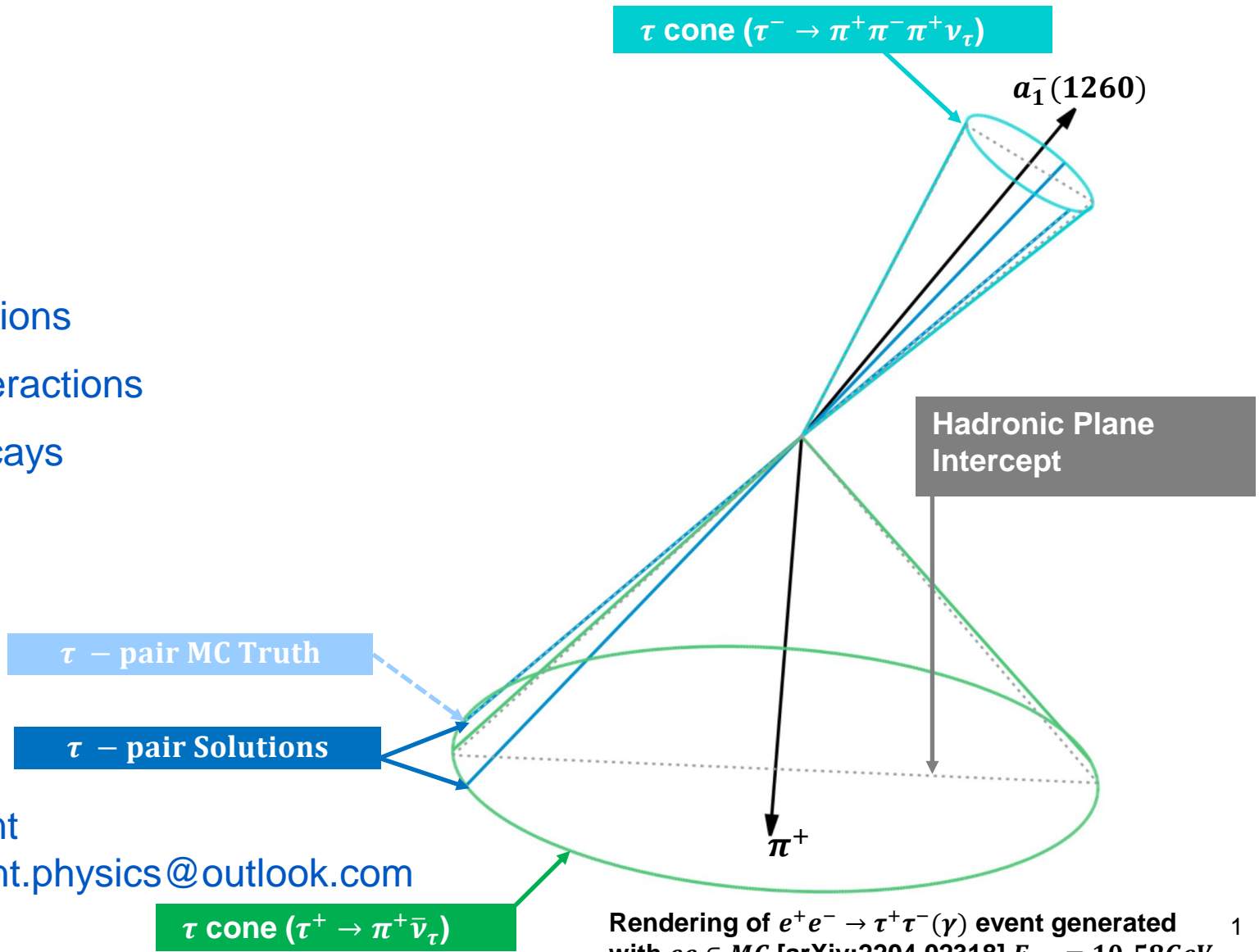
Introduction

QED Interactions

Hadronic Interactions

τ Lepton Decays

Summary



Ian M. Nugent

Email: inugent.physics@outlook.com

τ cone ($\tau^+ \rightarrow \pi^+ \bar{\nu}_\tau$)

Rendering of $e^+e^- \rightarrow \tau^+\tau^-(\gamma)$ event generated
with $ee \in MC$ [arXiv:2204.02318] $E_{cm} = 10.58\text{GeV}$ 1

Introduction

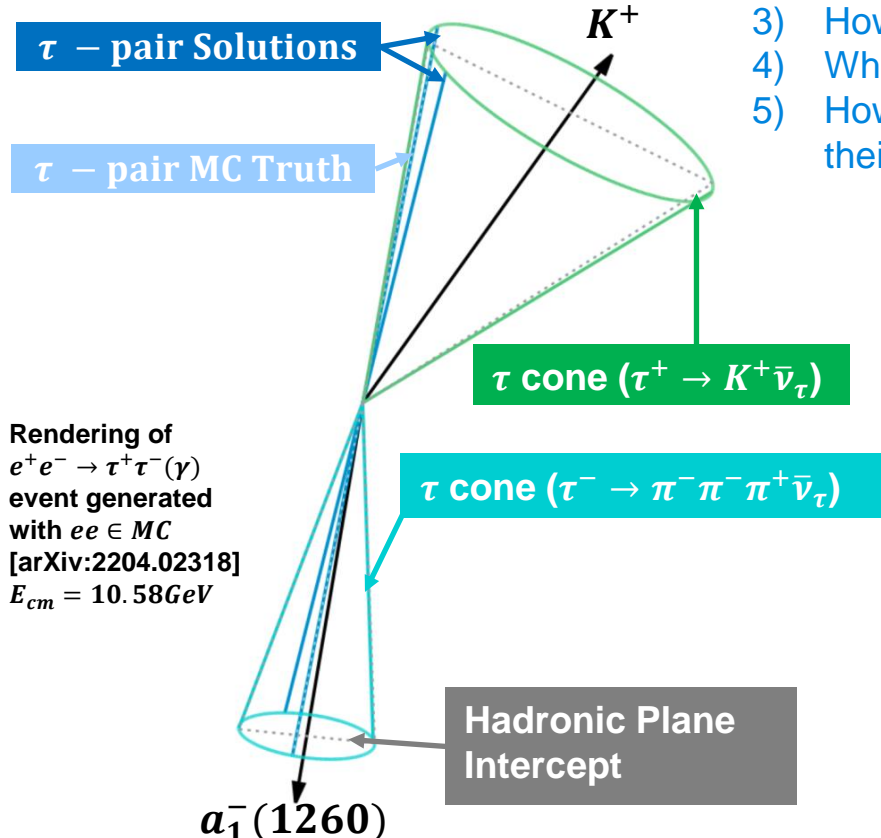
Based on: arXiv:2204.02318, arXiv:2211.10548, arXiv:2212.05388, arXiv:2303.02597 & 2312.01470

Monte-Carlo (MC) simulations play a pivotal role both as a technique to compare theoretical predictions to experiments and to facilitate the interpretation of the measured experimental results in particle physics.

⇒ require Infra-red safe calculation for QED interactions for comparisons between data and theory.

Fundamental open questions:

- 1) What is the origin of the quark-constituent mass? Is it related to Chiral-symmetry breaking?
- 2) What are the physical hadronic states that we observe and are they resonances?



- 3) How do hadronic states radiate?
- 4) What is the mixing between the singlet and triplet states?
- 5) How do we describe the resonant states, taking into account their finite size?

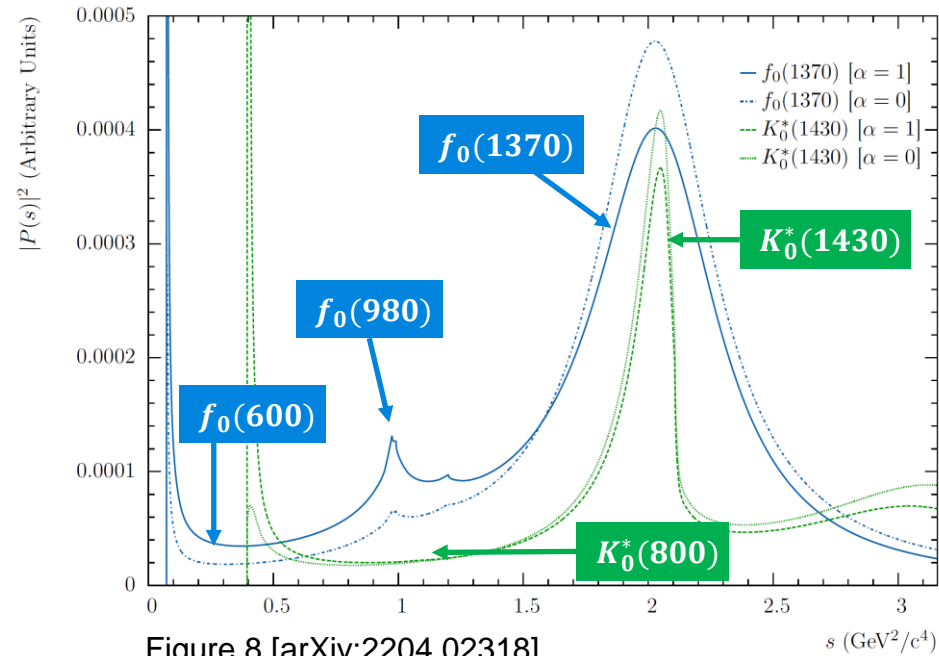


Figure 8 [arXiv:2204.02318]

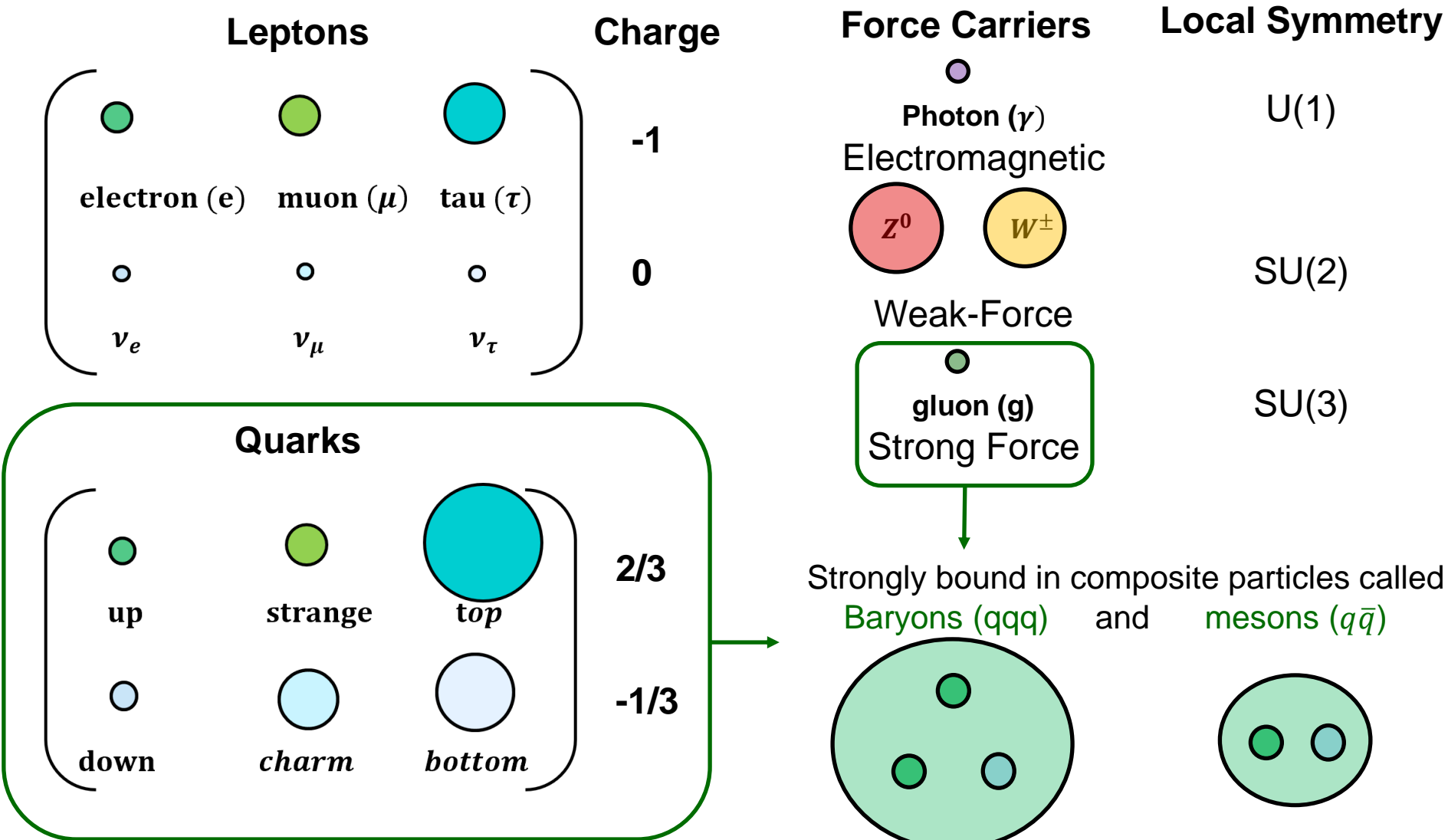
Standard Model

Nature is described on the smallest scale in terms of fundamental particles...

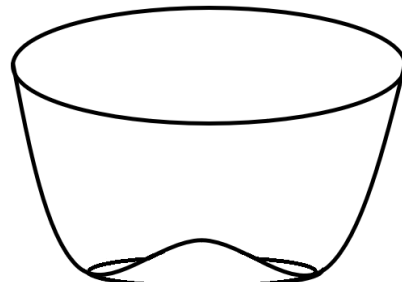
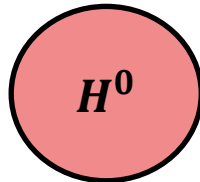
Leptons	Charge	Force Carriers	Local Symmetry
 electron (e) ν_e	 muon (μ) ν_μ	 tau (τ) ν_τ	-1
			0
Quarks		Weak-Force Photon (γ) Electromagnetic Z^0 W^\pm gluon (g) Strong Force	
 up down	 strange charm	 top bottom	 $2/3$ $-1/3$

Standard Model

Nature is described on the smallest scale in terms of fundamental particles...



Quark-Constituent Mass



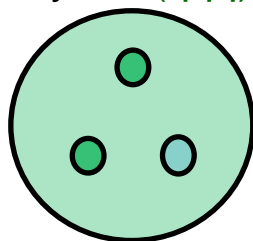
In the Standard Model, the mass of the fundamental particles is generated through electro-weak symmetry breaking with a scalar field \Rightarrow the Higgs

Symmetry breaking was developed to explain super-conductors (BCS-Theory 1957)

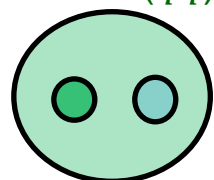
The Higgs interaction accounts for $\sim 1\%$ of the mass of the proton.

The remainder of the mass believed to be generated through the strong interactions....
 \Rightarrow referred to as the “Quark-Constituent Mass”.

Baryons (qqq)



Mesons ($q\bar{q}$)



In many hadronic models, the generation of the Quark-Constituent Mass is associated with the low mass scalar resonances through a Chiral-symmetry Breaking mechanism:

- Chiral Lagrangian Models [44, 45, 46, 47], Linear Sigma Models [48, 49, 50, 51, 52, 53, 54]
 $\Rightarrow \mathcal{L} \propto m^2 \rightarrow$ decay rate directly dependent on $m^2 \Rightarrow$ tends to have $\sigma/\Gamma \propto m^2$
 \Rightarrow scalar states are resonances
- Additionally, Non-Linear Sigma Models [55] (Skyrme Model [56, 57, 58]) and Nambu-Jona-Lasinio Model [59] also generate mass through a Chiral-symmetry Breaking mechanism, but can incorporate vector and pseudo-scalar states in addition to the scalar meson states [43, 58].

In other theoretical constructs the mass generation is not necessarily directly related Chiral-symmetry Breaking and scalar mesons [60, 61, 62, 63, 64, 65, 66, 67] ...

Approach to QED Calculations

In QED, the interaction can be described in terms of the free field Lagrangian density and interactions Lagrangian density [112]: $L = L_0 + L_I$

$$L_0 = N[\bar{\psi}(x)(i\gamma^\mu \partial_\mu - m)\psi(x) - \frac{1}{2}(\partial_\mu A_\nu(x)\partial^\mu A^\nu(x))]$$

$$L_I = N[e\bar{\psi}(x)\gamma^\mu A_\mu(x)\psi(x)]$$

Within the “Interaction picture” the corresponding equation of motion is $H_I|\phi(t)\rangle = i\frac{d}{dt}|\phi(t)\rangle$

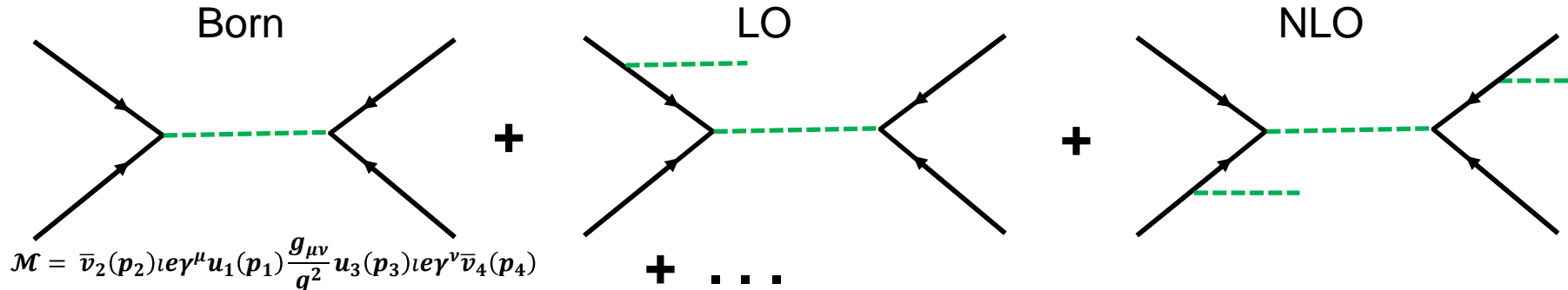
Dyson showed that this can be solved iteratively using perturbation theory if the coupling constant $\alpha \ll 1 \dots$ [112]

$$|\phi(t)\rangle = |\phi(-\infty)\rangle - i \int_{-\infty}^t dt_1 H_I(t_1)|\phi(-\infty)\rangle + (-i)^2 \int_{-\infty}^t dt_1 \int_{-\infty}^{t_1} dt_2 H_I(t_1)H_I(t_2)|\phi(-\infty)\rangle + \dots$$

Taking into account the time-ordering such that later times are on the left in the limit that $t \rightarrow \infty$

$$\Rightarrow s = \sum_{n=0}^{\infty} \frac{(-i)^n}{n!} \int_{-\infty}^{\infty} dx_1^4 \int_{-\infty}^{\infty} dx_2^4 \dots \int_{-\infty}^{\infty} dx_n^4 T[H_I(x_1)H_I(x_2) \dots H_I(x_n)]$$

Where $\langle \psi(\infty)|s|\psi(-\infty)\rangle$ represents the transition amplitude. After applying Wicks Theorem to write the s matrix in terms of normal products which are reduced to the non-vanishing propagators and vertices[112]. The individual terms in the s matrix expansion can then be associated with individual interactions [88,89]



Approach to QED Calculations

The Feynman matrix amplitude/matrix element (\mathcal{M}) is related to the transition amplitude $\langle \psi(\infty) | s | \psi(-\infty) \rangle$ by spinor normalization, phase-space factor and normalized per unit time and volume. The cross-section is defined relative to the transition amplitude divided by the incident flux per unit time thus removing the arbitrary time and volume dependency[112,88,89].

$$d\sigma = \frac{\sum_{n=0}^{\infty} \left| \sum_{k=1}^{\infty} \bar{\mathcal{M}}_n^k \right|^2 dPS_n}{4(\left| \vec{P}_{e^-} \right| E_{e^+} + \left| \vec{P}_{e^+} \right| E_{e^-})}$$

This cross-section is determined in terms of the **spin-averaged sum matrix element** $|\bar{\mathcal{M}}_n^k|$ for n hard-photon emissions and k photon exchanges.

The differential phase-space is represented by dPS_n for each of the n hard-photon configurations. The phase-space integral in the MC generator is based on the recursive mass formulation [84] modified with embedded Importance Sampling [85,86] to optimize the simulation efficiency and Jacobian Normalization factors

$$R_n(\sqrt{s}) = \int_{(m_1+\dots+m_n)^2}^{(\sqrt{s}-m_n)^2} dM_{n-1}^2 \int_{-1}^1 d\cos(\theta) \int_{-\pi}^{\pi} d\phi \frac{\sqrt{\lambda(s, M_{n-1}^2, m_n^2)}}{8s} \times R_{n-1}(M_{n-1}) \quad [\text{Eq. 3.84}]$$

Phase-Space Simulation

The phase-space [84] has been extended with importance sampling to simulate n hard-photons in all combinations of Initial-State, Final-State photon geometries including admixtures of Initial/Final-State photons. Importance sampling is embedded in each of the geometric configurations approximating the expected QED structure allowing for a more efficient calculation of the near-divergent differential cross-section.

$$R_n(\sqrt{s}) = \int_{(m_1 + \dots + m_n)^2}^{\frac{(\sqrt{s}-m_n)^2}{(m_1 + \dots + m_n)^2}} dM_{n-1}^2 \int_{-1}^1 d\cos(\theta) \int_{-\pi}^{\pi} d\phi \frac{\sqrt{\lambda(s, M_{n-1}^2, m_n^2)}}{8s} \times R_{n-1}(M_{n-1}) \quad [\text{Eq. 3,84}]$$

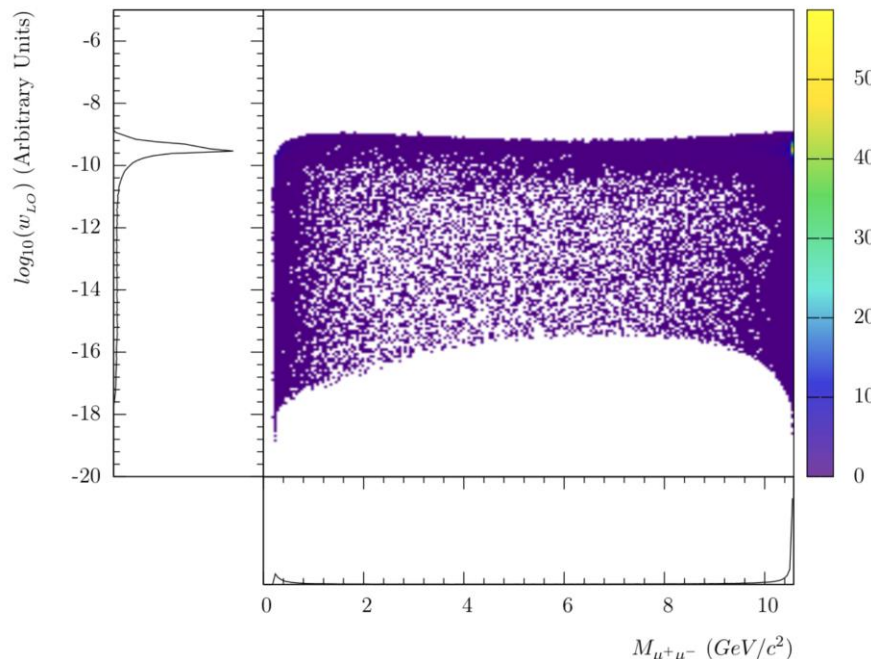
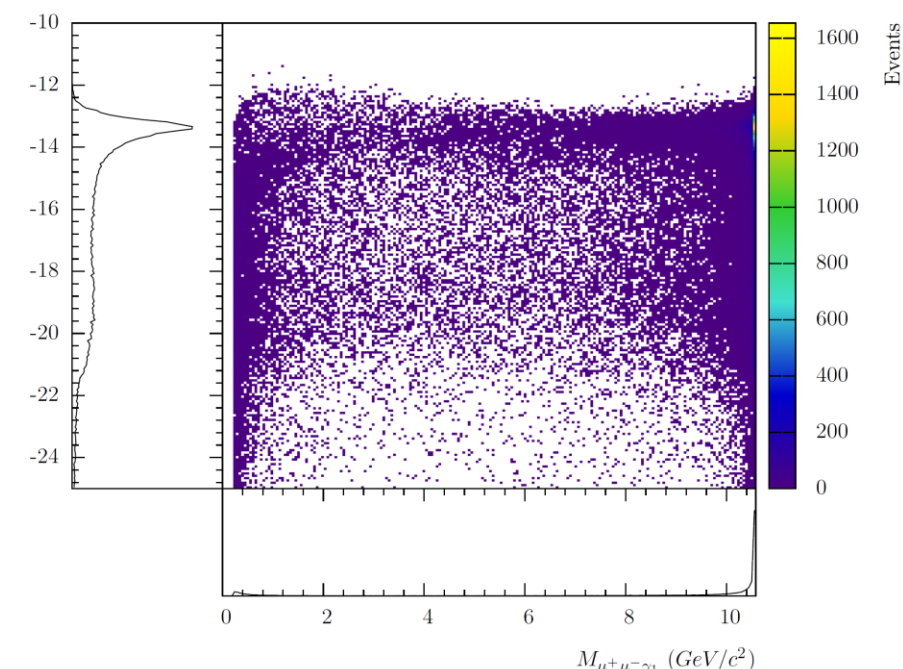


Figure 1 [arXiv:2212.05388]



Soft-photon cut-off of 1MeV

Liverpool Seminar (January 23, 2024)

Phase-Space Simulation

The phase-space [84] has been extended with importance sampling to simulate n hard-photons in all combinations of Initial-State, Final-State photon geometries including admixtures of Initial/Final-State photons. Importance sampling is embedded in each of the geometric configurations approximating the expected QED structure allowing for a more efficient calculation of the near-divergent differential cross-section.

$$R_n(\sqrt{s}) = \int_{(m_1 + \dots + m_n)^2}^{(\sqrt{s} - m_n)^2} dM_{n-1}^2 \int_{-1}^1 d\cos(\theta) \int_{-\pi}^{\pi} d\phi \frac{\sqrt{\lambda(s, M_{n-1}^2, m_n^2)}}{8s} \times R_{n-1}(M_{n-1}) \quad [\text{Eq. 3.84}]$$

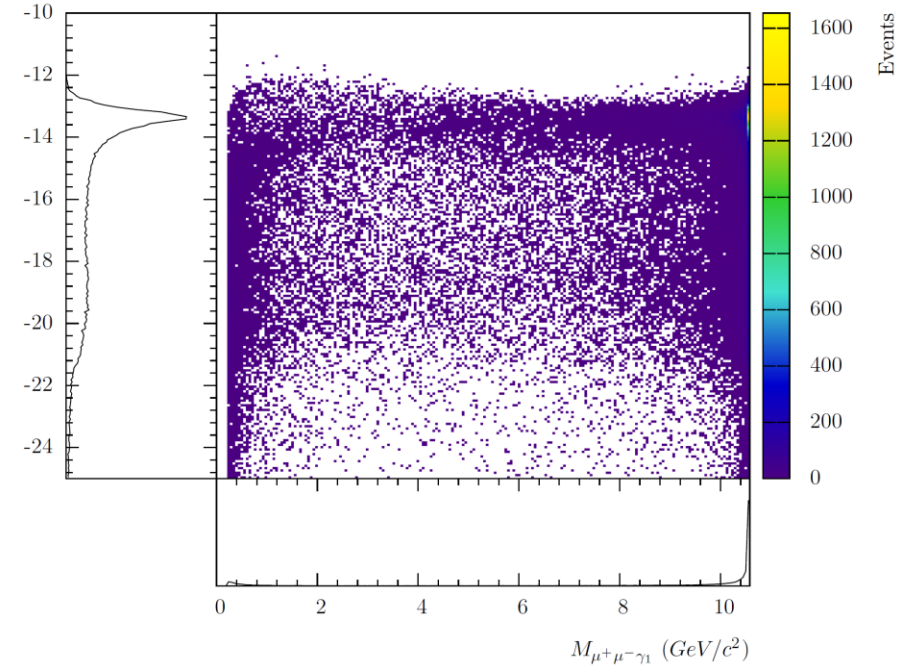
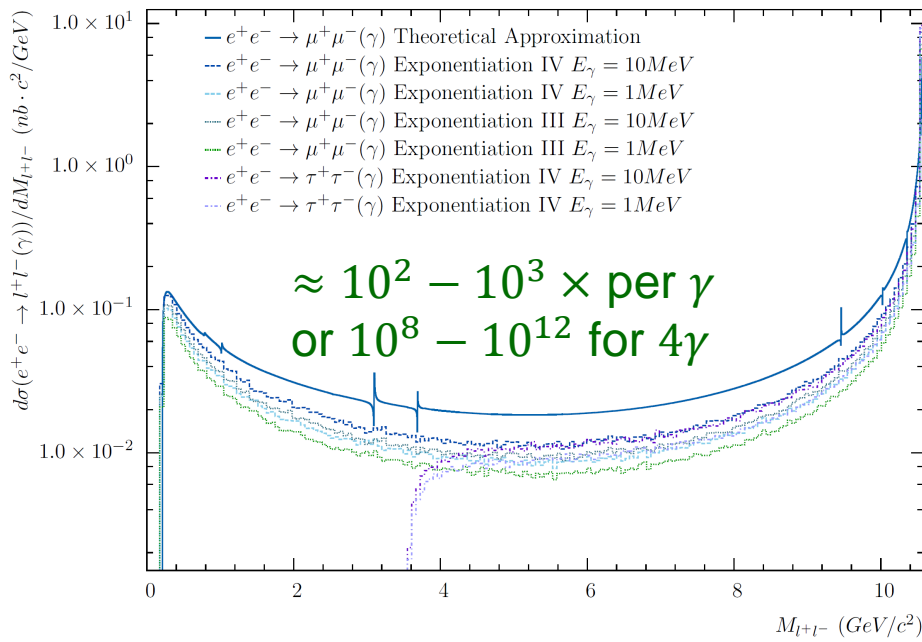


Figure 1 [arXiv:2212.05388]

Soft-photon cut-off of 1MeV

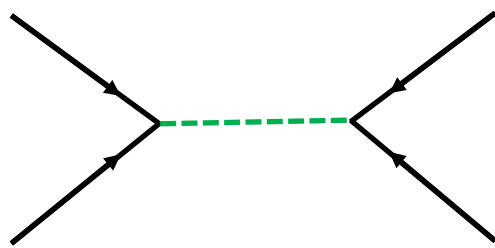
Liverpool Seminar (January 23, 2024)

Divergencies...

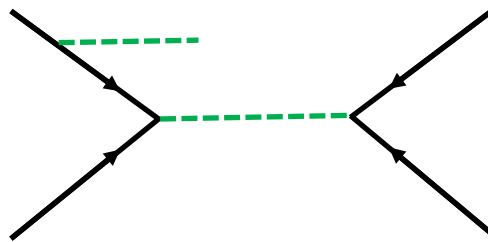
In the perturbative expansion, represented here in terms of Feynman Diagrams, there are two problematic sources of divergencies....

1

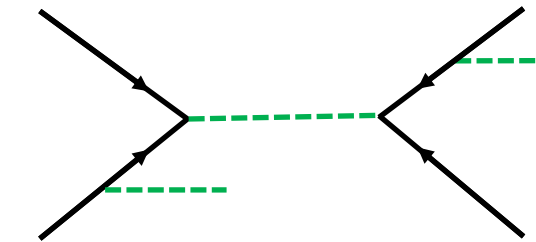
Born



LO

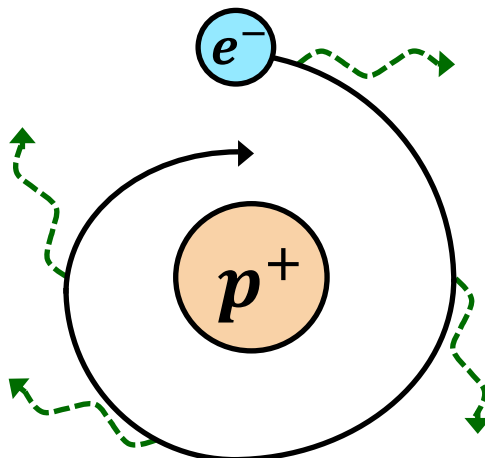


NLO



$$\mathcal{M} = \bar{v}_2(p_2) i e \gamma^\mu u_1(p_1) \frac{g_{\mu\nu}}{q^2} u_3(p_3) i e \gamma^\nu \bar{v}_4(p_4)$$

Additional Photon emissions $\propto \frac{\gamma^n P'_\eta + m}{P'^2 - m^2}$



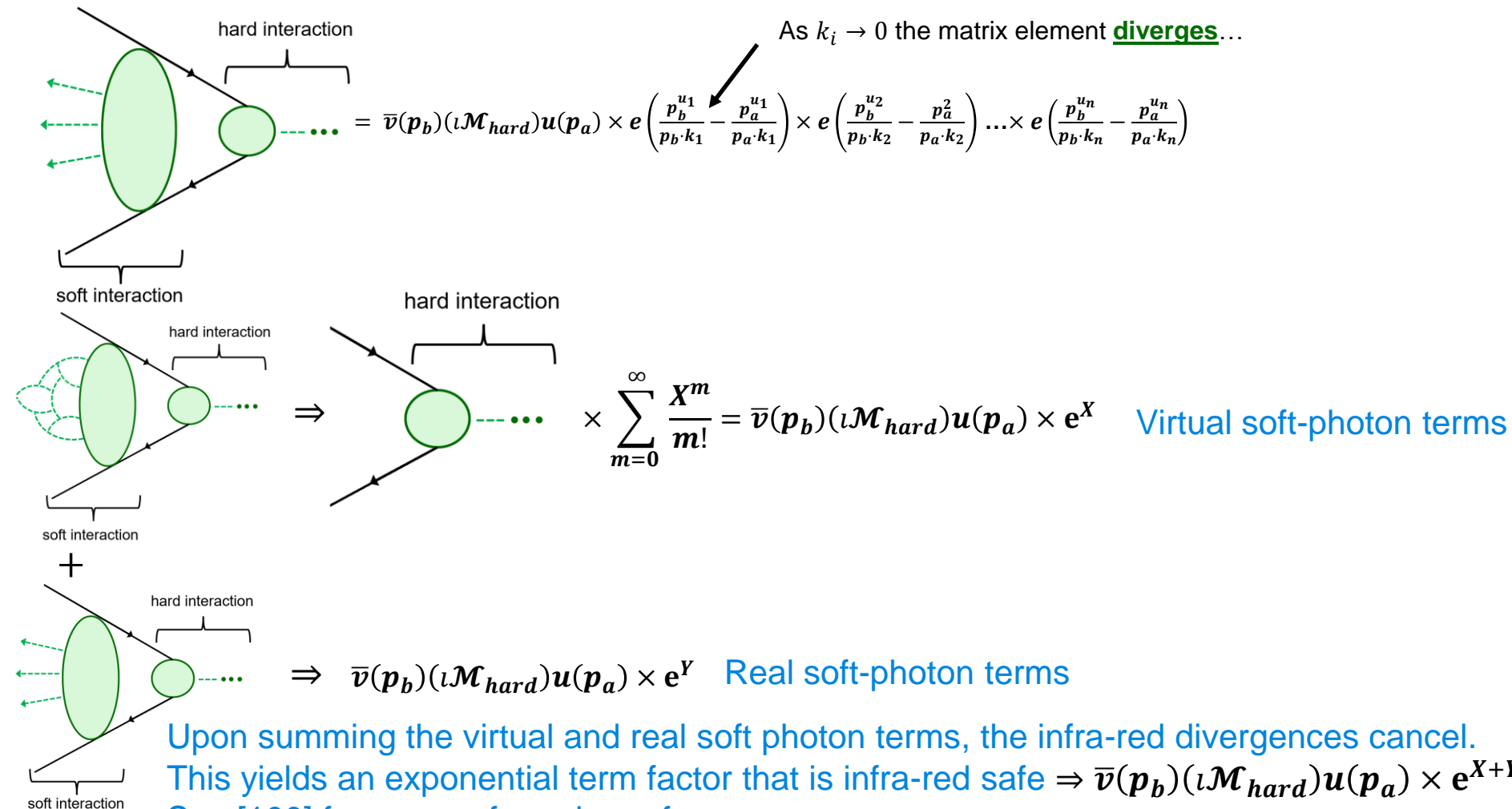
Diverges in limit $\Delta E_l \rightarrow 0$
Infra-red divergences...

This is analogous to the
“electron falling into the proton”
by J. Lamour [176]

Poisson Distribution

Infrared Divergencies...

Infra-red divergencies in the theory [89,99,100]...



This **Yennie-Frautschi-Suura** exponential term is a multiplicative subtraction [100].

Approach to QED Calculations

⇒ The cross-section must be modified to include the multiplicative **Yennie-Frautschi-Suura Exponentiation procedure**, to remove the infra-red divergencies, where δM is taken as the soft-photon cut-off.

$$d\sigma = \frac{\sum_{n=0}^{\infty} Y_i(Q_i^2) Y_f(Q_f^2) |\sum_{k=1}^{\infty} \bar{M}_n^k|^2 dPS_n}{4(\vec{P}_{e^-}|E_{e^+} + \vec{P}_{e^+}|E_{e^-})}$$

Requiring Lorentz invariants of the cross-section it follows, that in general, there must exist a Lorentz invariant representation of the single variable upon which the Yennie-Frautschi-Suura Exponentiation Form-Factor depends and the soft-photon cut-off associated with this term must also be Lorentz invariant

$$M' - M = \delta M$$

For consistency with E_{min} of the experimental detector, $\delta M \ll E_{min}$ so that the impact of neglected γ emissions is negligible after reconstruction.

Gauge invariance of the fermions self-energy and vertex graphs are taken into account through the association of the cut-off criteria applied to each individual vertex, where ordering is taken into account for multiple photons

This satisfies all of the conditions for the generalized Yennie-Frautschi-Suura Exponential Form-Factor [100]. Taking $M' = \sqrt{s}$, we equate this to the “special case” through

$$E_l = \frac{s - (\sqrt{s} - \delta M)^2}{2\sqrt{s}}$$

The E_l is a “**special case**” of the more generalized Yennie-Frautschi-Suura Exponential Form-Factor in the e^+e^- centre-of-mass frame [100].

YFS Exponentiation Form-Factor

In addition to the **Yennie-Frautschi-Suura** calculation [100]

$$Y_I = e^{-\frac{\alpha}{\pi} \left(\ln \frac{s-2m_l^2}{m_l^2} - 1 \right) \ln \left(\frac{s}{4E_{soft}^2} \right) + \frac{\alpha}{2\pi} \ln \frac{s-2m_l^2}{m_l^2}} \quad \text{ultra-relativistic approximation + neglected terms}$$

we include the ultra-relativistic approximations from **KK2F** [3]

$$Y_{II} = e^{\frac{2\alpha}{\pi} \left(\ln \frac{s-2m_l^2}{m_l^2} - 1 \right) \ln \left(\frac{2^2 E_{soft}}{\sqrt{s}} \right) + \frac{\alpha}{2\pi} \left(\ln \frac{s-2m_l^2}{m_l^2} - 1 \right) + \frac{\alpha}{\pi} \left(-\frac{1}{2} + \frac{\pi^2}{3} \right)} \quad \text{ultra-relativistic approximation + neglected terms}$$

and the **Sudakov Form-Factor** [89]

$$Y_{III} = e^{-\frac{\alpha}{2\pi} \left(\int_0^1 \frac{m^2 - q^2/2}{m^2 - q^2 \zeta(1-\zeta)} d\zeta - 1 \right) \ln \left(\frac{-q^2}{E_{soft}} \right)} \quad \text{divergent only components}$$

The **Schwinger's** approach to LO QED [101] with Yennie-Frautschi-Suura Exponentiation [100] is merged in $ee \in MC$ [2204.02318]

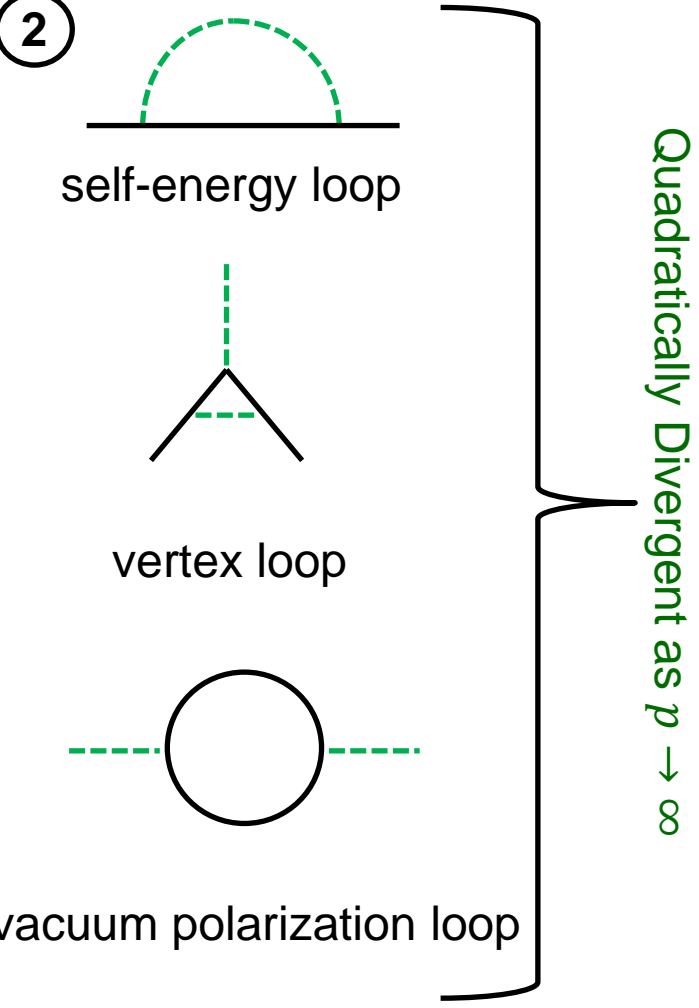
$$Y_{IV} = e^{\frac{2\alpha}{\pi} \left[\left((1-\nu^2)\chi(\nu) - 1 \right) \left[\ln \left(\frac{\delta M}{m_l} \right) + 1 \right] + \chi(\nu) - \frac{(1+\nu)}{\nu} \int_0^\nu dv' \frac{\chi(v')}{1-v'^2} \right] - \frac{\alpha}{\pi} \left(P \int_0^1 dv' \frac{(1+v'^2) \ln \frac{v'^2}{1-v'^2}}{v^2 - v'^2} + \chi(\nu) + \frac{3(1-\nu^2)}{3-\nu^2} \chi(\nu) \right) - F_c |_{O(\alpha)}}$$

where the **Coulomb attraction** [94,101] is removed from the exponentiation and included through a separate series for Type IV

$$Y_{IV} \rightarrow Y_{IV} \times \frac{\pi\alpha/\nu}{1 - e^{-\left(\frac{\pi\alpha}{\nu}\right)}}$$

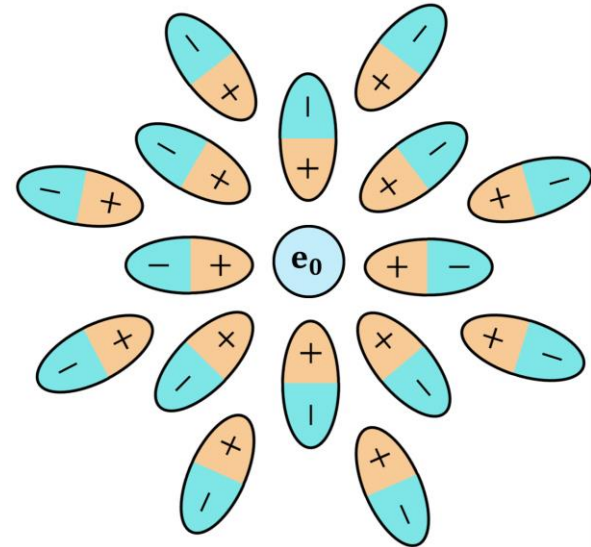
Renormalization and Wards Identity

There are additional higher order terms that contain ultra-violet divergence



Ultra-violet divergences are removed by applying a regularization parameter and then take the $\lim_{\Lambda \rightarrow \infty}$.

Regulators are chosen to preserve the required physics.



Using Ward Identity $\Lambda^\mu(p, p) = \frac{\partial \Sigma(p)}{\partial p_\mu} \Rightarrow Z_1 = Z_2$

$$e = e_0 z_1^{-1} Z_2 \sqrt{z_3} \rightarrow e = e_0 \sqrt{z_3}$$

\Rightarrow renormalization is described by the photon vacuum polarization.

$$\frac{-i g_{\mu\nu}}{q^2} \rightarrow \frac{-i g_{\mu\nu}}{q^2} \left(\frac{1}{1 - \Pi'(q^2)} \right) \xrightarrow{\sigma(\alpha)} \frac{-i g_{\mu\nu}}{q^2} \left(\frac{1}{1 - \Pi(q^2) - \Pi(0)} \right)$$

This was proven to be true for all orders by Itzykson and Zuber in 1980 [88, 89, 112].

Running of α_{QED}

Renormalization is included through the running of the coupling constant [17, 96] by means of **Wards Identity** [88] for the first order leptonic [96] and hadronic vacuum [17] polarizations within the “on-shell” renormalization scheme.

The hadronic contribution is factorized into the perturbative

$$\delta\alpha_{QED}^{\text{pert-had}}(s) = \frac{\alpha}{3\pi} \sum_{f=u,s,d,c} Q_f^2 N_{cf} \left(\ln \left(\frac{s}{m_f^2} \right) - \frac{5}{3} \right) \delta\alpha(s)$$

and non-perturbative regime

$$\delta\alpha_{QED}^{\text{nonpert-had}}(s) = -\frac{\alpha s}{3\pi} \left[P \int_{m_{thres}}^{s_{cut}} \frac{ds' R_{data}(s')}{s'(s'-s)} + P \int_{m_{cut}}^{\infty} \frac{ds' Q_f^2 N_{cf}}{s'(s'-s)} \right]$$

Narrow resonances are included through the approximation:

$$\Pi'_{\gamma ren}(s) \simeq \frac{-3\Gamma_{e^+e^-} s (s - M_R^2 - \Gamma^2)}{\alpha M_R [(s - M_R^2)^2 + M_R^2 \Gamma^2]}$$

[17] for the J/ψ , $\psi(2s)$, $\psi(3s)$, $\Upsilon(1s)$, $\Upsilon(2s)$,
 $\Upsilon(3s)$, $\Upsilon(4s)$ resonances [43]

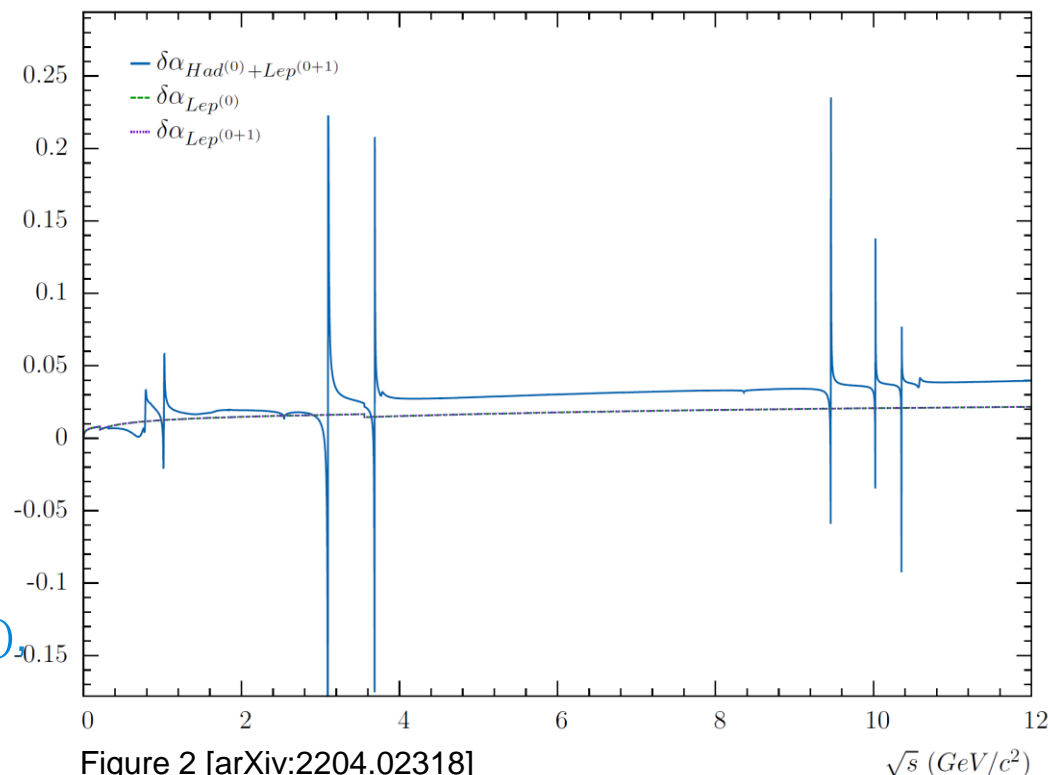


Figure 2 [arXiv:2204.02318]

*Uehling-Seber [94] effect is implicitly included through the running of α_{QED}

Additional Feynman Diagrams Results

$ee \in MC$ contains the Feynman diagram for Born ($\overline{\mathcal{M}}_{n=0}^{k=1}$) and all radiative emission diagrams at LO ($\overline{\mathcal{M}}_{n=1}^{k=1}$), NLO ($\overline{\mathcal{M}}_{n=2}^{k=1}$), NNLO ($\overline{\mathcal{M}}_{n=3}^{k=1}$) for Initial-State and Final-State including Initial/Final-State Interference. Additionally all NNNLO ($\overline{\mathcal{M}}_{n=4}^{k=1}$) diagrams corresponding to Initial-State radiative emissions are also included.

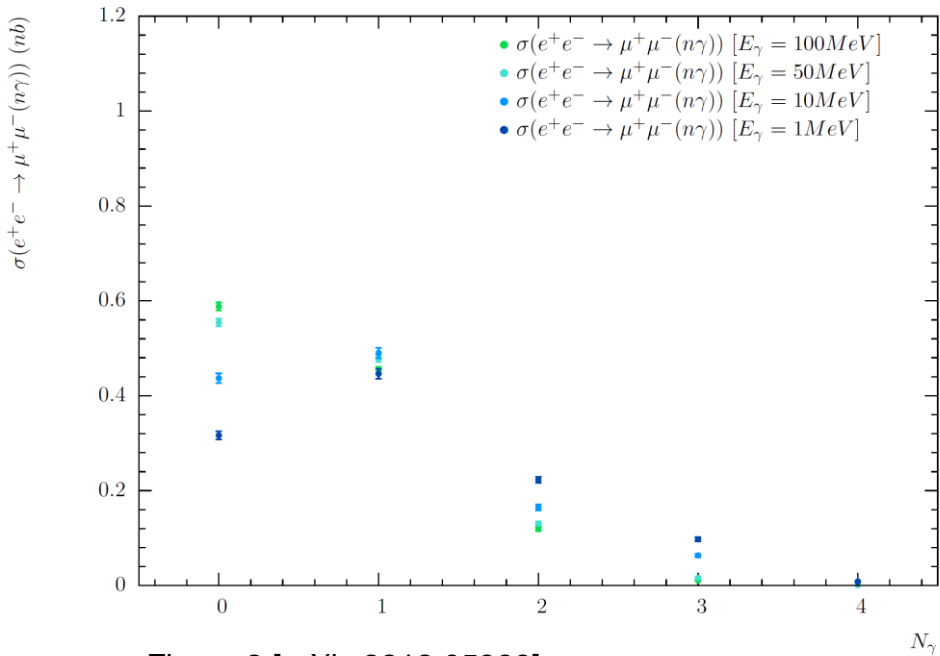
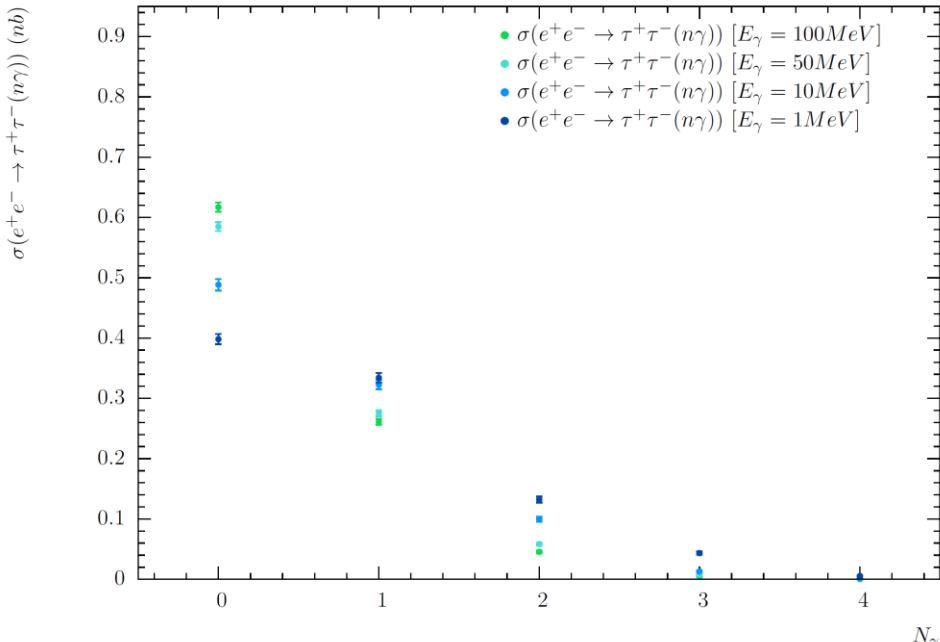


Figure 2 [arXiv:2212.05388]



At $E_l = 1\text{MeV}$, the $e^+e^- \rightarrow \mu^+\mu^-(n\gamma)$ NNNLO ($\overline{\mathcal{M}}_{n=4}^{k=1}$) contribution is $\sim 0.006\text{-}0.008\text{nb}$

Given the expected relative ISR+FSR and FSR contribution for NNNLO expect a truncation error of $\sim 1 - 1.5\%$ on any NNLO calculation for a 1MeV soft-photon cut-off.

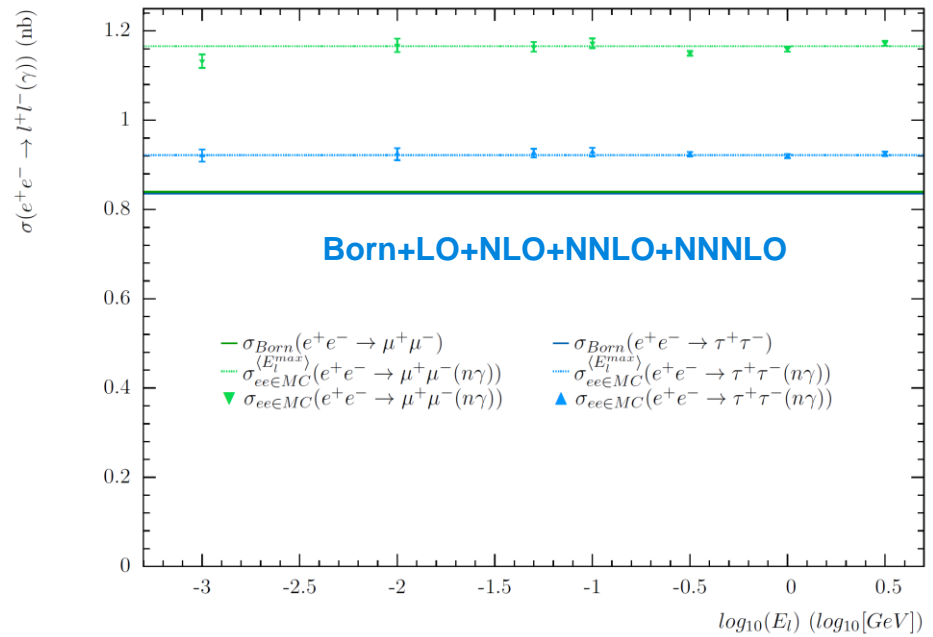
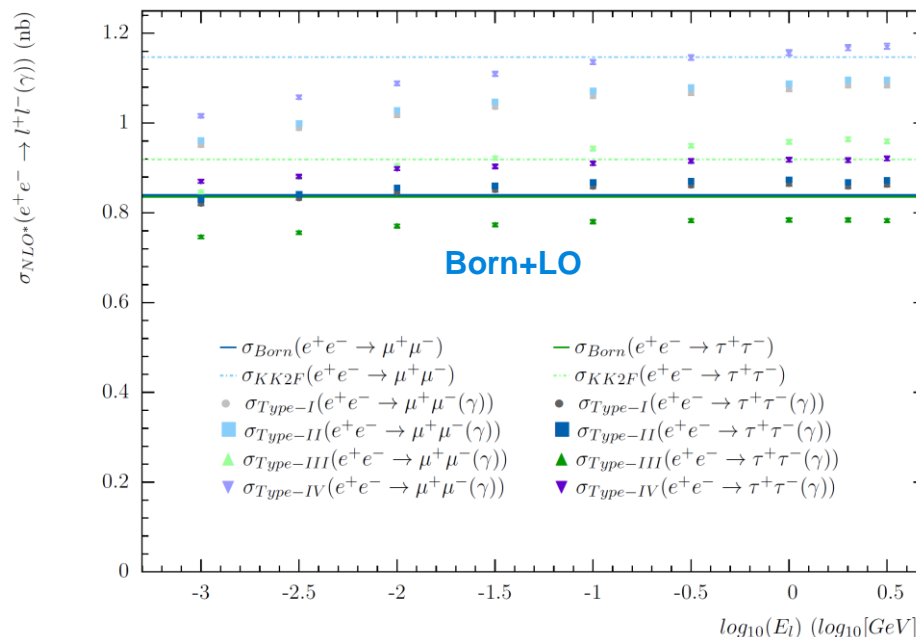
For comparison, KK2F is only up to NNLO (3γ).

YFS Exponentiation an Infinite Perturbative Series

YFS Exponentiation subtracts the infra-red divergences for all orders of Feynman diagrams, however, only a small sub-set of the Feynman diagrams are included into the simulation.

- This necessarily implies that there is a theoretical error on the predictions due to the truncation of the infinite Feynman series.
- Since the multiplicative subtract of the Infra-red divergences is positive definite, the predicted cross-sections tend to be reduced by the truncation.

⇒ Born ($\overline{\mathcal{M}}_{n=0}^{k=1}$) and all radiative emission diagrams at LO ($\overline{\mathcal{M}}_{n=1}^{k=1}$), NLO ($\overline{\mathcal{M}}_{n=2}^{k=1}$), NNLO ($\overline{\mathcal{M}}_{n=3}^{k=1}$) for Initial-State and Final-State including Initial/Final-State Interference are included. Additionally all NNNLO ($\overline{\mathcal{M}}_{n=4}^{k=1}$) diagrams corresponding to Initial-State radiative emissions are also included.



YFS Exponentiation an Infinite Perturbative Series

YFS Exponentiation subtracts the infra-red divergences for all orders of Feynman diagrams, however, only a small sub-set of the Feynman diagrams are included into the simulation

- This necessarily implies that there is a theoretical error on the predictions due to the truncation of the infinite Feynman series.
- Since the multiplicative subtract of the Infra-red divergences is positive definite, the predicted cross-section tends to be reduced by the truncation.
- As with the Feynman mass approach to subtracting infra-red divergencies as the soft-photon cut-off is reduced, the contribution of higher order terms to the perturbative Feynman series increases.

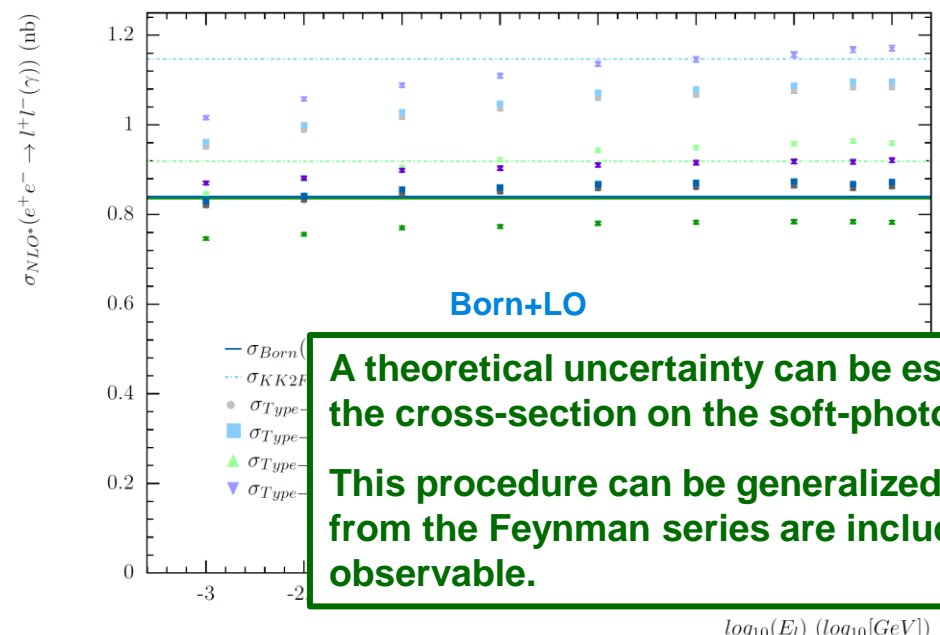


Figure 5 [arXiv:2204.02318]

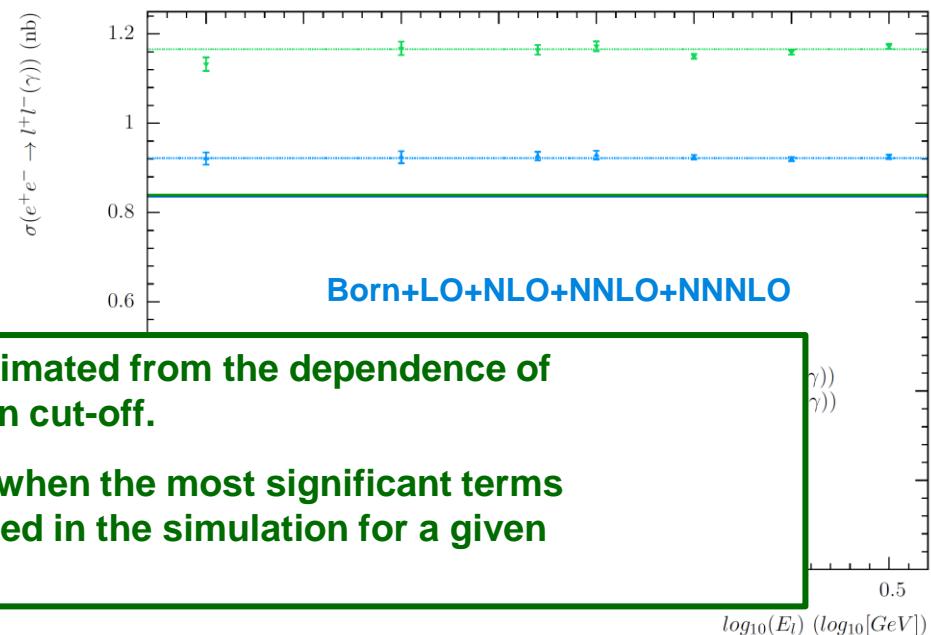


Figure 3 [arXiv:2212.05388]

Conditions for Infra-Red Safe Photons

Within the **Yennie-Frautschi-Suura Exponentiation Formalism**, the number of hard-photons is an infra-red safe observable when the soft-photon energy in the laboratory frame, δM , is less than the minimum detectable energy in the experiment, E_{min} , [100].

- For a soft-photon cut-off using δM : If δM is chosen to be sufficiently small, $\delta M c^2 \ll E_{min}$, then the number of “soft-photons” above E_{min} can be made arbitrarily small or negligible in the laboratory frame.
- When there is a negligible truncation error, this condition can be verified, by computing two values of δM . If the change in the number of hard-photons is negligible, both values of δM satisfy the condition for the number of photons being an infra-red safe observable. If the condition is met or the deviation is sufficiently small, a theoretical uncertainty can be applied. Otherwise a lower value of δM is required.

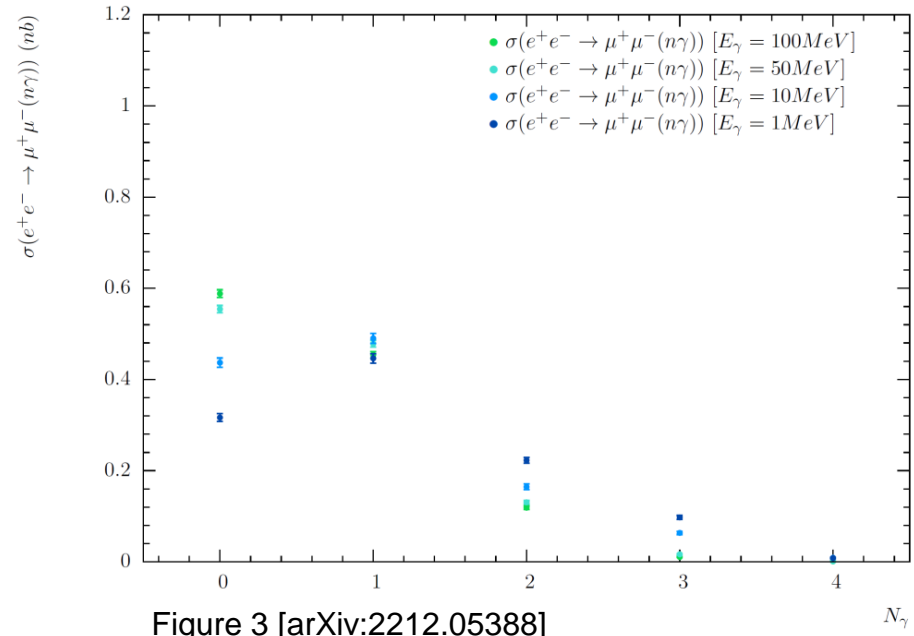
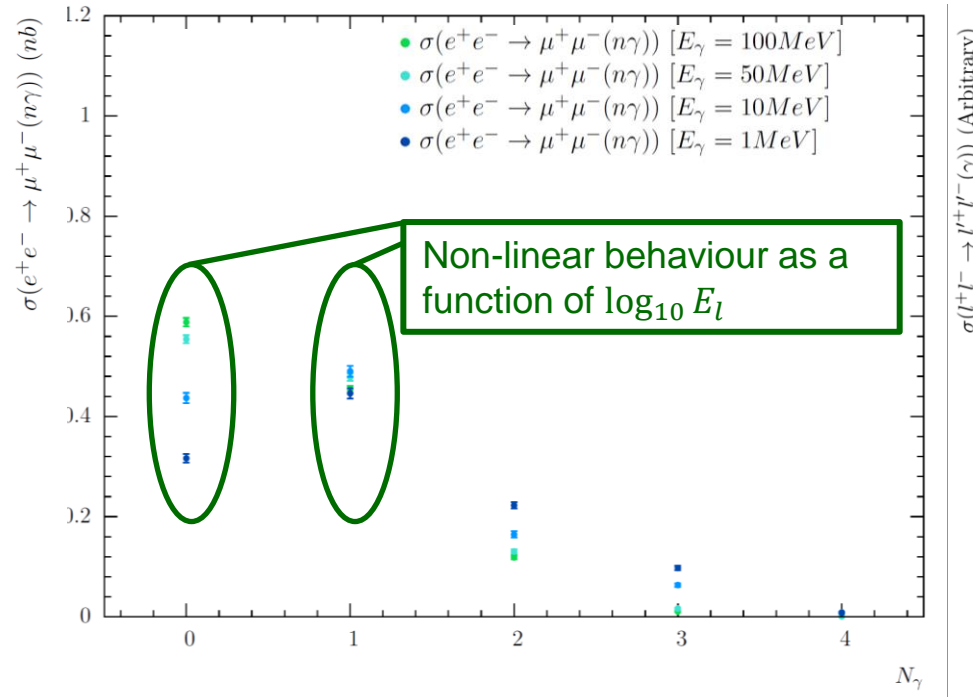


Figure 3 [arXiv:2212.05388]

This condition is essential for any analysis that applies a selection criteria on the number of photons or applies a statistical method which includes the photons. To have a physically meaningful comparison between the data and MC the observables being studied must be infra-red safe within the given theoretical prediction.

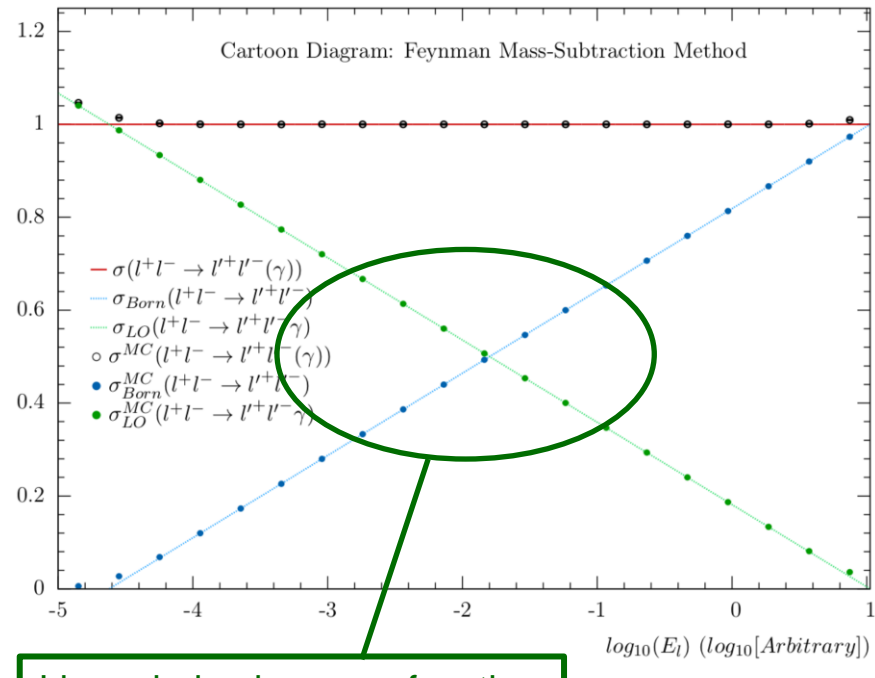
Exponentiation vs Feynman Mass Subtraction

YFS Exponentiation



Feynman Mass-Subtraction

- Method used in MC for e^+e^- hadron vacuum polarization measurements (g-2)



Naively, ratio of 1 γ to 2 γ events are inconsistent at 1MeV and 10MeV with exponentiations
⇒ only one value of E_γ where the two methods will coincide

Approach to $e^+e^- \rightarrow Hadrons(n\gamma)$ Calculations

For a $e^+e^- \rightarrow V \rightarrow PP$ interaction the Born level matrix element may be written as

$$\mathcal{M}_a^b = (\bar{v}_2 i e \gamma^\mu u_1) \frac{g_{\mu\nu}}{q^2} (\bar{u}_3 i e Q_f v_4)$$

Within the hadronic current formalism from which the hadronic τ decays are constructed this becomes:

$$\mathcal{M}_a^b \approx (\bar{v}_2 i e \gamma^\mu u_1) \frac{g_{\mu\nu}}{q^2} i e Q_f \times \mathbf{J}^\nu$$

Effective hadronic current

Where

$$\mathbf{J}^\nu = \mathbf{N} F(s) \left(g^{\nu\alpha} - \frac{q^\nu q^\alpha}{q^2} \right) (\mathbf{p}_a - \mathbf{p}_b)_\alpha$$

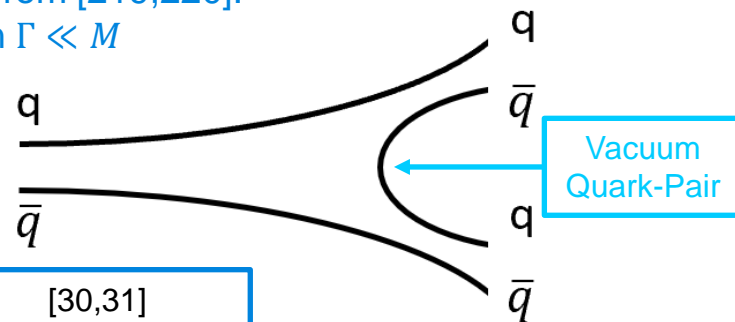
- $F(s)$ is the model dependent Form-Factor (Vector-Dominance, χRL , Flux-Tube Breaking, Quark-Pair-Creations Model, ...)
- $(g^{\nu\alpha} - \frac{q^\nu q^\alpha}{q^2})$ is the tensor component of the spin 1 propagator
- $(\mathbf{p}_a - \mathbf{p}_b)_\alpha$ is the $V \rightarrow PP$ vertex coupling
- \mathbf{N} is the current amplitude calculated in the given hadronic model
 - Within the effective theories constructed from the SU(3) generator [129] \mathbf{N} implicitly includes the colour factor N_c [89]. Therefore we use the convention that N_c is implicitly included in \mathbf{N}

$$e^+ e^- \rightarrow \Upsilon(4s)(m\gamma) \rightarrow B^+ B^- / B^0 \bar{B}^0(n\gamma)$$

The $e^+ e^- \rightarrow \Upsilon(4s)(m\gamma) \rightarrow B^+ B^- (n\gamma)$ and $e^+ e^- \rightarrow \Upsilon(4s)(m\gamma) \rightarrow B^0 \bar{B}^0 (n\gamma)$ decay models are modelled with the Quark-Pair-Creation Model [216,217,218] using the parameterization from [219,220].

Form-Factor is normalized within the Chiral limit under the assumption $\Gamma \ll M$

$$F(s) \rightarrow \frac{M^2}{(s - \bar{m}^2(s)) + iM\Gamma_{total}(s)}$$



With

$$\Gamma_{total}(s) = \frac{1}{8\pi} |g_{BBY} \sum_{m=\pm 1} I_4(m, \mathbf{q})| \frac{q(s)}{s} \quad [30,31]$$

$$I_4(m, \mathbf{q}) = \sqrt{\frac{1}{35}} \left(14R^2 \frac{\partial}{\partial R^2} + 16R^4 \left(\frac{\partial}{\partial R^2} \right)^2 + \frac{16}{3} R^6 \left(\frac{\partial}{\partial R^2} \right)^3 \right) I_1(m, \mathbf{q})$$

$$I_1(m, \mathbf{q}) = \frac{8\sqrt{6}}{\pi^2} \left(\frac{RR_B}{R^2+2R_B^2} \right)^{3/2} \left(1 - \frac{hR_B^2}{R^2+2R_B^2} \right) e^{-\frac{R^2 R_B^2 h^2 q^2}{4(R^2+2R_B^2)}} \epsilon \cdot \mathbf{q} \quad h = \frac{2m_B}{m_B+m_q}$$

Current amplitude is normalized within the SU(3) Chiral limit where the heavy-quarks are treated as singlets \Rightarrow the effective Lagrangian is constructed from only the light quarks in the heavy-quark meson $\rightarrow 3$ and $\bar{3}$.

The resonance structure is dependant on the harmonic-oscillator wave-function in the Quark-Pair-Creation Model [216,217,218] and this impacts the phase-space. Therefore, the Form-Factor is further modified to take this into account, normalizing at the pole-mass to remove the phase-space contribution from the channel dependant width $\Gamma_{B_x \bar{B}_y(s)}$

$$F(s) \propto \frac{\Gamma_{B_x \bar{B}_y}(s) \times (s/\beta^3)}{(s - \bar{m}^2(s)) + iM\Gamma_{total}(s)}$$

This allows for the phase space difference to be taken into account between the $e^+ e^- \rightarrow \Upsilon(4s)(m\gamma) \rightarrow B^+ B^- (n\gamma)$ and $e^+ e^- \rightarrow \Upsilon(4s)(m\gamma) \rightarrow B^0 \bar{B}^0 (n\gamma)$ decay modes.

B mesons decays are currently not simulated

Radiation Models

Radiation models are extensions based on: J.P Lees, *et al*, Measurement of the Initial-State-Final-State Radiation Interference in the Processes $e^+e^- \rightarrow \mu^+\mu^-\gamma$ and $e^+e^- \rightarrow \pi^+\pi^-\gamma$, Phys. Rev. D, 92:072015, 2015 [221].

The models for the outgoing mesons in [221] are:

- i. Assume $\tau_{QED} \gg \tau_{QCD} \Rightarrow \gamma$ radiates off the Final-State meson \rightarrow Klein-Gordon
- ii. Assume γ radiates off the particles at quark level \rightarrow Dirac-Spinors

Final-State radiation models need to be applied to both the Exponentiation with radiative emission and the Coulomb potential. Therefore the models are extended as:

Model 1: Assume $\tau_{QED} \gg \tau_{QCD}$
 $\Rightarrow \gamma$ radiates off the Final-State meson \rightarrow Klein-Gordon

The **Schwinger's** approach to LO QED of scalar particles [101] is merged with the Yennie-Frautschi-Suura Exponentiation [100] following the procedure in $ee \in MC$ [2204.02318]

$$Y_{spin=0} = e^{\frac{2\alpha Q_f^2}{\pi} \left([(1-\nu^2)\chi(\nu)-1] \left[\ln\left(\frac{\delta M}{m_l}\right) + 1 \right] + \chi(\nu) - \frac{(1+\nu)}{\nu} \int_0^\nu d\nu' \frac{\chi(\nu')}{1-\nu'^2} \right) - \frac{\alpha Q_f^2}{\pi} \left(P \int_0^1 d\nu' \frac{(1+\nu'^2) \ln \frac{\nu'^2}{1-\nu'^2}}{\nu'^2 - \nu'^2} \right) - F_c |_{O(\alpha)}}$$

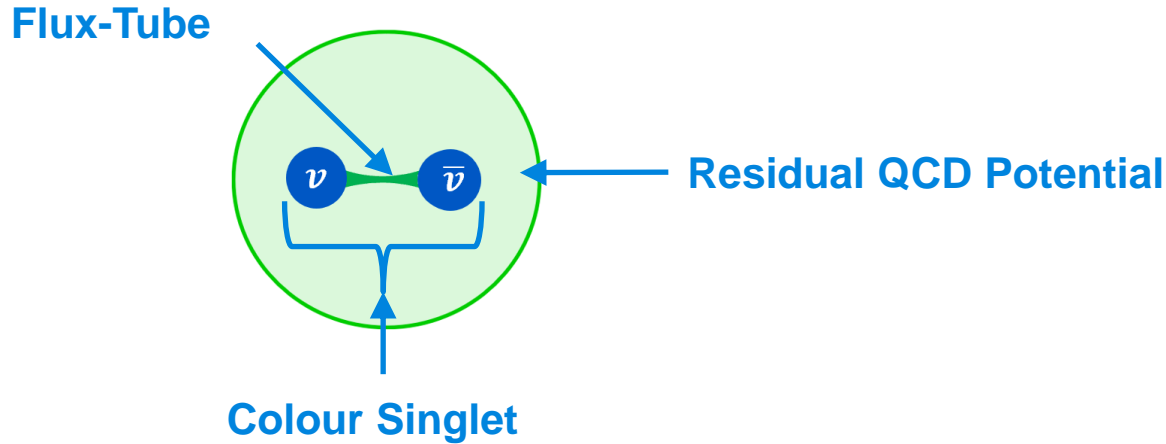
where the **Coulomb attraction** [94,101] is removed from the exponentiation and included through a separate series

$$Y \rightarrow Y \times F_c = Y \times \frac{\pi\alpha/\nu}{1 - e^{-(\frac{\pi\alpha}{\nu})}}$$

\Rightarrow Coulomb potential interacts with Final-State mesons \rightarrow meson charge and mass is applied to F_c

Radiation Models

Model 2: Is constructed in terms of colour singlets and flux-tube breaking...

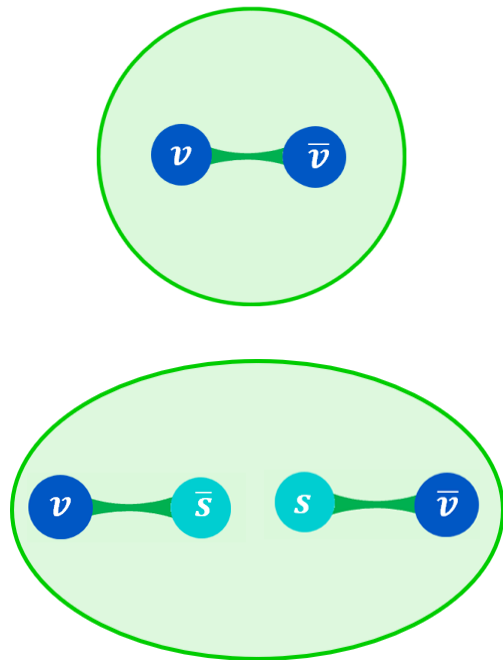
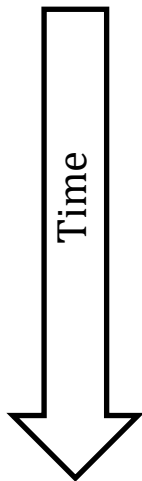


Vector mesons are formed from a colour singlet of valence quarks bound by a “Flux-tube” surrounded by sea of residual gluons and sea quarks.

- Model based on the assumptions that
 - i. Confinement in QCD by flux-tubes
 - ii. Conservation of angular momentum.
 - iii. $\alpha_{QED} \ll \alpha_s$
 - iv. Colour singlet size \ll wave-length of photon emissions
⇒ colour singlet can be approximated as a point particle when radiating off a photon

Radiation Models

Model 2: Is constructed in terms of colour singlets and flux-tube breaking...

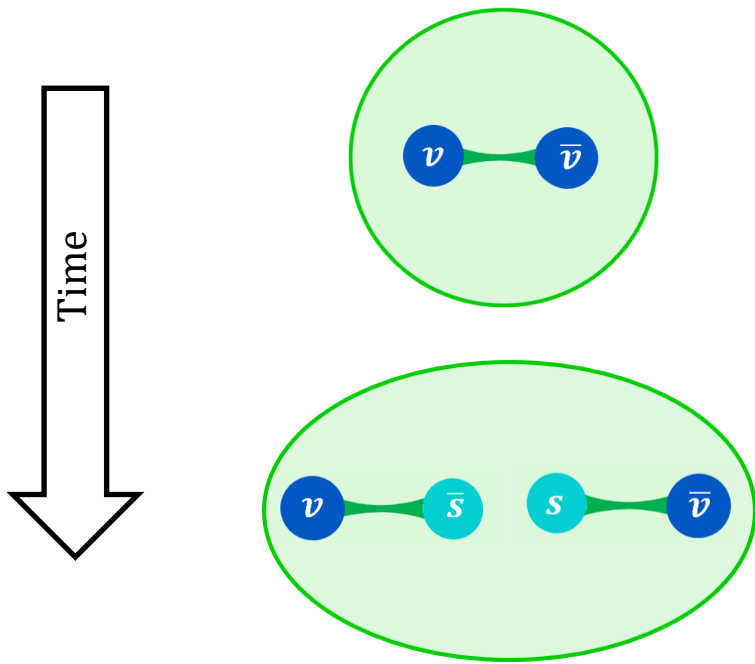


Vector meson formed from colour singlet of valence quarks bound by “Flux-tube”. Surrounded by sea of residual gluon field and sea quarks.

Sea quark pair created as the “Flux-Tube” between valence quarks breaks and two new colour singlets are formed.

Radiation Models

Model 2: Is constructed in terms of colour singlets and flux-tube breaking...



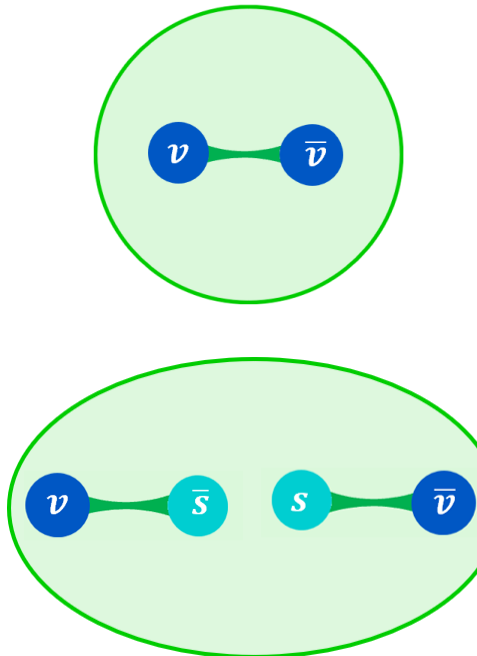
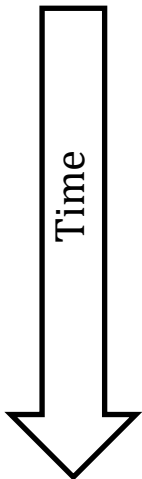
Vector meson formed from colour singlet of valence quarks bound by “Flux-tube”. Surrounded by sea of residual gluon field and sea quarks.

Sea quark pair created as the “Flux-Tube” between valence quarks breaks and two new colour singlets are formed.

- Bound by residual QCD potential
- Coulomb potential is dominated by small distance scales $m_{eff} \approx m_v + m_s$ with meson charge
- Initial singlet states can be spin-0 or integer spin
- $\alpha_{QED} \ll \alpha_s \Rightarrow$ spin transferred to gluon field

Radiation Models

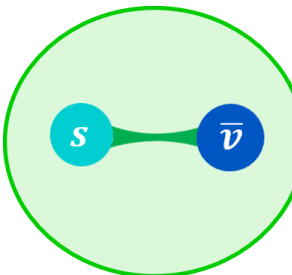
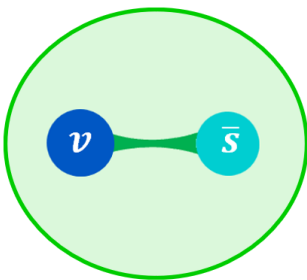
Model 2: Is constructed in terms of colour singlets and flux-tube breaking...



Vector meson formed from colour singlet of valence quarks bound by “Flux-tube”. Surrounded by sea of residual gluon field and sea quarks.

Sea quark pair created as the “Flux-Tube” between valence quarks breaks and two new colour singlets are formed.

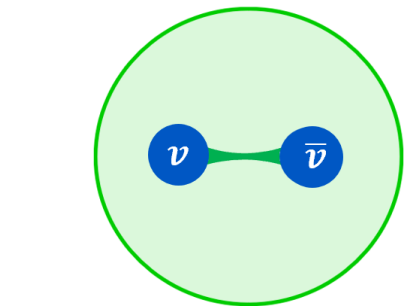
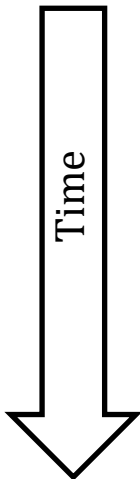
- Bound by residual QCD potential
- Coulomb potential is dominated by small distance scales $m_{eff} \approx m_v + m_s$ with meson charge
- Initial singlets state can be spin-0 or integer spin
- $\alpha_{QED} \ll \alpha_s \Rightarrow$ spin transferred to gluon field



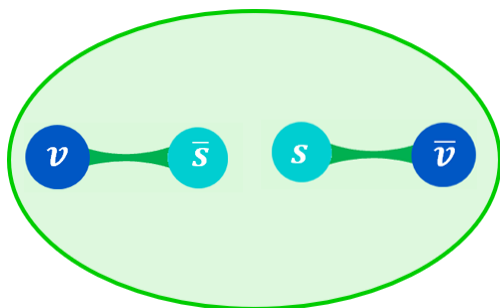
The vector meson disintegrates and forms the two independent pseudo-scalar meson total angular momentum of the system being conserved.

Radiation Models

Model 2: Is constructed in terms of colour singlets and flux-tube breaking...

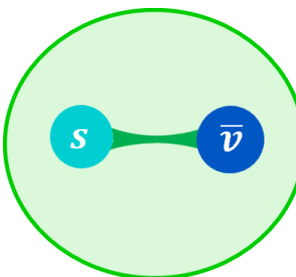
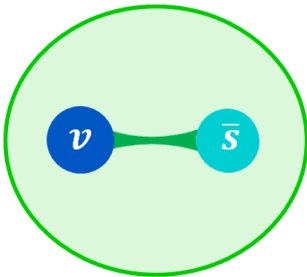


Vector meson formed from colour singlet of valence quarks bound by “Flux-tube”. Surrounded by sea of residual gluon field and sea quarks.



Sea quark pair created as the “Flux-Tube” between valence quarks breaks and two new colour singlets are formed.

- Bound by residual QCD potential
- Coulomb potential is dominated by small distance scales $m_{eff} \approx m_v + m_s$ with meson charge
- Initial singlets state can be spin-0 or integer spin
- $\alpha_{QED} \ll \alpha_s \Rightarrow$ spin transferred to gluon field



The vector meson disintegrates and forms the two independent pseudo-scalar meson total angular momentum of the system being conserved.

- Colour singlet size \ll wave-length of photon emissions $\Rightarrow \gamma$ radiated from singlet with $m_{eff} \approx m_{meson}$ and meson charge

Radiation Models

Model 3: Assume $\tau_{QED} \gg \tau_{QCD}$ for the YFS Exponentiation and radiative emission

⇒ γ radiate off of the Final-State meson → Klein-Gordon

Assume Coulomb potential acts on small distance scales and ⇒ at quark level

→ quark charge and mass is applied to F_c for the quark with the lowest $v = \beta = \sqrt{1 - 4m_q/s}$

Model 4: Assume γ radiate off the particles at quark level [221]

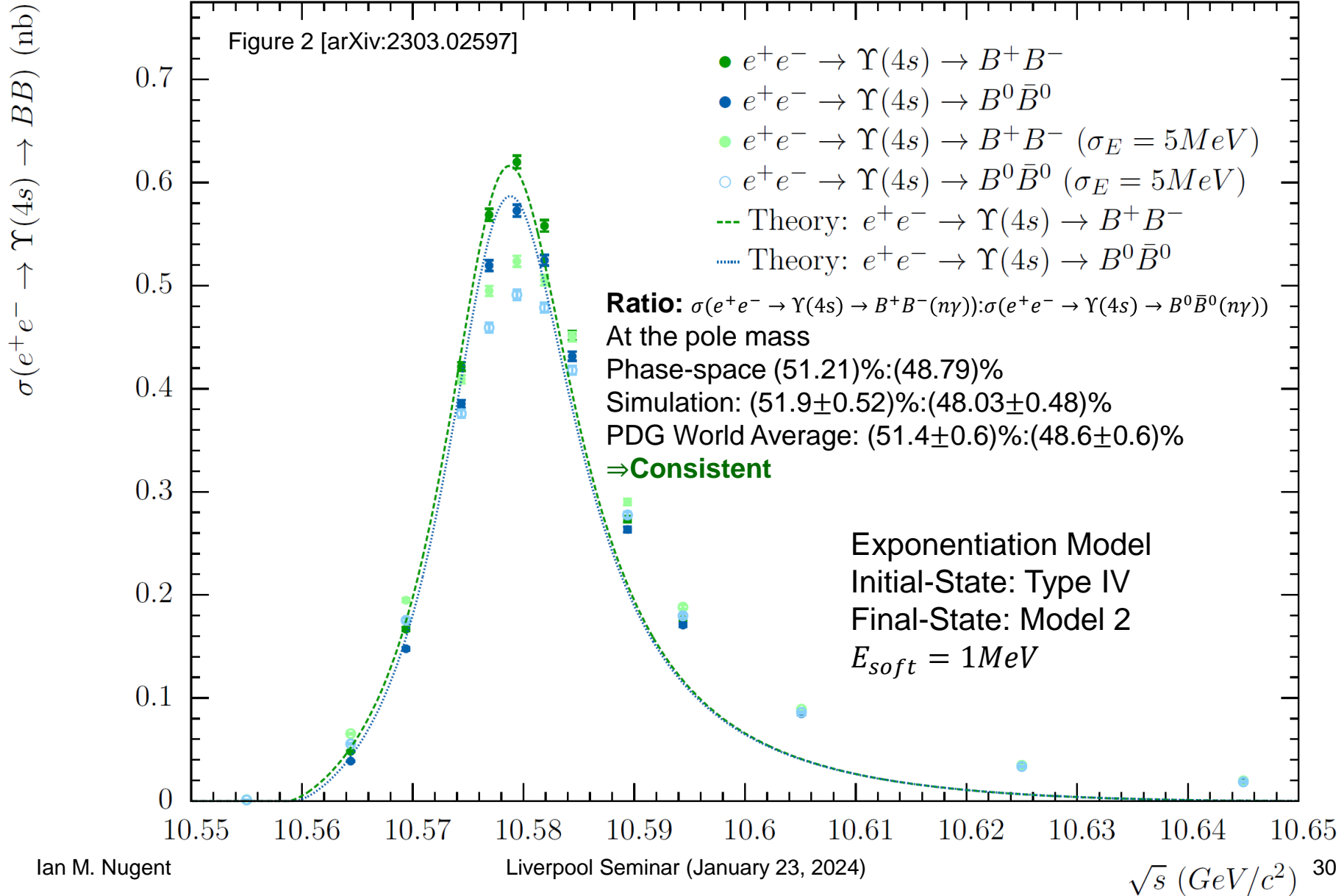
→ Dirac-Spinors

Assume Coulomb potential acts on small distance scales and ⇒ at quark level

→ quark charge and mass is applied to F_c for the quark with the lowest $v = \beta = \sqrt{1 - 4m_q/s}$

Models 1 & 2 are preferred based on arguments of confinement with Flux-Tubes. This is supported with the results from [221].

$$e^+ e^- \rightarrow \Upsilon(4s)(m\gamma) \rightarrow B^+ B^- / B^0 \bar{B}^0(n\gamma)$$



$$e^+ e^- \rightarrow \Upsilon(4s)(m\gamma) \rightarrow B^+ B^- / B^0 \bar{B}^0(n\gamma)$$

By exploiting the constrained phase-space of $\Upsilon(4s) \rightarrow B^+ B^-(n\gamma)$ and $\Upsilon(4s) \rightarrow B^0 \bar{B}^0(n\gamma)$ processes, a comparison of the relative enhancement due to the Coulomb potential can be used to discriminate between the Radiative Models.

Relative enhancement: Model 1:Model 2: Model 3/4 $\rightarrow 20.28\%:1.98\%:0\%$ at the pole-mass
 \Rightarrow Model 1 can be excluded. This implies that the Coulomb potential must be applied at either quark or singlet level and **not** at the meson or baryon level. Supported by [222] on $e^+ e^- \rightarrow p^+ p^-$.

An uncertainty of $\sim 0.3\text{-}0.4\%$ is required on the ratio: $\sigma(e^+ e^- \rightarrow \Upsilon(4s) \rightarrow B^+ B^-(n\gamma)):\sigma(e^+ e^- \rightarrow \Upsilon(4s) \rightarrow B^0 \bar{B}^0(n\gamma))$ to distinguish between Model 2 and Model 3 [Test assumption of QCD confinement with Flux-Tubes].

Figure 4 [arXiv:2303.02597]

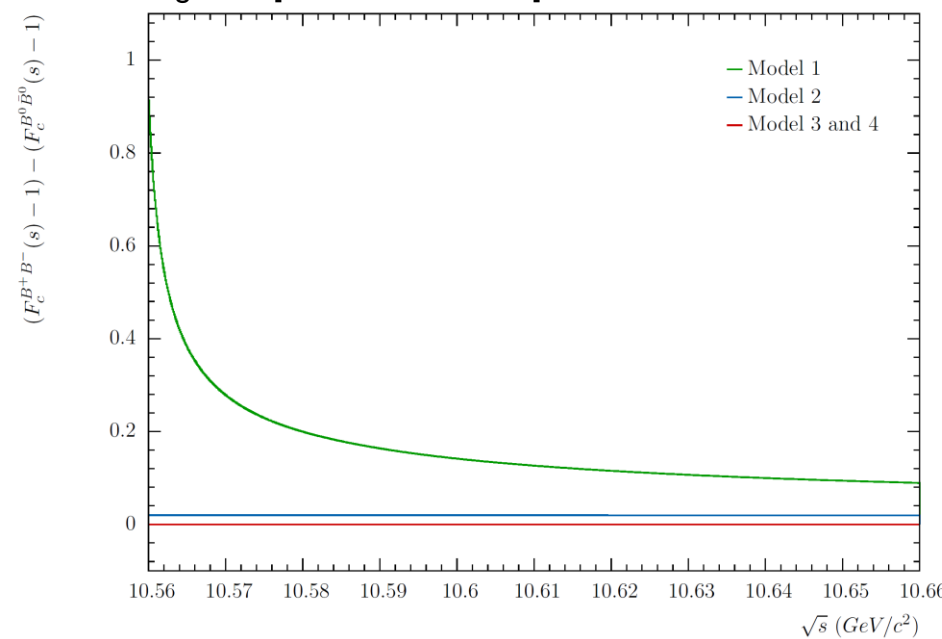
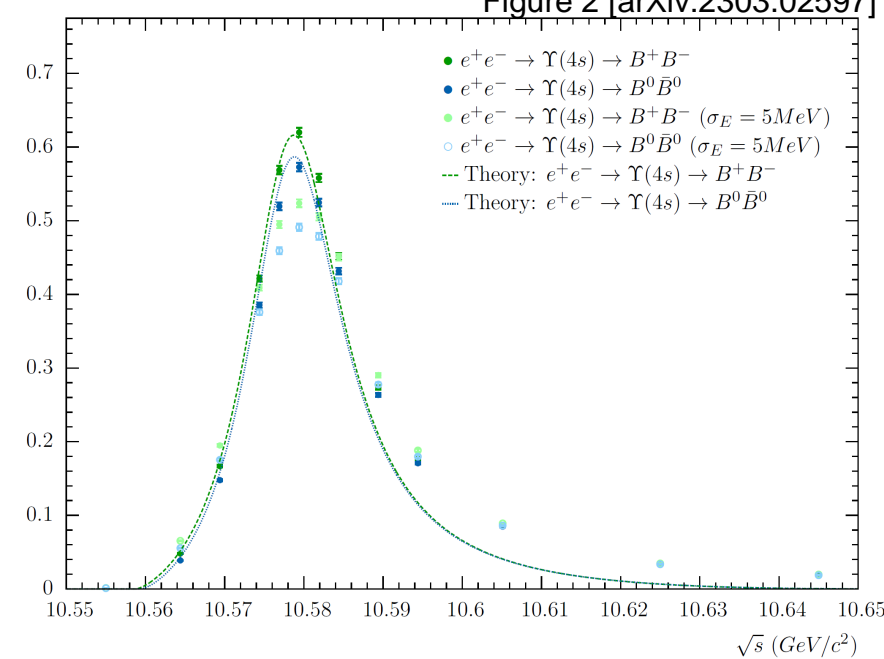
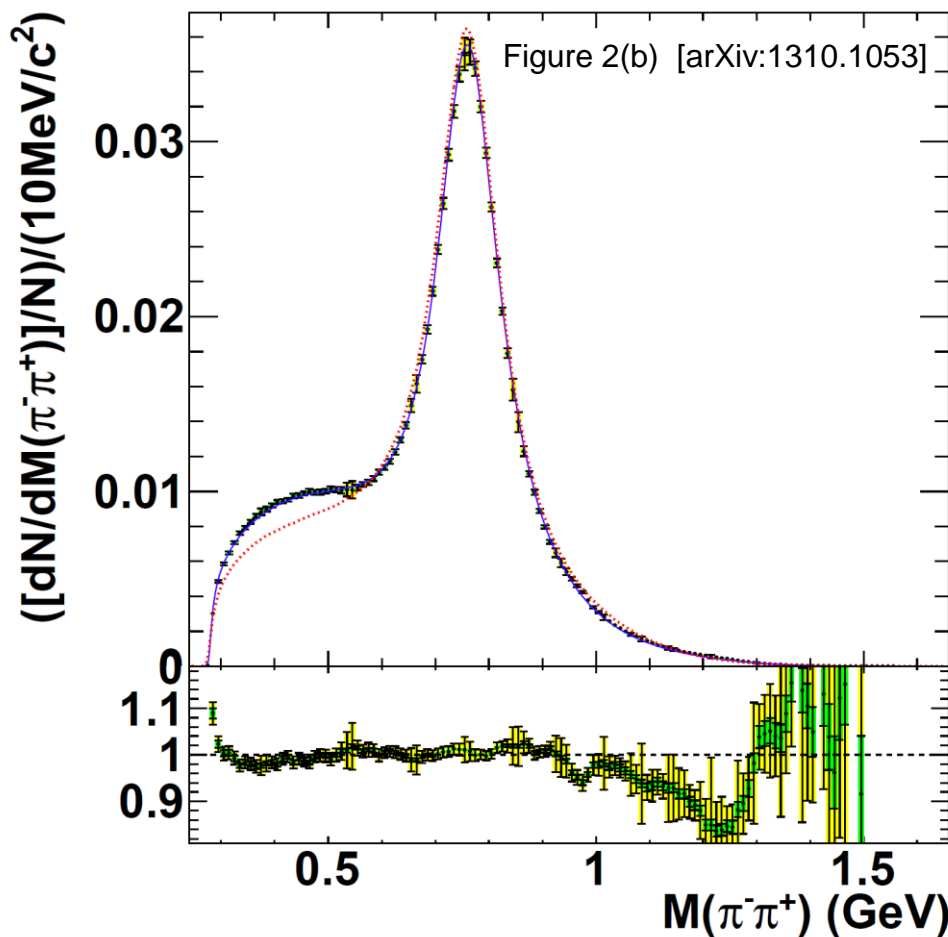
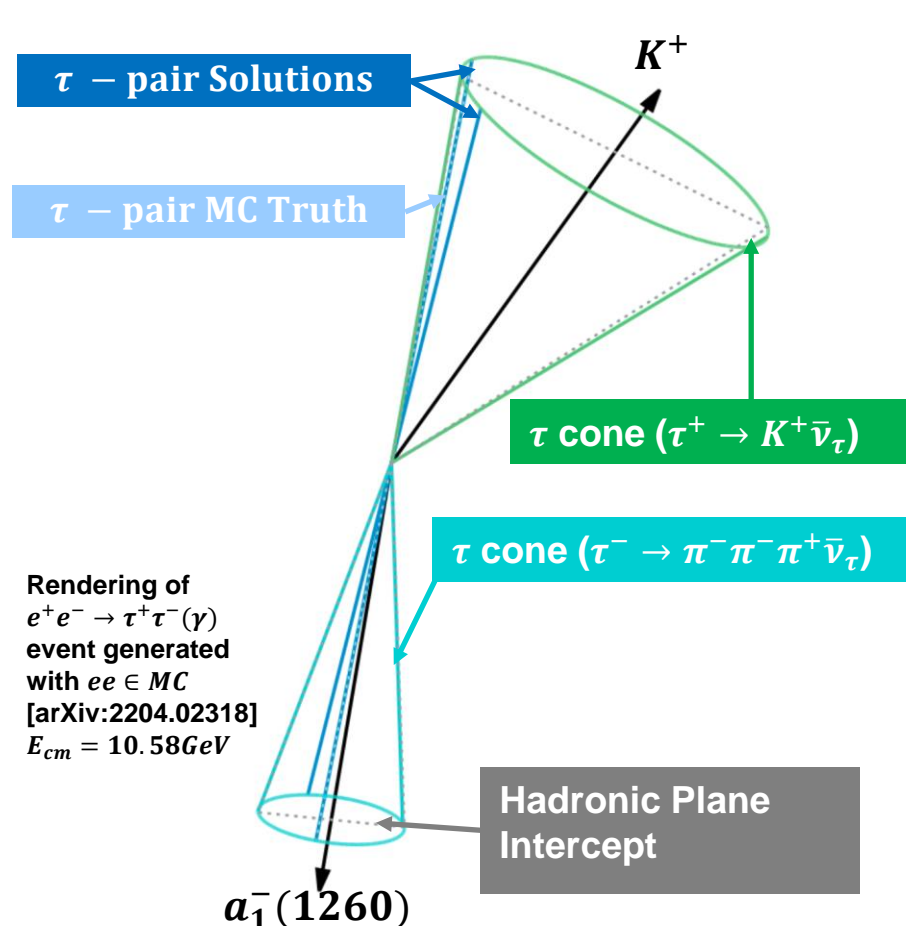


Figure 2 [arXiv:2303.02597]



$$e^+ e^- \rightarrow \Upsilon(4s)(m\gamma) \rightarrow B^+ B^- / B^0 \bar{B}^0 (n\gamma)$$

- The Coulomb potential is often taken into account at the meson level $e^+ e^- \rightarrow \text{Hadrons}$ measurements which are used for determining the hadronic vacuum polarization to g-2 [223,224,225,226].
- This implies that the Coulomb potential can not be a viable explanation for the low mass excess found in hadronic τ decays which are commonly interpreted as scalars [227].



Overview of τ Decays

The differential decay rate of the τ lepton at Born level is,

$$d\Gamma = \frac{1}{2m_\tau} |\mathcal{M}|^2 \times dPS$$

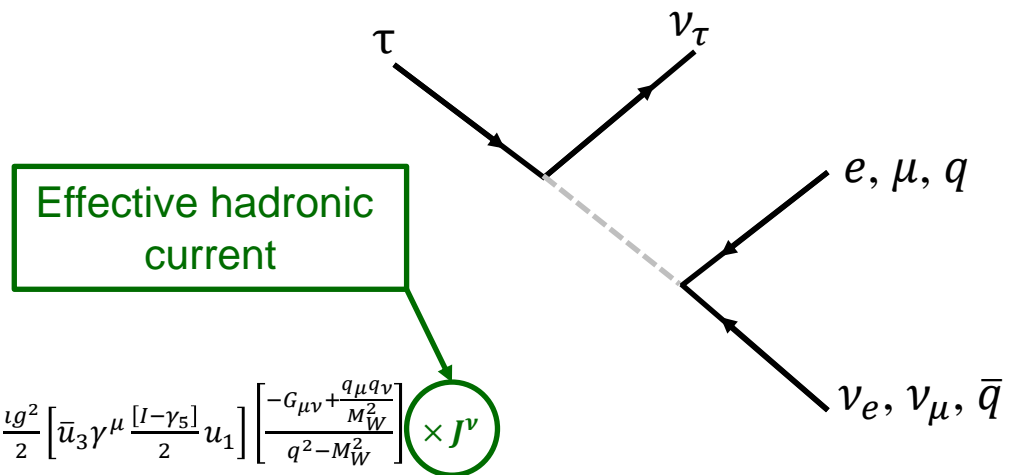
where

Leptonic Decay

$$\mathcal{M} = -\frac{\imath g^2}{2} \left[\bar{u}_3 \gamma^\mu \frac{[I-\gamma_5]}{2} u_1 \right] \left[\frac{-G_{\mu\nu} + \frac{q_\mu q_\nu}{M_W^2}}{q^2 - M_W^2} \right] \left[\bar{v}_2 \gamma^\mu \frac{[I-\gamma_5]}{2} l_4 \right]$$

Semi-Leptonic decay

$$\mathcal{M} = -\frac{\imath g^2}{2} \left[\bar{u}_3 \gamma^\mu \frac{[I-\gamma_5]}{2} u_1 \right] \left[\frac{-G_{\mu\nu} + \frac{q_\mu q_\nu}{M_W^2}}{q^2 - M_W^2} \right] \left[\bar{q}_2 \gamma^\mu \frac{[I-\gamma_5]}{2} q_4 \right] \rightarrow -\frac{\imath g^2}{2} \left[\bar{u}_3 \gamma^\mu \frac{[I-\gamma_5]}{2} u_1 \right] \left[\frac{-G_{\mu\nu} + \frac{q_\mu q_\nu}{M_W^2}}{q^2 - M_W^2} \right] \times J^\nu$$



J^ν represents the hadronic current for a given decay mode and hadronic model. All Final-State spins are summed over. The Initial-State spin average depends on the QED polarization interface algorithm.

Categories of Hadronic Models

- i. Chiral-Resonance Lagrangian Models
- ii. Vector-Dominance Models
- iii. Empirical Models from previous Experiments
- iv. Flux-Tube Breaking Model: "Chromoelectric Flux-Tube Breaking Model" constructed in the context on the "strong coupling lattice formulation" [61, 121, 122] combined with a "revitalized $[{}^3P_0]$ quark model" [33, 60, 61, 121, 122]

Hadonic τ Decays

Model	Decay Modes	Resonances
Tsai [111]	$\tau^- \rightarrow \pi^- \nu_\tau, \tau^- \rightarrow K^- \nu_\tau$	
Kuhn-Santamaria [18,70]	$\tau^- \rightarrow \pi^- \pi^0 \nu_\tau, \tau^- \rightarrow K^- K^0 \nu_\tau, \tau^- \rightarrow \pi^- \pi^- \pi^+ \nu_\tau, \tau^- \rightarrow \pi^- \pi^0 \pi^0 \nu_\tau$	$\rho(770), \rho'(1450), \rho''(1700), a_1(1260)$
Decker-Mirkes-Sauer-Was [118]	$\tau^- \rightarrow \pi^- \pi^- \pi^+ \nu_\tau, \tau^- \rightarrow \pi^- \pi^0 \pi^0 \nu_\tau, \tau^- \rightarrow K^- \pi^- \pi^+ \nu_\tau, \tau^- \rightarrow K^- \pi^0 \pi^0 \nu_\tau, \tau^- \rightarrow \pi^- \bar{K}^0 \pi^0 \nu_\tau, \tau^- \rightarrow K^- \pi^- K^+ \nu_\tau, \tau^- \rightarrow K^0 \pi^- \bar{K}^0 \nu_\tau, \tau^- \rightarrow K^- \pi^0 K^0 \nu_\tau, \tau^- \rightarrow K^- K^- K^+ \nu_\tau, \tau^- \rightarrow \pi^- \pi^0 \eta \nu_\tau$	$\rho(770), \rho'(1450), \rho''(1700), a_1(1260), K^*(892), K^{*'}(1410), K^{*''}(1680), K_1(1400)$
Finkemeier-Mirkes [68,127]	$\tau^- \rightarrow \pi^- \pi^0 \nu_\tau, \tau^- \rightarrow K^- \pi^0 \nu_\tau, \tau^- \rightarrow \pi^- K^0 \nu_\tau, \tau^- \rightarrow K^- K^0 \nu_\tau, \tau^- \rightarrow K^- \eta \nu_\tau, \tau^- \rightarrow K^- \eta(958) \nu_\tau, \tau^- \rightarrow K^- \pi^- \pi^+ \nu_\tau, \tau^- \rightarrow K^- \pi^0 \pi^0 \nu_\tau, \tau^- \rightarrow \pi^- \bar{K}^0 \pi^0 \nu_\tau, \tau^- \rightarrow K^- \pi^- K^+ \nu_\tau, \tau^- \rightarrow K^0 \pi^- \bar{K}^0 \nu_\tau, \tau^- \rightarrow K_S^0 \pi^- K_S^0 \nu_\tau, \tau^- \rightarrow K_L^0 \pi^- K_S^0 \nu_\tau, \tau^- \rightarrow K_L^0 \pi^- K_L^0 \nu_\tau, \tau^- \rightarrow K^- \pi^0 K^0 \nu_\tau, \tau^- \rightarrow K^- K^- K^+ \nu_\tau$	$\rho(770), \rho'(1450), \rho''(1700), a_1(1260), K^*(892), K^{*'}(1410), K^{*''}(1680), K_0^*(1430), K_1(1270), K_1(1400)$
Tauola [87]	$\tau^- \rightarrow \pi^- \pi^- \pi^0 \pi^+ \nu_\tau$	$\rho(770), \rho'(1450), \rho''(1700), \omega(782),$
Feindt [119]	$\tau^- \rightarrow \pi^- \pi^- \pi^+ \nu_\tau, \tau^- \rightarrow \pi^- \pi^0 \pi^0 \nu_\tau$	$\rho(770), a_1(1260)$
CLEO [35][38][39][123]	$\tau^- \rightarrow \pi^- \pi^0 \nu_\tau, \tau^- \rightarrow \pi^- \pi^- \pi^+ \nu_\tau, \tau^- \rightarrow \pi^- \pi^0 \pi^0 \nu_\tau, \tau^- \rightarrow \pi^- \pi^- \pi^0 \pi^+ \nu_\tau, \tau^- \rightarrow K^- \pi^- \pi^+ \nu_\tau,$	$\rho(770), \rho'(1450), \rho''(1700), f_0(600), \omega(782), a_1(1260), a_1(1640), K^*(892), K^{*'}(1410), K^{*''}(1680), K_1(1270), K_1(1400)$
Novosibirsk [40]	$\tau^- \rightarrow \pi^- \pi^- \pi^0 \pi^+ \nu_\tau$	$\rho(770), f_0(600), \omega(782), a_1(1260)$
Kuhn-Was [128]	$\tau^- \rightarrow \pi^- \pi^- \pi^- \pi^+ \nu_\tau, \tau^- \rightarrow \pi^- \pi^+ \pi^0 \pi^0 \nu_\tau, \tau^- \rightarrow \pi^- \pi^0 \pi^0 \pi^0 \nu_\tau$	$\rho(770), f_0(600), \omega(782), a_1(1260)$
Phenomenological [2204.02318]	$\tau^- \rightarrow K^- \pi^- \pi^+ \pi^0 \nu_\tau, \tau^- \rightarrow K^- \pi^- K^+ \pi^0 \nu_\tau$	$\rho(770), \rho'(1450), \rho''(1700), \omega(782), h_1(1170), h_1(1415), a_1(1260), K^*(892), K^{*'}(1410), K^{*''}(1680), K_1(1270), K_1(1400)$
Flux-Tube Breaking [33,60,61,121,122,134]	$\tau^- \rightarrow \pi^- \pi^0 \nu_\tau, \tau^- \rightarrow K^- \pi^0 \nu_\tau, \tau^- \rightarrow \pi^- K^0 \nu_\tau, \tau^- \rightarrow \pi^- \pi^- \pi^+ \nu_\tau, \tau^- \rightarrow \pi^- \pi^0 \pi^0 \nu_\tau, \tau^- \rightarrow K^- \pi^- \pi^+ \nu_\tau, \tau^- \rightarrow K^- \pi^0 \pi^0 \nu_\tau, \tau^- \rightarrow \pi^- K^0 \pi^0 \nu_\tau, \tau^- \rightarrow K^- \pi^- \pi^0 \pi^+ \nu_\tau,$	$\rho(770), a_1(1260), f_0(1370), K^*(892), K_1(1270), K_1(1400), K_0^*(1430), K(1460)$
Generic Scalar PS	Any mode – defined at run time from input arguments	

$e^+e^- \rightarrow \tau^+\tau^-(\gamma)$ Polarization: An Interface Approach

The spin dynamics of the QED interaction and subsequent τ decays are implemented by means of the **modified Altarelli-Parisi Density Function** [5,6,175]

$$\frac{\rho_{\lambda_i, \lambda_j}}{|\mathcal{M}|^2} \times \mathcal{M}_{\lambda_i, \lambda_j, \lambda_k, \lambda_l, \dots, \lambda_n} \mathcal{M}_{\lambda_i, \lambda_j, \lambda_{k'}, \lambda_{l'}, \dots, \lambda_{n'}}^* \times \prod_{\alpha=k}^n D_{\lambda_\alpha, \lambda'_\alpha}$$

Where $D_{\lambda_\alpha, \lambda'_\alpha} = \frac{1}{|\mathcal{M}|^2} \mathcal{M}_{\lambda_\alpha, \lambda_\beta, \lambda_\gamma, \dots, \lambda_\nu}^{(D)} \mathcal{M}_{\lambda'_\alpha, \lambda'_\beta, \lambda'_\gamma, \dots, \lambda'_\nu}^{(D)*}$ for the τ leptons and $D_{\lambda_\alpha, \lambda'_\alpha} = \delta_{\lambda_\alpha, \lambda'_\alpha}$ for the photons [5,6].

The **probability for a given spin configuration (P)** is determined using the modified Altarelli-Parisi Density function where a $SU(2) \rightarrow SO(3)$ transformation is applied using the **completeness relation and projection operators** to obtain a positive definite probability

$$P = \frac{\rho_{\lambda_i, \lambda_j}}{|\mathcal{M}|^2} \times \mathcal{M}_{\lambda_i, \lambda_j, \lambda_k, \lambda_l, \dots, \lambda_n} \mathcal{M}_{\lambda_i, \lambda_j, \lambda_{k'}, \lambda_{l'}, \dots, \lambda_{n'}}^* \times \prod_{\alpha=k}^n D_{\lambda_\alpha, \lambda'_\alpha}$$

The modified Altarelli-Parisi Density function allows for a partial factorization of the spin and matrix element algorithms, where the QED and τ decay processes can be computed separately. Initial-State polarizations are implemented

- i. A change of basis for the Initial-State electron and positron polarization by means of constructing the wave-function from a linear super-positioning of states where $\vec{P} = |\vec{P}| \times \hat{n}$.

$$\langle s_{\hat{n}} \rangle = \langle s_{1/2, m} | \hat{s}_{\hat{n}} | s_{1/2, m} \rangle = \left\langle s_{1/2, m} \left| \frac{\hbar}{2} [n_x \hat{\sigma}_x + n_y \hat{\sigma}_y + n_z \hat{\sigma}_z] \right| s_{1/2, m} \right\rangle$$

- ii. An extension of the modified Altarelli-Parisi Density function to include an arbitrary Initial-State polarization.

$$\frac{\rho_{\lambda_i, \lambda_{i'}}^{e^+} \times \rho_{\lambda_j, \lambda_{j'}}^{e^-}}{|\mathcal{M}|^2} \times \mathcal{M}_{\lambda_i, \lambda_j, \lambda_k, \lambda_l, \dots, \lambda_n} \mathcal{M}_{\lambda_{i'}, \lambda_{j'}, \lambda_{k'}, \lambda_{l'}, \dots, \lambda_{n'}}^* \times \prod_{\alpha=k}^n D_{\lambda_\alpha, \lambda'_\alpha}$$

Where $\rho_{\lambda_i, \lambda_{i'}}^{e^+}$ and $\rho_{\lambda_j, \lambda_{j'}}^{e^-}$ are the SU(2) representations of the polarimetric vectors and $\rho_{\lambda_i, \lambda_j} \rho_{\lambda_i, \lambda_{i'}=i}^{e^+} \times \rho_{\lambda_j, \lambda_{j'}=j}^{e^-}$.

$e^+e^- \rightarrow \tau^+\tau^-(\gamma)$ Polarization: An Interface Approach

Accept/Reject Algorithm (SDM[L+T]):

- $e^+e^- \rightarrow \tau^+\tau^-(\gamma)$ events are simulated using the spin averaged matrix element with exponentiation.
- Both τ s are simulated as unpolarized.
- The decay products of the τ s are rotated longitudinally and transversely in their respective centre-of-mass frames before being boosted back to the e^+e^- centre-of-mass frame. After applying the $SU(2) \rightarrow SO(3)$ transformation, the acceptance/rejection is determined using the modified Altarelli-Parisi Density Function relative to a normalized random die (repeat c if fails).

Accept/Reject Algorithm (L-Decoupled+SDM[T]):

- $e^+e^- \rightarrow \tau^+\tau^-(\gamma)$ events are simulated using the spin averaged matrix element with exponentiation.
- Both τ s are simulated with longitudinal polarization using an accept/reject algorithm with probability

$$P_{\lambda_k, \lambda_l} = \frac{\sum_i \sum_j \rho_{\lambda_i, \lambda_j} \sum_{m, \dots, n} |\mathcal{M}_{\lambda_i, \lambda_j, \lambda_m, \dots, \lambda_n}|}{|\bar{\mathcal{M}}|}$$

- The decay products of the τ s are rotated transversely. After applying the $SU(2) \rightarrow SO(3)$ transformation, the acceptance/rejection is determined using the modified Altarelli-Parisi Density Function relative to a normalized random die (repeat c if fails).

Possible to develop a more generic interface which incorporates these algorithms for use at the LHC (LHCb).

- This could include being compatible with LHE events, SANC Files for the Z, + ... etc.

* Transverse spin correlations related Quantum Mechanical solution for Bell's Inequality

Ian M. Nugent

Liverpool Seminar (January 23, 2024)

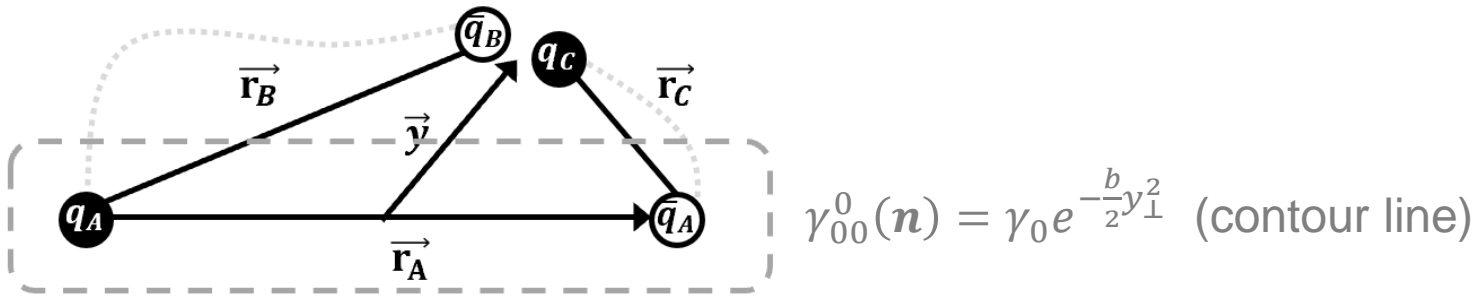
Flux-Tube Breaking Model

A ``chromoelectric flux-tube breaking model'' constructed in the context of the ``strong coupling lattice formulation'' [61,122,123] combined with a ``revitalized $[^3P_0]$ quark model'' [30,61,122,123].

Mesons are described by $q\bar{q}$ wave-function solutions for the Schrödinger equation with the potential

$$H_{ij}(\mathbf{p}, \mathbf{r}) = H_{ij}^{conf} + H_{ij}^{hyp} + H_{ij}^{so} + H_A \text{ where } H_{ij}^{conf} = \left(\frac{3}{4}c + \frac{3}{4}br - \frac{\alpha_s(r)}{r} \right) \frac{\lambda_i \cdot \lambda_j^*}{4} = \left(c + br - \frac{4\alpha_s(r)}{3r} \right).$$

Wave-function described in terms of harmonic oscillator $\psi \sim \text{polynomial} \times e^{-\beta^2 r^2}$, where β characterizes the wave-number and is constrained by the meson properties (ie charge radius)



$$M(A \rightarrow BC) = \int d^3r \int d^3y \psi_B^*(\frac{\mathbf{r}}{2} + \mathbf{y}) \psi_C^*(\frac{\mathbf{r}}{2} - \mathbf{y}) \times \alpha \cdot (\imath \vec{\nabla}_B + \imath \vec{\nabla}_C + \mathbf{q}) \times \psi_A(r) e^{\imath \mathbf{q} \cdot \frac{\mathbf{r}}{2}} \gamma_{00}^0(r, y)$$

Breaking point for B(C) is $\frac{\mathbf{r}}{2} + \mathbf{y}$ ($\frac{\mathbf{r}}{2} - \mathbf{y}$)

\mathbf{q} is the momentum of B(C) in rest frame of A

Vertex Structure defined in terms of Transverse Vertices: $p_\rho^\mu \Gamma_\mu = p_{a_1}^\mu \Gamma_{\mu\nu} = p_\rho^\nu \Gamma_{\mu\nu} = 0$

$$J_{A \rightarrow BC \dots \rightarrow DE}^\mu = f_A(s) P_A^{\mu\nu} f_{A \rightarrow BC}(s) \Gamma_{\nu\gamma} P_B^{\gamma\eta} \dots f_{L \rightarrow MN} \Gamma_{\zeta\omega} P_M^\omega$$

Causal effect of the width dependence on the effective mass of the propagator taken into account through dispersion relations.

Model developed to build a bridge between Lattice QCD and experiment - has extensions to C and B-mesons.

Description of the Scalar Sector

In contrast to the Unitarized Quark Model [144] which associate the lowest mass scalar state to the $f_0(500)$ or the $qq\bar{q}\bar{q}$ state for the Flux-Tube Breaking Model in [60], our Flux-Tube Breaking Model takes the $f_0(1370)$ as the lowest mass scalar state.

For the strange modes we take $K_0^*(1430)$ as the lowest mass scalar state.

After taking into account the causal effect of the width dependence on the effective mass through dispersion relations

$$\hat{m}_n(s) = m_0^2 - \frac{1}{2\pi} P \int_{m_{thres}}^{\infty} ds' m_0 \left[\frac{\Gamma_n(s'^2)}{s' - s} - \frac{\Gamma_n(s'^2)}{s' - m_0^2} \right] \quad \bar{m}(s) = m_0 - \frac{1}{2\pi} P \int_{m_{thres}}^{\infty} dm' \left[\frac{\Gamma_n(m'^2)}{m' - \sqrt{s}} - \frac{\Gamma_n(m'^2)}{m' - m_0} \right]$$

Within the construct of the 3P_0 model there are significant distortions of the resonance line-shape particularly near the production threshold.

Where the “bare” propagator for the covariant amplitude is described in terms of an “on-shell” spin-one massive vector boson [33] with α being a free parameter that relates the “purely resonant time-ordered” component of the propagator and non-resonant contribution [33].

$$P(s) = \frac{\alpha}{s - \hat{m}^2(s) + i m_0 \Gamma(s)} + \frac{1 - \alpha}{2 m_0 (\sqrt{s} - \bar{m}(s)) + i m_0 \Gamma(s)}$$

Note: Within the Flux-Tube Model, the amplitudes of the scalar states are independent of their masses.

Description of the Scalar Sector

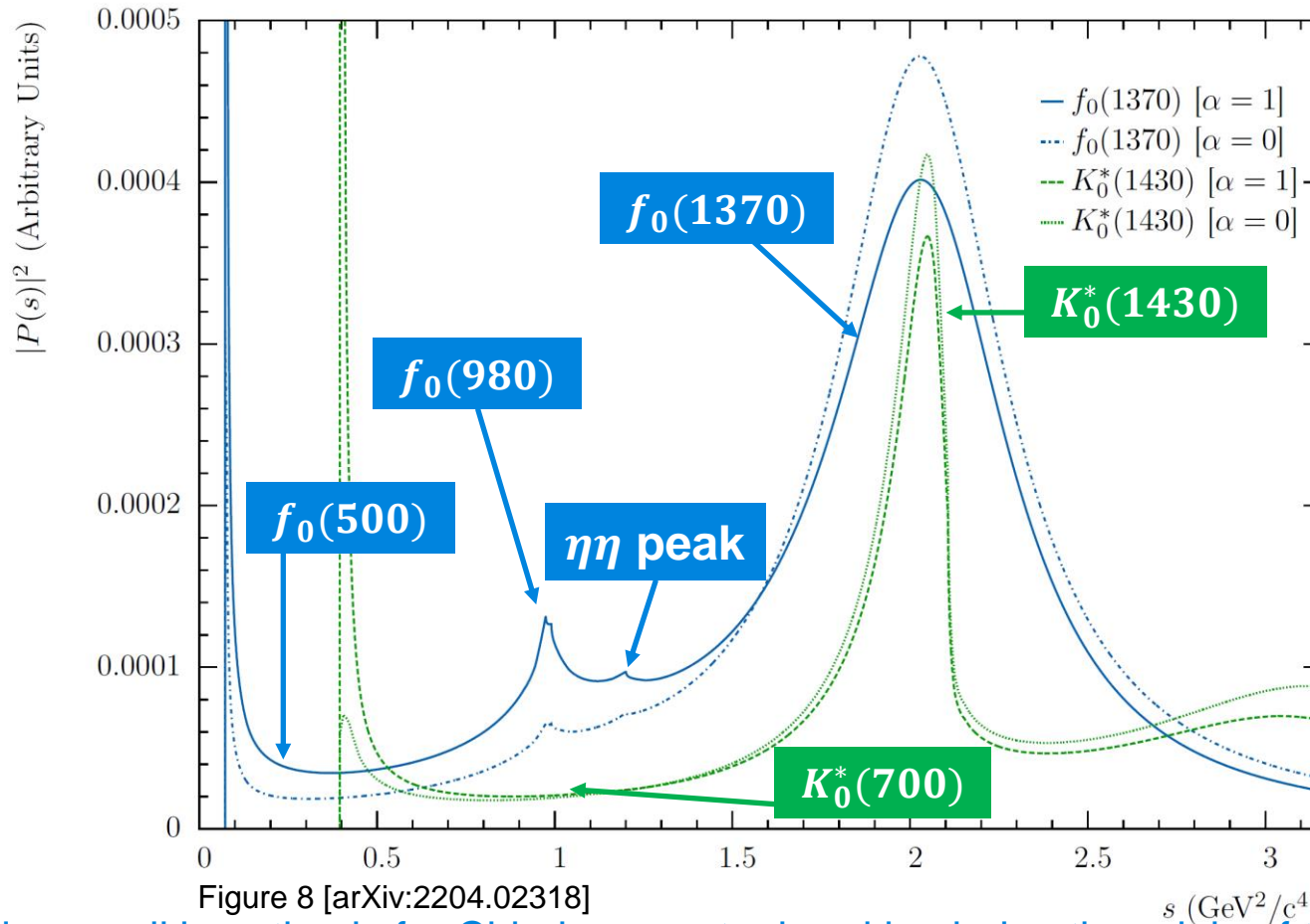
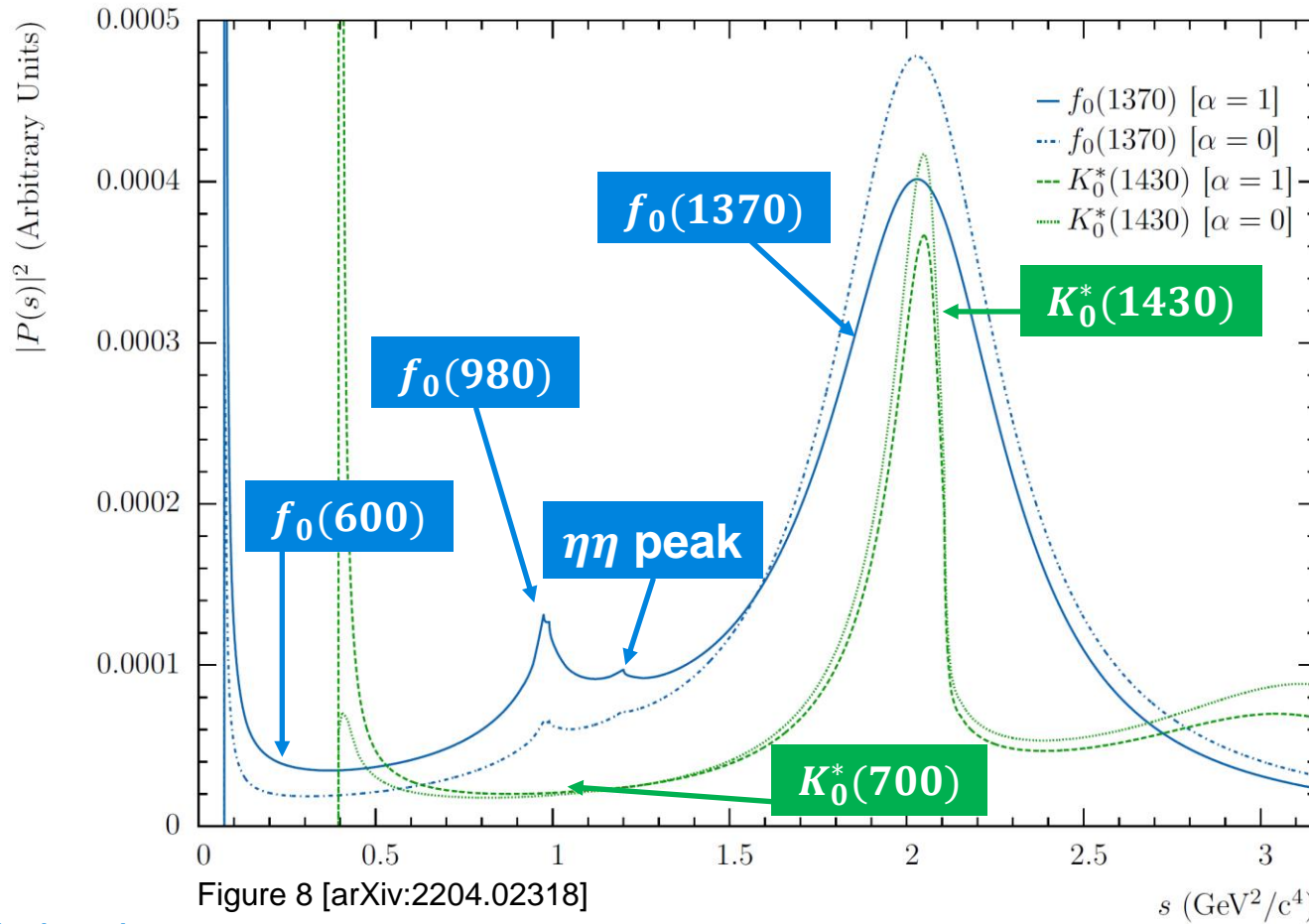


Figure 8 [arXiv:2204.02318]

This provides a null hypothesis for Chiral-symmetry breaking being the origin of the composite-quark mass

- 1) $f_0(980)$ exhibits a double peak structure corresponding to the two pair-production threshold K^+K^- & $K^0\bar{K}^0$
- 2) No change in sign of interference between $f_0(500)$, $f_0(980)$ and $K_0^*(700)$ at other resonances at their peak
- 3) $f_0(1370) \rightarrow \eta\eta$ produces a small peak at $10.96\text{GeV}/c$ ($2 \times m_\eta$)

Description of the Scalar Sector

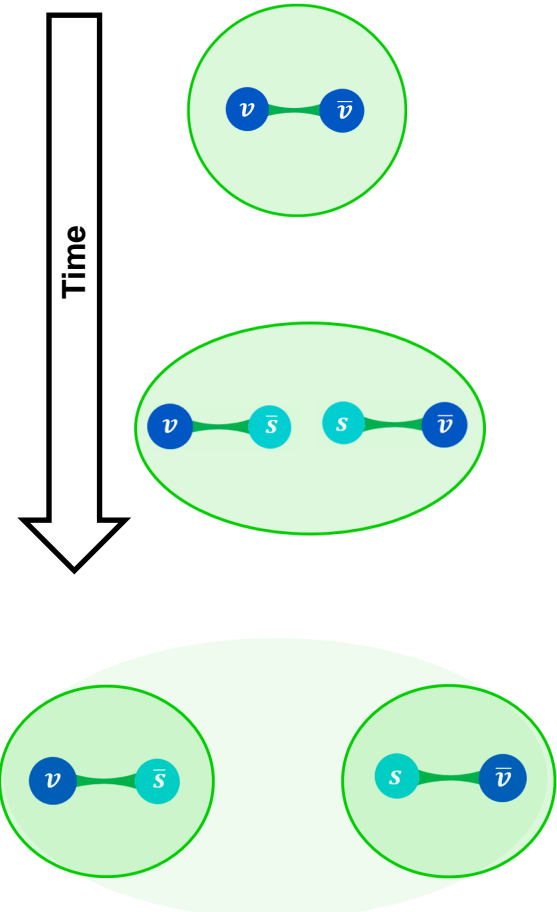


By associating the

- $\epsilon_s(1360) \rightarrow f_0(1500)$ with threshold interface from $\eta\eta'(958)$, $\epsilon(1780) \rightarrow f_0(1710)$ and $\epsilon_s(1990) \rightarrow f_0(2020)$ for the non-strange sector
- $\kappa(1890) \rightarrow K_0^*(1950)$ for the strange sector

the Flux-Tube model provides a complete description of the observed scalar sector.

Residual QCD Interaction in Hadron Production...



Although mesons are colour singlets, there is still a residual QCD potential between the mesons. This residual QCD potential modified the Final-State production through both a wave-function distortion and the modification of the propagator [228,229,230]. At low energies, only the wave function distortions play a significant role [230].

$$R_{h_1 h_2} = s_{h_1 h_2}^2 = \frac{\sigma(h_0 \rightarrow h_1 h_2 | V(r))}{\sigma(h_0 \rightarrow h_1 h_2)} \approx \frac{|\psi(\mathbf{r} = \mathbf{0} | V(r)|^2}{|\psi(\mathbf{r} = \mathbf{0})|^2}$$

In the non-relativistic static limit, the wave-function amplitude distortion for potential $V(r)$ can be determined from the radial solution to the Schrodinger Equation.

$$R''(r) = -\frac{2}{r} R'(r) + 2\mu \left(\frac{l(l+1)}{2\mu r^2} + V(r) - E_{h_1 h_2} \right) R(r)$$

The relative amplitude is determined numerically [258,259] where the initial conditions are defined using the Spherical Bessel Functions [260] $J_0(x)$, $J_1(x)$ and $J_2(x)$ for the S, P and D waves respectively.

As $t \rightarrow \infty$ the residual QCD potential goes to zero

Tetra-Quark States: Scalar States and Residual QCD Potential

In the S states, the colour hyperfine spin-spin interaction produces a strong amplification near threshold [230]. This extension to the modified line-shape for scalar resonances presented in [228,229,230,231,232] can explain the strong KK contribution in the $f_0(980)$ [230,233,234,235], while explaining the $f_0(500)$ and $K_0^*(700)$.

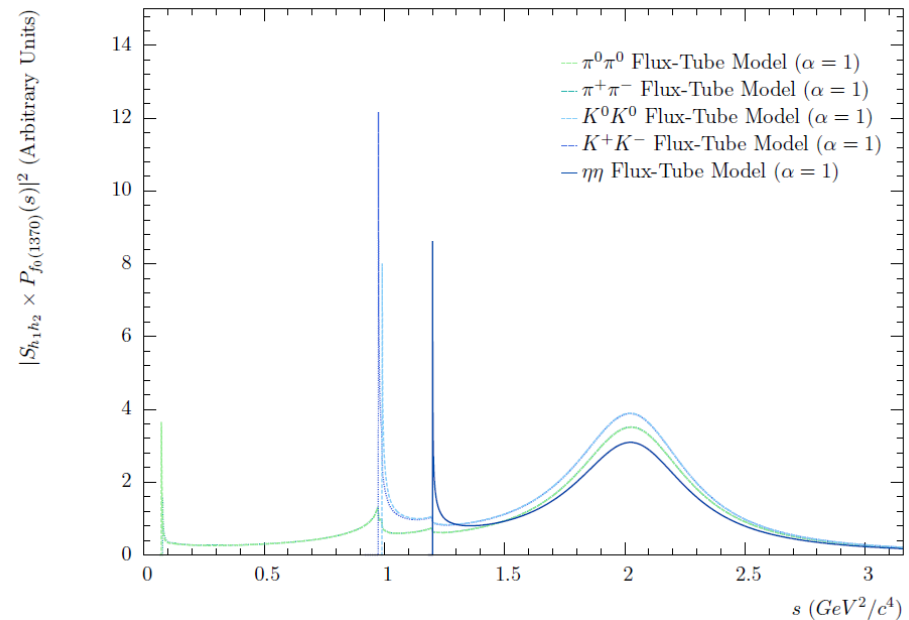
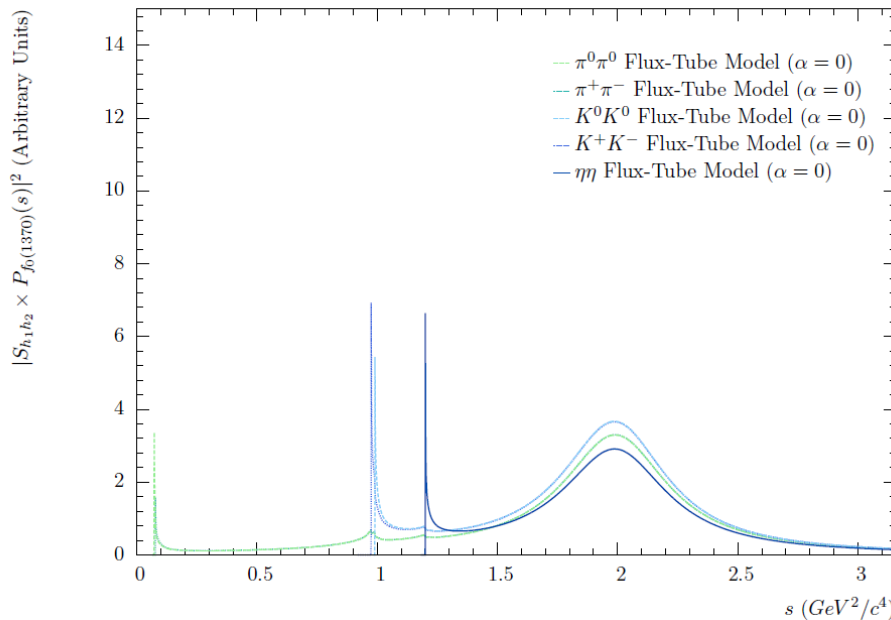


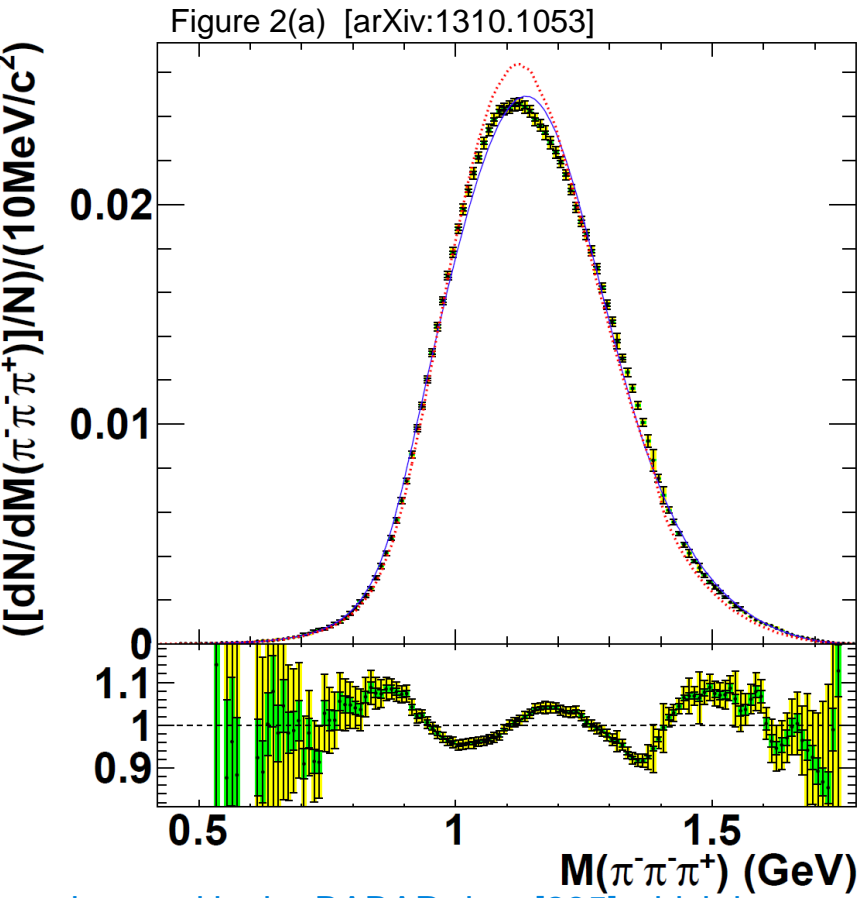
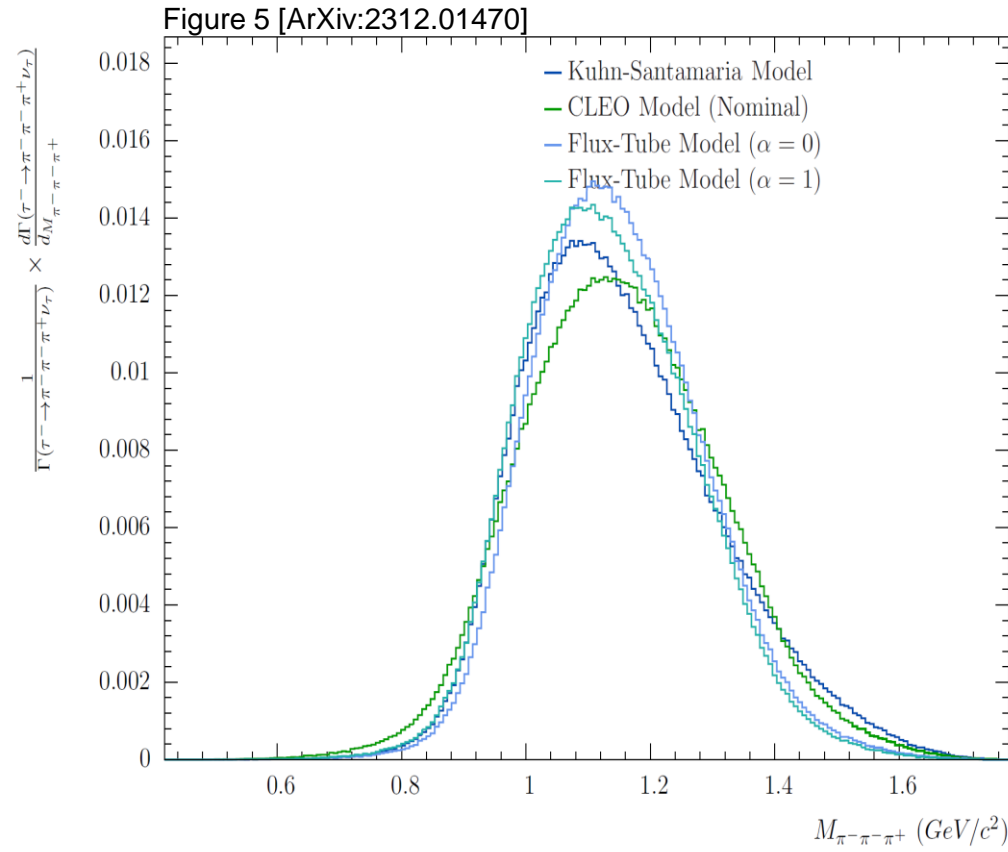
Figure 2 [ArXiv:2312.01470]

This provides another null hypothesis in terms of Tetra-quarks for Chiral-symmetry breaking being the origin of the composite-quark mass.

Depending in the model for the strong annihilation there may or may not be an additional wavefunction amplification of $f_0(1370) \rightarrow \eta\eta$ near the $\eta\eta$ threshold.

S-Wave, P-Wave and D-Wave in Axial-Vectors Decays

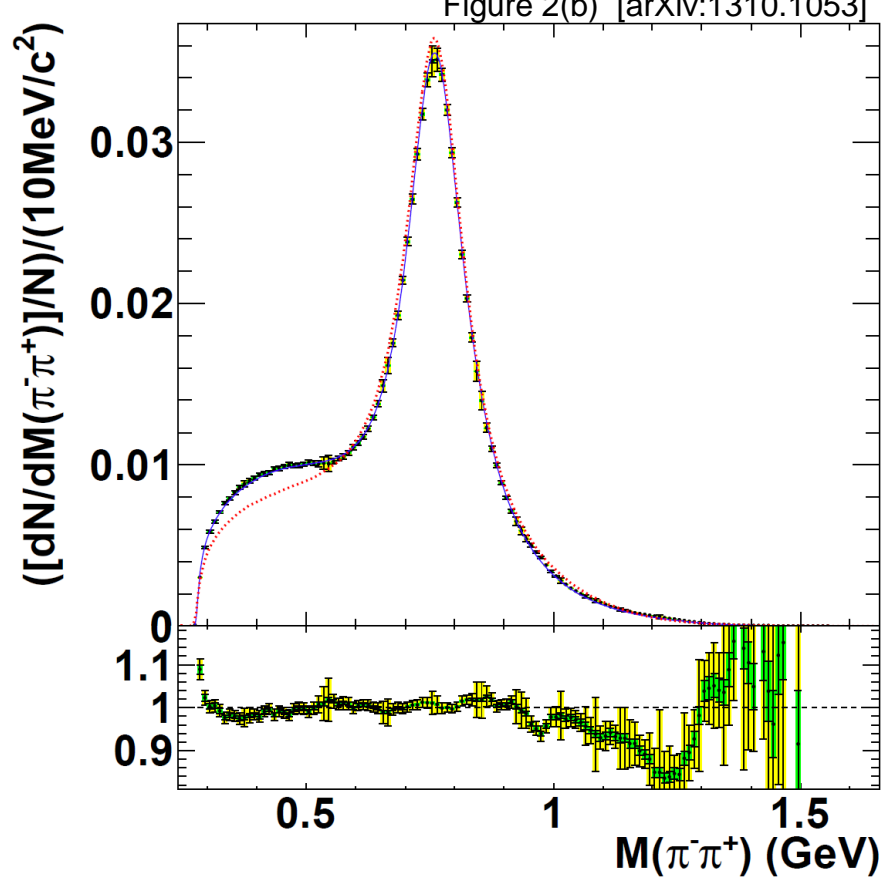
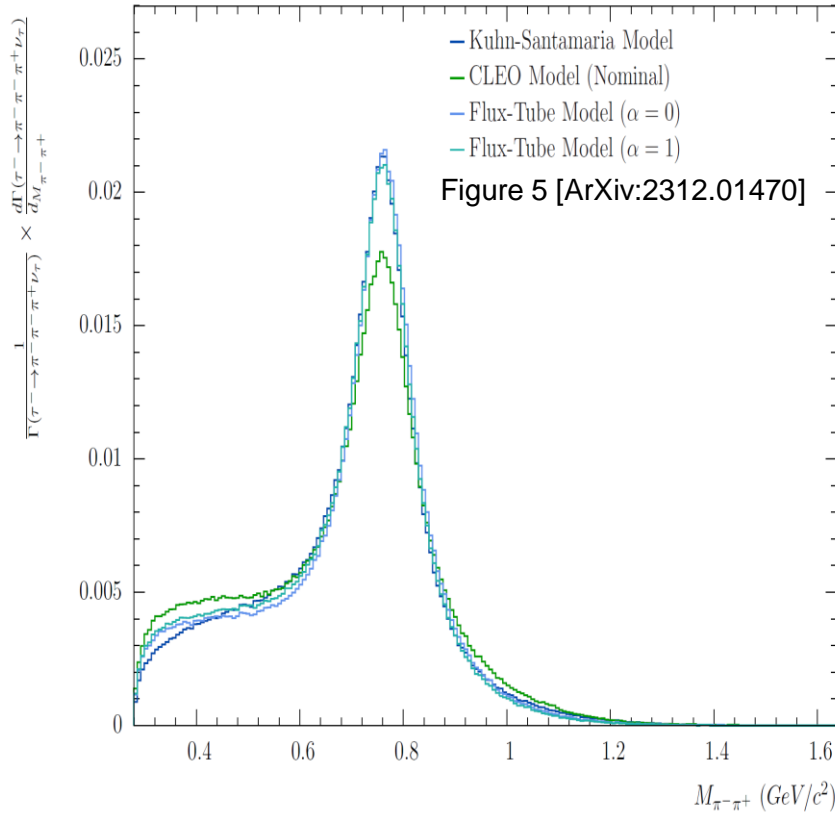
The residual QCD potential also plays a role in the evolutionary dynamics of other hadronic systems... In the S-wave decay of Axial-vector mesons, the colour hyperfine spin-spin interaction is the primary contribution to the residual QCD potential. This has a significant impact on the hadronic width, $\Gamma(s)$, of the meson and consequently, \bar{m} , and \hat{m}^2 .



This provides a possible explanation for the $a_1(1260)$ line shape observed in the BABAR data [285] which is narrower than the Flux-Tube Prediction. [Improved agreement expected after tuning.]

S-Wave, P-Wave and D-Wave in Axial-Vectors Decays

In the S-wave decay of Axial-vector mesons, the colour hyperfine spin-spin interaction is the primary contribution to the residual QCD potential. This has a significant impact on the hadronic width, $\Gamma(s)$, of the meson and consequently, \bar{m} , and \hat{m}^2 .



While also providing a possible explanation for the low mass-excess in the $\pi^+\pi^-$ line shape which has also been associated with the presence of the low mass scalars [285].

Residual QCD and Mixing of Singlet and Triplet States

In the K_1 system, the expectation of the spin-spin operator $\hat{S}_i \cdot \hat{S}_j$ differs between the singlet and triplet state. The wave-function amplitude distortions must be included in the mixing of the singlet and triplet states to construct the $K_1(1270)$ and $K_1(1400)$ states.

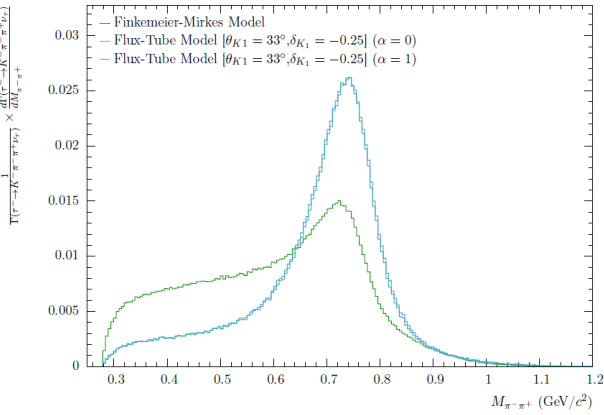
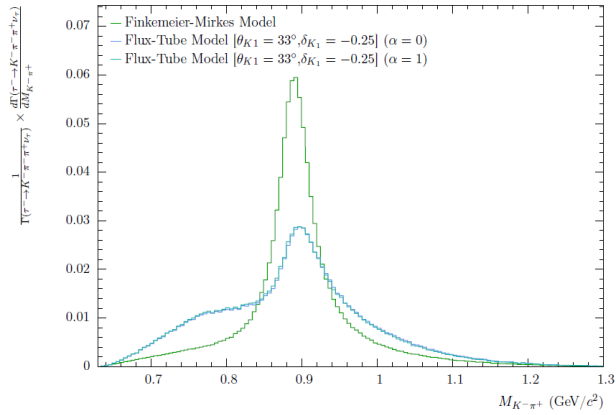
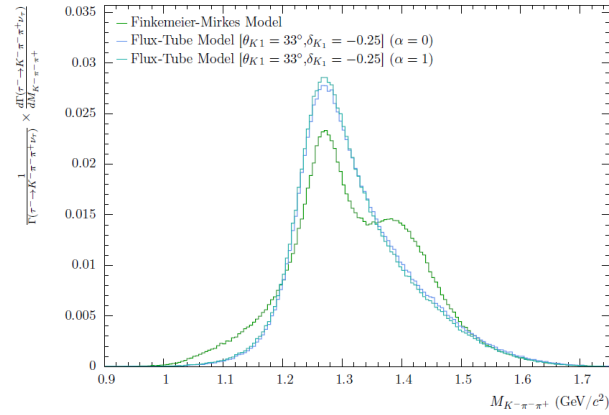
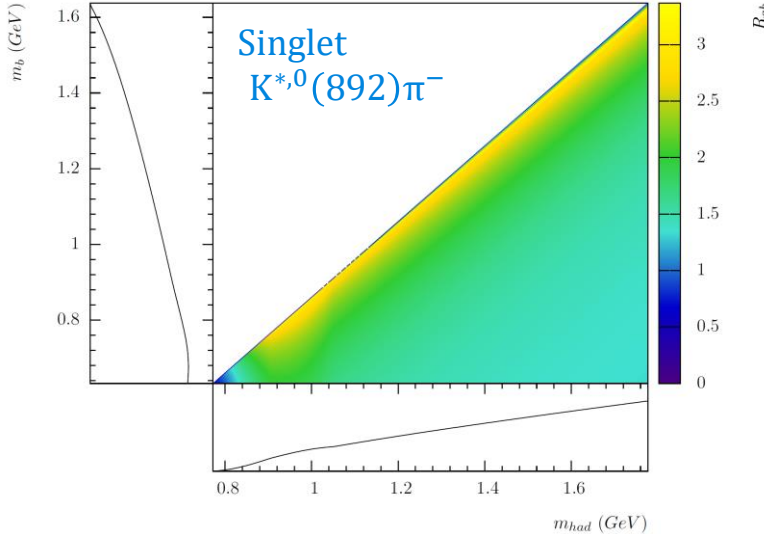
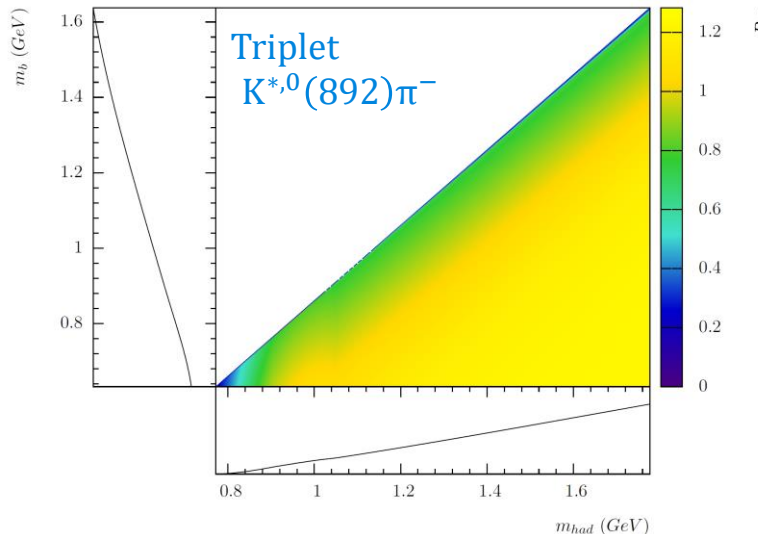


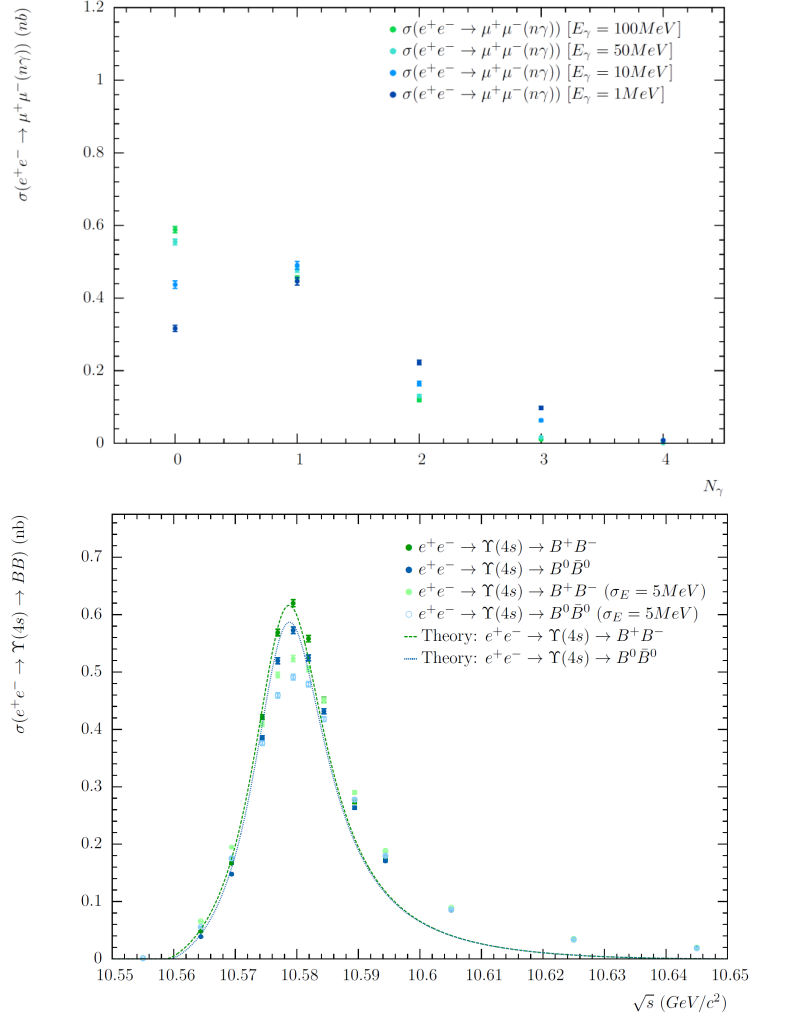
Figure 5 [ArXiv:2312.01470]



Summary

MC generators play a pivotal role in comparing theoretical predictions to experiments and in facilitating the interpretation of the experimental measurements and therefore the physics phenomena which can be probed experimentally depend on the theoretical construct and physics phenomena included in the Monte-Carlo simulation. QED calculations in $ee \in MC$ provides insight into the modelling of radiation which have implications for the interpretation of experimental measurements including g-2.

- i. Infrared safe calculations for number of γ even with selection criteria applied to the radiated photons.
- ii. Contribution from $n_\gamma = 4$, non-negligible at 10.58GeV.
- iii. Requires Higher Orders to reach the precision necessary for the Initial-State Radiation Method [29] in the low mass region $\sigma(e^+e^- \rightarrow \pi^+\pi^-(n\gamma))/\sigma(e^+e^- \rightarrow \mu^+\mu^-(n\gamma))$.
- iv. $e^+e^- \rightarrow \Upsilon(4s)(m\gamma) \rightarrow B^+B^- (n\gamma)$ to $e^+e^- \rightarrow \Upsilon(4s)(m\gamma) \rightarrow B^0\bar{B}^0 (n\gamma)$ ratio provides separation between the descriptions of the Coulomb potential in the Radiative Models
 - a. Excludes Model 1 where the Coulomb potential acts on the mesons
 - b. Excludes the Coulomb potential from explaining the low mass excess in [42] associated with scalars.
 - c. This impacts the $e^+e^- \rightarrow$ Hadrons measurements for the hadronic vacuum polarization to g-2 [38,39,40,41] which apply the Coulomb potential.



Summary

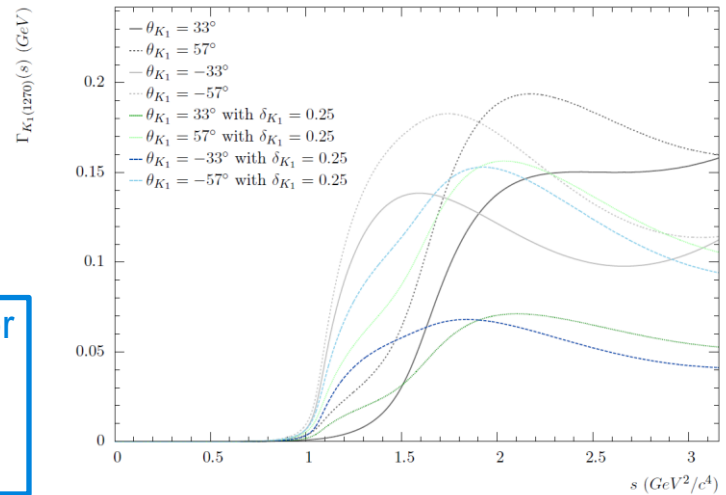
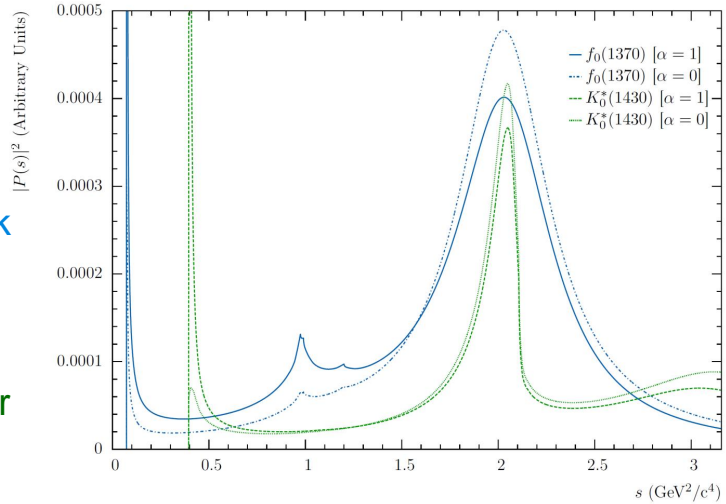
MC generators play a pivotal role in comparing theoretical predictions to experiments and in facilitating the interpretation of the experimental measurements and therefore the physics phenomena which can be probed experimentally depend on the theoretical construct and physics phenomena included in the Monte-Carlo simulation.

ee ∈ MC provides a broad range of tools for investigating the hadronic structure in τ decays

- An experimentally testable null hypothesis for Chiral-symmetry breaking being the origin of the composite-quark mass
- Extension of Flux-Tube Breaking Model to include Tetra-quark states.
- Models to investigate the singlet and triplet states and their mixing in the strange and non-strange sectors.
 - Model dependent method for a simultaneous extraction of K_1 mixing, θ_{K_1} , and $SU(3)_f$ suppression factor $\delta_{K_1} \sim \frac{m_s - m_u}{(m_s + m_u)}$, where δ_{K_1} may provide some discrimination between various quark models.
- Lepton universality, $|V_{us}|$, m_s , g-2 hadronic vacuum polarization (CVC), Michel parameters, α_s , rich hadronic structure: OZI, Wess-Zumino,....

Plan is to make the ***ee ∈ MC*** software publicly available for the e^+e^- community

⇒ However, there are still some additions and updates planned before this can be done



Thank you

References

- [1] S. Jadach, J. H. Kuhn, Z. Was, *Comput. Phys. Commun.* 64 (1990) 275–299. doi:10.1016/0010-4655(91)90038-M.
- [2] S. Jadach, Z. Was, *Comput. Phys. Commun.* 64 (1991) 267–274. doi:10.1016/0010-4655(91)90037-L.
- [3] S. Jadach, B. Ward, Z. Was, *Comput. Phys. Commun.* 130 (2000) 260–325. doi:10.1016/S0010-4655(00)00048-5.
- [4] P. Ilten, *Nuclear Phys B - Proc. Suppl.* 253-255 (2014) 77–80. doi:10.1016/j.nuclphysbps.2014.09.019.
- [5] J. C. Collins, *Nucl. Phys. B* 304 (1987) 794–804. doi:10.1016/0550-3213(88)90654-2.
- [6] I. G. Knowles, *Comput. Phys. Commun.* 58 (1990) 271–284. doi:10.1016/0010-4655(90)90063-7.
- [7] P. Richardson, *JHEP* 2001 (11) (2001) 029–029. doi:10.1088/1126-6708/2001/11/029.
- [8] ALEPH Collaboration, DELPHI Collaboration, L3 Collaboration, OPAL Collaboration, SLD Collaboration, LEP Electroweak Working Group, SLD Electroweak, *Physics Reports* 427 (5)(2006) 257–454. doi:10.1016/j.physrep.2005.12.006.
- [9] A. Stahl, *Springer Tracts Mod. Phys.* 160 (2000) 1–316. doi:10.1007/BFb0109630.
- [10] E. Braaten, S. Narison, A. Pich, *Nucl. Phys. B* 373 (1991) 581–612. doi:10.1016/0550-3213(92)90267-F.
- [11] M. Davier, S. Descotes-Genon, A. Hocker, B. Malaescu, Z. Zhang, *Eur. Phys. J. C* 55 (2008) 305–322. doi:10.1140/epjc/s10052-008-0666-7.
- [12] G. Aad, et al., *Phys. Lett. B* 805 (2020) 135426. doi:10.1016/j.physletb.2020.135426.
- [13] A. Sirunyan, el al., *Phys Rev. D* 100 (2019) 112002 doi:10.1103/PhysRevD.100.112002.
- [14] Z. Czyczula, T. Prezedzi'nski, Z. Was, *Euro. Phys. J. C* (4) (2012). doi:10.1140/epjc/s10052-012-1988-z.
- [15] S. Binner, J. H. Kuhn, K. Melnikov, *Phys. Lett.* B459 (1999) 279–287. doi:10.1016/S0370-2693(99)00658-9.
- [16] H. Czyz, J. H. Kuhn, *Eur. Phys. J. C* 18 (2001) 497–509. doi:10.1007/s100520000553.
- [17] F. Jegerlehner, *Springer Tracts in Modern Physics* 226, Heidelberg, Germany, 2007.
- [18] J. Lees, et al., *Phys. Rev. D* 86 (2012) 032013. doi:10.1103/PhysRevD.86.032013.
- [19] D. Babusci, et al., *Phys. Lett. B* 720 (4-5) (2013) 336–343. doi:10.1016/j.physletb.2013.02.029.
- [20] F. Campanario, H. Czyz, J. Gluza, M. Gunia, T. Riemann, G. Rodrigo, *JHEP* 02 (2014) 114. doi:10.1007/JHEP02(2014)114.
- [21] M. Ablikim, et al., *Phys. Lett. B* 753 (2016) 629–638. doi:10.1016/j.physletb.2015.11.043.
- [22] D. Davier, A. Hocker, M. Bogdan, Z. Zhang, *Eur. Phys. J. C* 77 (12) (2017) 827. doi:10.1140/epjc/s10052-017-5161-6.
- [23] R. Alemanu, M. Davier, A. Hocker, *Eur. Phys. J. C* 2 (1998) 123. doi:10.1007/s100520050127.
- [24] M. Davier, A. Hocker, *Phys. Lett. B* 419 (1998) 419–431. doi:10.1016/S0370-2693(97)01512-8.
- [25] M. Davier, S. Eidelman, A. Hocker, Z. Zhang, *Eur. Phys. J. C* 27 (2003) 497–521. doi:10.1140/epjc/s2003-01136-2.
- [26] M. Nenayoun, P. David, L. DelBuono, F. Jegerlehner, Z. Was, *Eur. Phys.J. C* 75 (12) (2015) 613. doi:10.1140/epjc/s10052-015-3830-x.
- [27] G. Lopez Castro, P. Roig, G. Toledo, Sanchez, *Nucl. Part. B Proc. Supp.* 260 (2015) 70–74. doi:10.1016/j.nuclphysbps.2015.02.014.
- [28] A. Pich, *Precision Tau Physics*, *Prog. Part. Nucl. Phys.* (2014) 41–85doi:10.1016/j.ppnp.2013.11.002.
- [29] M. Bruno, T. Izubuchi, C. Lehner, A. Meyer, *POS LATTICE2018* (2018) 135.doi:10.22323/1.334.0135.
- [30] J. A. Miranda, P. Roig, *Phys. Rev. D* 102 (2020) 114017. doi:10.1103/PhysRevD.102.114017.
- [31] T. Aoyama, et al., *Phys. Rept.* 887 (2020) 1–166. doi:10.1016/j.physrep.2020.07.006.
- [32] K. Maltman, J. Kambor, *Phys. Rev. D* 64 (9) (2001) 093014. doi:10.1103/PhysRevD.64.093014.
- [33] N. Isgur, C. Morningstar, C. Reader, *Phys. Rev. D* 39 (1989) 1357. doi:10.1103/PhysRevD.39.1357.
- [34] M. Suzuki, *Phys. Rev. D* 42 (1993) 1252–1255. doi:10.1103/PhysRevD.47.1252.
- [35] D. Asner, et al., *Phys. Rev. D* 62 (2000) 072006. doi:10.1103/PhysRevD.62.072006.
- [36] M. Alexeev, et al(2020). arXiv:2006.05342.
- [37] C. Adolph, et al., *Phys. Rev. Lett.* 115 (2015) 082001. doi:10.1103/PhysRevLett.115.082001.
- [38] D. M. Asner, et al., *Phys. Rev. D* 61 (1999) 012002. doi:10.1103/PhysRevD.61.012002.
- [39] K. Edwards, et al., *Phys. Rev. D* 61 (2000) 072003. doi:10.1103/PhysRevD.61.072003.
- [40] A. Bondar, S. Eidelman, A. Milstein, T. Pierzchała, N. Root, Z. Was, M. Worek, *Computer Physics Communications* 146 (2) (2002) 139 – 153. doi:10.1016/S0010-4655(02)00262-X.
- [41] S. Paramesvaran, PhD dissertation, Royal Holloway, University London (2010).
- [42] I. Nugent, T. Przedzinski, P. Roig, O. Shekhovtsova, Z. Was, *Phys. rev. D* 88 (2013) 093012. doi:10.1103/PhysRevD.88.093012.
- [43] P. Zyla, et al., *Review of Particle Physics*, *Prog. Theor. and Exp. Phys.* 2020 (8), 082C01 (2020). doi:10.1093/ptep/ptaa104. URL https://pdg.lbl.gov/2020/hadronic-xsections/rpp2020-hadronicrpp_page1001.dat

References

- [44] J. Oller, E. Oset, J. Pelaez, Phys. Rev. D 59 (1999) 074001. doi:10.1103/PhysRevD.59.074001.
- [45] J. Pelaez, Mod. Phys. Lett. A 19 (39) (2004) 2879–2894. doi:10.1142/s0217732304016160.
- [46] A. Dobado, J. Pelaez, Phys. Rev. D 56 (5) (1997) 3057–3073. doi:10.1103/PhysRevD.56.3057.
- [47] J. Oller, Nucl. Phys. A 714 (1-2) (2003) 161–182. doi:10.1016/S0375-9474(02)01360-X.
- [48] N. A. Tornqvist, Euro. Phys. J. C 11 (2) (1999) 359–363. doi:10.1007/s100529900192.
- [49] M. Napsuciale, S. Rodriguez, Phys. Lett. B 603 (3-4) (2004) 195–202. doi:10.1016/j.physletb.2004.10.018.
- [50] M. Napsuciale, S. Rodriguez, Phys. Rev. D 70 (9) (2004) 094043. doi:10.1103/PhysRevD.70.094043.
- [51] M. Ishida, Prog. Of Theor. Phys. 101 (3) (1999) 661–669. doi:10.1143/ptp.101.661.
- [52] M. Scadron, Euro. Phys. J. C 6 (1) (1999) 141–145. doi:10.1007/s100520050327.
- [53] A. Fariborz, J. Schechter, S. Zarepour, S. Zebarjad, Phys. Rev. D 90 (2014) 033009. doi:10.1103/PhysRevD.90.033009.
- [54] D. Black, A. Fariborz, F. Sannino, J. Schechter, Phys. Rev. D 59 (7). doi:10.1103/PhysRevD.59.074026.
- [55] M. Gell-Mann, M. Levy, Il Nuovo Cimento 16 (1960) 705–726. doi:10.1007/BF02859738.
- [56] T. H. R. Skyrme, A non-linear field theory, Proc. Roy. Soc. Lond. A 260 127–138. doi:10.1098/rspa.1961.0018.
- [57] T. H. R. Skyrme, Nucl. Phys. 31 (1962) 556–569. doi:10.1016/0029-5582(62)90775-7.
- [58] J. M. Speight, Phys. Lett. B 781 (2018) 455–458. doi:10.1016/j.physletb.2018.04.026.
- [59] Y. Nambu, G. Jona-Lasinio, Phys. Rev. 122 (1961) 345–358. doi:10.1103/PhysRev.122.345.
- [60] S. Godfrey, N. Isgur, Phys. Rev. D 32 (1985) 189–231. doi:10.1103/PhysRevD.32.189.
- [61] R. Kokoski, N. Isgur, Phys. Rev. D 35 (1987) 907. doi:10.1103/PhysRevD.35.907.
- [62] A. N. Mitra, Phys. Rev. 142 (1966) 1119–1125. doi:10.1103/PhysRev.142.1119.
- [63] S. Capstick, W. Roberts, Prog. Part. Nucl. Phys. 45 (2000) S241–S331. doi:10.1016/S0146-6410(00)00109-5.
- [64] A. Chodos, R. L. Jae, K. Johnson, C. B. Thors, V. F. Weisskopf, Phys. Rev. D 9 (1974) 3471–3495. doi:10.1103/PhysRevD.9.3471.
- [65] A. Chodos, R. L. Jae, K. Johnson, C. B. Thors, Phys. Rev. D 10 (1974) 2599–2604. doi:10.1103/PhysRevD.10.2599.
- [66] T. DeGrand, R. L. Jae, K. Johnson, J. Kiskis, Phys. Rev. D 12 (1975) 2060–2076. doi:10.1103/PhysRevD.12.2060.
- [67] J. Maldacena, Adv. Theor. Math. Phys. 2 (1998) 231–252. doi:10.1023/A:1026654312961.
- [68] M. Finkemeier, E. Mirkes, Z. Phys. C 69 (1996) 243–252. arXiv:hep-ph/9503474.
- [69] G. Gounaris, J. Sakurai, Phys. Rev. Lett. 21 (1968) 244–247. doi:10.1103/PhysRevLett.21.244.
- [70] J. H. Kuhn, A. Santamaria, Z. Phys. C 48 (1990) 445–452. doi:10.1007/BF01572024.
- [71] N. A. Tornqvist, Z. Phys. J. C 11 (2) (1987) 641–648. doi:10.1007/BF01630606.
- [72] G. Lopez Castro, G. Toledo Sanchez, J. Phys. G 27 (2001) 2203–2210. doi:10.1088/0954-3899/27/11/301.
- [73] A. Flores-Tlalpa, F. Flores-Baez, G. Lopez Castro, G. Toledo Sanchez, Phys. Rev. D 72 (2005) 113003. doi:10.1103/PhysRevD.72.113003.
- [74] F. Flores-Baez, A. Flores-Tlalpa, G. Lopez Castro, G. Toledo Sanchez, Phys. Rev. D 74 (2006) 071301. doi:10.1103/PhysRevD.74.071301.
- [75] A. Flores-Tlalpa, F. Flores-Baez, G. Lopez Castro, G. Toledo Sanchez, Nucl. Phys. B - Proc. Suppl. 169 (2007) 250–254. doi:10.1016/j.nuclphysbps.2007.03.011.
- [76] J. Lees, et al., Phys. Rev. D 92 (7) (2015) 072015. doi:10.1103/PhysRevD.92.072015.
- [77] T. Abe, et al., (2010). arXiv:1011.0352.
- [78] E. Kou, other, Progress of Theoretical and Experimental Physics 2019 (12) (2019). doi:10.1093/ptep/ptz106.
- [79] M. Matsumoto, T. Nishimura, ACM Trans. Model. Comput. Simul. 8 (1998) 3–30. doi:10.1145/272991.272995.
- [80] T. Nishimura, ACM Trans. Model. Comput. Simul. 10 (2000) 348–357. doi:10.1145/369534.369540.
- [81] S. Harase, T. Kimoto, ACM Trans. on Mathematical Software 44 (2018) 1–11. doi:10.1145/3159444.
- [82] S. Vigna, arXiv:1402.6246.
- [83] D. E. Knuth, Addison-Wesley, Reading, USA, 1981.
- [84] E. Byckling, K. Kajantie, Nucl. Phys. B 9 (1969) 568–576. doi:10.1016/0550-3213(69)90271-5.
- [85] D. Gamanian, H. F. Lopes, Chapman & Hall/CRC Taylor & Francis Group, 2006.
- [86] A. Gelman, J. B. Carlin, H. S. Stern, D. B. Dunson, A. Vehtari, D. B. Rubin, CRC Press Taylor & Francis Group, 2014.
- [87] S. Jadach, Z. Was, R. Decker, J. H. Kuhn, Comput. Phys. Commun. 76 (1993) 361–380. doi:10.1016/0010-4655(93)90061-G.
- [88] F. Mandl, G. Shaw, John Wiley & Sons, Great Britain, 1985.

References

- [89] M. E. Peskin, D. V. Schroeder, Addison-Wesley, Reading, USA, 1995.
- [90] F. Halzen, A. D. Martin, John Wiley & Sons, USA, 1984.
- [91] L. Ryder, Cambridge University Press, New York, USA, 1996.
- [92] A. M. Steane, (12 2013). arXiv:1312.3824.
- [93] T. Dray, C. Manogue, World Scientific Co. Pte. Ltd., Singapore, 2015.
- [94] B. Smith, M. Voloshin, Phys. Lett. B 324 (1) (1994) 117–120. doi:10.1016/0370-2693(94)00095-6.
- [95] J.D. Walecka. World Scientific Co. Pte. Ltd., Singapore, 2013. ISBN:978-9814436-89-2.
- [96] Christian Sturm. Nuclear Physics B, 874(3):698{719, Sep 2013. ISSN 0550-3213. doi:10.1016/j.nuclphysb.2013.06.009.
- [97] M. Tanabashi et al. Review of Particle Physics. Phys. Rev.D, 98:030001, Aug 2018. doi:10.1103/PhysRevD.98.030001.
- [98] S. Actis et al. Euro. Phys. J. C, 66(3-4):585{686, 2010. doi:10.1140/epjc/s10052-010-1251-4.
- [99] F. Bloch and A. Nordsieck, Phys. Rev., 52:54, 1937. doi: 10.1103/Phys-Rev.52.54.
- [100] D. R. Yennie, S. C. Frautschi, and H. Suura. Annals of Physics, 13:379{452, 1961. doi: 10.1016/0003-4916(61)90151-8.
- [101] J. Schwinger. Particle, Sources, and Fields Volumes I-III. Perseus Books Publishing, L.L.C., Reading, Massachusetts, USA, 1998.
- [102] B. Banerjee, S. Pietryk, J.M. Roney, and Z. Was, Phys. Rev. D, 77(5), 2008. doi:10.1103/physrevd.77.054012.
- [103] G. Balossini, C. Bignamini, C. M. Carloni Calame, G. J. C, 22:423{430, 2001. doi: 10.1007/s100520100818. Montagna,
- O. Nicrosini, and F. Piccinini, Nucl. Phys. B, 758(1-2):227{253, 2006. doi: 10.1016/j.nuclphysb.2006.09.022.
- [104] M. Cao et al. Z Physics at LEP1, volume 1. A. Altarelli and R. Kleiss, C. Verzegnassi eds., CERN Report 89-08, CERN, Geneva, Switzerland, 1989.
- [105] J.P. Lees et al., Nucl. Phys. Meth. A, 726:203{213, 2013. doi: 10.1016/j.nima.2013.04.029.
- [106] F. Abudinen et al., Chin. Phys. C, 44(2):021001, 2020. doi: 10.1088/1674-1137/44/2/021001.
- [107] B. Aubert et al., Phys. Rev. D, 69(1):011103, 2004. doi: 10.1103/Phys-RevD.69.011103.
- [108] Yu.M. Bystritskiy, E.A. Kuraev, G.V. Fedotovich, and F.V. Ignatov, Phys. Rev. D, 72:114019, 2005. doi:
- [109] B. Aubert and et al., Phys. Rev. Lett., 103:231801, 2009. doi:10.1103/PhysRevLett.103.231801.
- [110] G. Balossini, C. Bignamini, C. M. Carloni Calame, G. Montagna, O. Nicrosini, and F. Piccinini, Phys. Lett. B, 663(3):209{213, 2008. doi:10.1016/j.physletb.2008.04.007.
- [111] Yung-Su Tsai. Phys. Rev. D, 4:2821{2837, Nov 1971. doi:10.1103/PhysRevD.4.2821. [Erratum: Phys. Rev. D 13 (1976) 771].
- [112] P. Renton. Cambridge University Press, New York, USA, 5 1990. ISBN 978-0-521-36692-2.
- [113] J. H. Kuhn and E. Mirkes. Z. Phys. C, 56:661{672, 1992. doi: 10.1007/BF01474741. [Erratum: Z.Phys.C 67 (1995) 364].
- [114] Z. Was, In Topical Conference on the Phenomenology of Unified Field Theories from Standard Model to Supersymmetries, 1984.
- [115] S. Jadach, B.L.F. Ward, and Z. Was, Eur. Phys. [116] S. Jadach, B.F.L. Ward, and Z. Was, Comput. Phys. Commun., 130:260{325, 2000. doi:10.1016/S0010-4655(00)00048-5.
- [117] S. Aoki et al., Eur. Phys. J. C, 77(2):112, 2017. doi: 10.1140/epjc/s10052-016-4509-7.
- [118] R. Decker, E. Mirkes, R. Sauer, and Z. Was, Z. Phys. C, 58:445{452, 1993. doi: 10.1007/BF01557702.
- [119] M. Feindt, Z. Phys. C, 48:681{688, 1990. doi: 10.1007/BF01614704.
- [120] A. E. Bondar, S. I. Eidelman, A. I. Milstein, and N. I. Root, Phys. Lett. B, 466(2-4):403{407, 1999. doi: 10.1016/s0370-2693(99)01081-3.
- [121] N. Isgur and J.E. Paton. Phys. Lett. B, 124:247{251, 1983. doi: 10.1016/0370-2693(83)91445-4.
- [122] N. Isgur and J.E. Paton. Phys Rev D., 31:2910, 1984. doi: 10.1103/Phys-RevD.31.2910.
- [123] S. Anderson et al., Phys. Rev. D, 61:112002, 2000. doi: 10.1103/Phys-RevD.61.112002.
- [124] J.M. Blatt and V.F. Weisskopf, John Wiley & Sons, USA, 1952.
- [125] Bernard Aubert et al., Phys. Rev. Lett., 100:011801, 2008. doi:10.1103/PhysRevLett.100.011801.
- [126] M. J. Lee et al. Phys. Rev. D. 81, page 113007, 2010. doi: 10.1103/PhysRevD.81.113007.
- [127] Markus Finckemeier and Erwin Mirkes, Phys. C, 72(4):619{626, 1996. doi:10.1007/s002880050284.
- [128] J. H. Kuhn and Z.Was. Acta Phys. Polon. B, 39:147{158}, 2008.
- [129] H. Georgi. Dover Publications INC, USA, 2009. ISBN 978-0-486-46904-1.
- [130] Bernhard Ketzer, Boris Grube, and Dmitry Ryabchikov. Prog. in Part. and Nuc. Phys., 113:103755, 2019. doi: 10.1016/j.ppnp.2020.103755.
- [131] J.H. Kuhn and F. Wagner. Nucl. Phys. B, 236(1):16-34, 1984. doi: 10.1016/0550-3213(84)90522-4.

References

- [132] A.N. Diddens, H. Pilkuhn, and K. Schlupmann. Landolt-Bornstein vol. 6, 1972.
- [133] M. G. Bowler. Phys. Lett. B, 182:400{404, 1986. doi: 10.1016/0370-2693(86)90116-4.
- [134] H. G. Bludell, S. Godfrey, and B. Phelps. Phys. Rev. D, 53:3712-3722, 1996. doi:10.1103/PhysRevD.53.3712.
- [135] H. Albrecht et al. Phys. Lett. B, 185:223, 1987. doi: 10.1016/0370-2693(87)91559-0.
- [136] R. Decker and E. Mirkes. Z. Phys. C, 57:495{500, 1993. doi:10.1007/BF01474344.
- [137] A. Abele et al., Eur. Phys. J. C, 21:261{269, 2001. doi:10.1007/s100520100735.
- [138] G. Zweig. Version 2. CERN Report N0 8419 TH 412, 1964.
- [139] S. Okubo. Phys. Lett., 5:165-168, 1963. doi: 10.1016/S0375-9601(63)92548-9.
- [140] J. Iizuka. Prog. Theor. Phys. Suppl., 37-38:21-34, 1966. doi:10.1143/PTPS.37.21.
- [141] M. Ablikim et al. Phys. Rev. D, 98(7):072005, 2018. doi:10.1103/physrevd.98.00772005.
- [142] David J. Griffiths. John Wiley & Sons, USA, 1987.
- [143] M. Schmidtler, Nucl. Phys. B – Proc. Suppl. 76, 271-282, 1999.
- [144] N. A. Tornqvist, Z. Phys. C, 68:647-660, 1995. doi: 10.1007/BF01565264.
- [145] N.A. Tornqvist, Z. Phys. C, 68(4):647{660, 1995. doi: 10.1007/bf01565264.
- [146] E. Van Beveren and G. Rupp. Eur. Phys. J. C, 22:493-501, 2001. doi: 10.1007/s100520100823.
- [147] M. Boglione and M.R. Pennington, Phys. Rev. D, 65(11):114010, 2002. doi:10.1103/PhysRevD.65.114010.
- [148] M. Alford and R.L. Jae. Nucl. Phys. B, 578(1-2):367-161{172, 2002. doi: 10.1016/S0370-2693(02)01168-1. 382, 2000. doi: 10.1016/s0550-3213(00)00155-3.
- [149] L. Maiani, F. Piccinini, A.D. Polosa, and V. Riquer. Phys. Rev. Lett., 93(21):212002, 2004. doi: 10.1103/PhysRevLett.93.212002.
- [150] G 't Hooft, G Isidori, L. Maiani, A.D. Polosa, and V. Riquer, Phys. Lett. B, 662(5):424{430, 2008. doi: 10.1016/j.physletb.2008.03.036.
- [151] S. Weinberg, Phys. Rev., 130:667-782, 1963. doi: 10.1103/PhysRev.130.776.
- [152] Y. S. Kalashnikova, A.E. Kudryavtsev, A. V. Nefediev, C. Hanhart, and J. Haidenbauer, Eur. Phys. J. A, 24(3):437{443, 2005. doi: 10.1140/epja/i2005-10008-4.
- [153] L.D. Landau. Nucl. Phys., 13(1):181{192, 1959. doi: 255:38-41, 2014. doi:10.1016/0029-5582(59)90154-3.
- [154] L.R. Dai, Q.X. Yu, and E. Oset. Phys. Rev. D, 99(1):016021, 2019. doi:10.1103/physrevd.99.016021.
- [155] A. Pich, Phys. Lett. B, 196(4):561-565, 1987. doi: 10.1016/0370-2693(87)90821-5.
- [156] Xiangdong Ji, Phys. Rev. Lett., 74:1071{1074, 1995. doi:10.1103/PhysRevLett.74.1071.
- [157] Xiangdong Ji, Phys. Rev. D, 52(1):271{281, 1995. doi: 10.1103/physrevd.52.271.
- [158] J. P. Chen, H. Gao, T. K. Hemmerick, Z. E. Meziani, and P. A. Souder. A White Paper on SoLID (Solenoidal Intensity Device). 2014.
- [159] M Davier, S. Eidelman, A. Hocker, and Z. Zhang, Eur. Phys. J. C, 27:497-521, 2003. doi:10.1140/epjc/s2003-01136-2.
- [160] M Davier, S. Eidelman, A. Hocker, and Z. Zhang, Eur. Phys. J. C, 31:503-510, 2003. doi: 10.1140/epjc/s2003-01362-6.
- [161] A. Aloisio et al., Phys. Lett. B, 606:12-24, 2005. doi:10.1016/j.physletb.2004.11.068.
- [162] R. R. Akhmetshin et al., Phys. Lett. B, 527: 384, 2006. doi: 10.1134/S106377610609007X.
- [163] M. N. Achasov et al., J. Exp. Theor. Phys., 103:380{384, 2006. doi: 10.1134/S106377610609007X.
- [164] D. G. Dumm and P. Roig, Eur. Phys. J. C, 73(8):2528, 2013. doi: 10.1140/epjc/s10052-013-2528-1.
- [165] M. Fukjikawa et al, Phys. Rev. D, 78(7):072006, 2008. doi: 10.1103/PhysRevD.78.072006.
- [166] S. Gonzalez-Sols. EPJ Web Conf., 212:08003, 2019. doi: 10.1051/epjconf/201921208003.
- [167] P. Gonzalez-Sols, S. an d Roig, Eur. Phys. J. C, 79(5):436, 2019. doi: 10.1140/epjc/s10052-019-6943-9.
- [168] I.M. Nugent, Nucl. Phys. B - Proc. Suppl., 253-255:38-41, 2014. doi:10.1016/j.nuclphysbps.2014.09.010.
- [169] O. Shekhovtsova, T. Przedzinski, P. Roig, and Z. Was, Phys. Rev. D, 86(11):113008, 2012. doi: 10.1103/PhysRevD.86.113008.
- [170] K. Ackersta et al., Z. Phys. C, 75:593-605, 1997. doi: 10.1007/s002880050505.
- [171] H Albrecht et al., Phys. Lett. B, 349:576{584, 1995. doi: 10.1016/0370-2693(95)00281-0.
- [172] P. Abreu et al., Phys. Lett. B, 326:411{427, 1998. doi:10.1016/S0370-2693(98)00347-5.
- [173] M. Wagner. PhD dissertation, Institut Fur Theoretische Physik, Justus-Liebig-Universitat Gieen, 2007.
- [174] G. Lopez Castro and J.H. Munoz. Phys. Rev. D, 83:094016, 2011. doi:10.1103/PhysRevD.83.094016.
- [175] S. Jadach and Z. Was, Acta Phys. Polon. B, 15:1151, 1984. [Erratum: Acta Phys. Polon. B 16 (1985) 483].
- [176] J. Lamour. LXIII. Philosophical Magazine, 544(271):503-512, 1897.
- [177] C. M. Carloni Calame, G. Montagna, O. Nicrosini, and F. Piccinini, Nucl. Phys. B - Proc. Suppl., 131:48{55, 2004. doi:10.1016/j.nuclphysbps.2004.02.008.

References

- [178] C. M. Carloni Calame, Phys. Lett. B, 520(1-2):16-24. doi: 10.1016/s0370-2693(01)01108-X.
- [179] C. M. Carloni Calame, C. Lunardini, G. Montagna, O. Nicrosini, and F. Piccinini, Nucl. Phys. B, 584(1-2):459-479. doi: 10.1016/s0550-3213(00)00356-4.
- [180] W. J. Marciano and A Sirlin, Phys. Rev. Lett., 61:1815-1-818, 1988. doi:10.1103/PhysRevLett.61.1815.
- [181] E. Braaten and C. S. Li, Phys. Rev D, 42:3888-3891. doi: 10.1103/PhysRevD.42.3888.
- [182] J. Erler, Rev. Mex. Fis., 50:200-202, 2004.
- [183] L. Michel, Proc. Phys. Soc. A, 63:514-531, 1950. doi: 10.1088/0370-1298/63/5/311.
- [184] C. Bouchiat and L. Michel, Phys. Rev., 106:170{172, 1957. doi: 10.1103/PhysRev.106.170.
- [185] W. Bacino et al., Phys. Rev. Lett., 42:749, 1979. doi: 10.1103/PhysRevLett.42.749.
- [186] S Behrends et al., Phys. Rev. D, 32:2468{2470, 1985. doi:10.1103/PhysRevD.32.2468.
- [187] W. T. Ford et al., Phys. Rev. D, 37:1971-1982, 1987. doi: 10.1103/PhysRevD.36.1971.
- [188] H. Janssen et al., Phys. Lett. B, 228:273{280, 1989. UK, 1982. doi: 10.1016/0370-2693(89)90670-9.
- [189] H Albrecht et al., Phys. Lett. B, 246:278{284, 1990. doi: 10.1016/0370-2693(90)91346-D.
- [190] H Albrecht et al., Phys. Lett. B, 316:608{614, 1993. doi: 10.1016/0370-2693(93)91051-N.
- [191] H Albrecht et al., Phys. Lett. B, 341:441{447, 1995. doi:10.1016/0370-2693(94)01386-Q.
- [192] H. Albrecht et al., Phys Lett. B, 431:179-187, 1998. doi: 10.1016/S0370-2693(98)00565-6.
- [193] K. Abe et al., Phys. Rev. Lett., 78:4691-4696, 1997. doi:10.1103/PhysRevLett.78.4691.
- [194] J. P Alexander et al., Phys. Rev. D, 56:5320{5329, 1997. doi: 10.1103/PhysRevD.56.5320.
- [195] K. Ackersta et al., Eur. Phys. J. C, 8:3{21, 1999. doi: 10.1007/s100529901080.
- [196] P. Seager., Nucl. Phys B. - Proc. Suppl., 76:141-146, 1999. doi:10.1016/S0920-5632(99)00446-6.
- [197] M. Wunsch, Nucl. Phys B. - Proc. Suppl., 76:159-164, 1999. doi: 10.1016/S0920-5632(99)00452-1.
- [198] B Oberhof, Nucl. Phys B. - Proc. Suppl., 260:12{15, 2015. doi:10.1016/j.nuclphysbps.2015.02.003.
- [199] A. Abdesselam, Nucl. Phys B. - Proc. Suppl., 287:11-14, 2017. doi:10.1016/j.nuclphysbps.2017.03.034.
- [200] D. A. Epifanov, Nucl. Phys B. - Proc. Suppl., 287:7{10, 2017. doi: 10.1016/j.nuclphysbps.2017.03.033.
- [201] Thomas Williams, Colin Kelley, et al. Gnuplot 4.2: An Interactive Plotting Program. <http://gnuplot.sourceforge.net/>, 2007.
- [202] M. Abramowitz and I. A. Stegun. Dover Publications Inc., New York, USA, 1964.
- [203] Wen Shen. World Scientific, 2016.
- [204] P. E. Gill, W. Murray, and M. H. Wright, Emerald,
- [205] P. Nyborg. Il Nuovo Cimento, LXV A(3):544, 1970.
- [206] O. Gituliar, V. Magerya, and A. Pikelner, PoS, LL2018:87, 2018. doi:10.22323/1.303.0087.
- [207] A. Jonquiere, Versigt af Kongl. Vetenskaps-Akademiens Forhandlingar, 46:257-268, 1888.
- [208] G. N. Watson, Quart. J. Math. Oxford Ser., 8:39-42, 1937. doi:10.1093/qmath/os-8.1.39.
- [209] L. Lewis. MR-0105524, 1958.
- [210] R. Morris. Mathematics of Computation, 33(146):778-787, 1979. doi:10.2307/2006312.
- [211] A. N. Kirillov. Prog. Theor. Phys. Suppl., 118:61-142, 1995. doi: 10.1143/ptps.118.61.
- [212] T. T. Pierzcha la, E. Richter-Was, Z. Was, and M. Worek, Acta Phys. Polon. 32, 1277-1296, 2001.
- [213] M. Finkemeier, 1997 hep-ph/9706465.
- [214] J. Wess and B. Zumino, Phys. Lett. B, 37:95{97, 1971. doi: 10.1016/0370-2693(71)90582-X.
- [215] J. F. Donoghue, E. Golowich, and B. R. Holstein. Cambridge University Press, New York, USA, 1996 (Reprint)
- [216] A. Le Yaouanc, L. Oliver, O Pene, and J.C. Raynal. Phys. Rev. D, 8:2223, 1973. doi:10.1103/PhysRevD.8.2223.
- [217] A. Le Yaouanc, L. Oliver, O Pene, and J.C. Raynal. Phys. Lett. B, 71:397, 1977. doi: 10.1016/0370-2693(77)90250-7.
- [218] S. Ono, Phys. Rev. D, 23:1118, 1981. doi: 10.1103/Phys-RevD.23.1118.
- [219] J.P Lee et al., Phys. Rev. D, 72:032005, 2005. doi: 10.1103/PhysRevD.72.032005.
- [220] H. Albrecht et al., Z. Phys. C, 65:619, 1995. doi: 10.1007/BF01578670.
- [221] J.P Lee et al., Phys. Rev. D, 92:072015, 2015. doi: 10.1103/PhysRevD.92.072015.
- [222] S. abd Zallo A. Baldini Ferroli, R.and Pacetti, Eur. Phys. J. A, 48:33,2012. doi: 10.1140/epja/i2021-12033-6.
- [223] S. Actis et al., Euro. Phys. J. C, 66(3-4):585-686, 2010. doi: 10.1140/epjc/s10052-010-1251-4.
- [224] J.P. Lees et al. Phys. Rev. D, 88:032013, 2013. doi: 10.1103/Phys-RevD.88.032013.
- [225] R. R. Akhmetshin et al., Phys. Lett. B, 669:217{222, 2008. doi:10.1016/j.physletb.2008.09.053.
- [226] J.P. Lees et al., Phys, Rev. D, 88(7), 2013. doi: 10.1103/physrevd.88.072009.
- [227] I.M. Nugent, T. Przedzinski, P. Roig, O. Shekhvotsova, and Z. Was. Phys. Rev. D, 88:093012, 2013. doi: 10.1103/PhysRevD.88.093012.

References

- [228] J.D. Weinstein and N. Isgur. Phys. Rev. Lett., 48:659, 1982. doi: 10.1103/PhysRevLett.48.659.
- [229] J.D. Weinstein and N. Isgur. Phys. Rev. D, 27:588, 1983. doi: 10.1103/PhysRevD.27.588.
- [230] T. Barnes, K. Dooley, and N. Isgur. Phys. Lett. B, 183: 210{214, 1987. doi: 10.1016/0370-2693(87)90440-0.
- [231] J.D. Weinstein and N. Isgur. Phys. Rev. D, 41: 2236, 1990. doi: 10.1103/PhysRevD.41.2236.
- [232] N. Isgur, K. Maltman, J.D. Weinstein, and T. Barnes. Phys. Rev. D, 64:161, 1990. doi: 10.1103/PhysRevD.64.161.
- [233] T. Barnes. Phys. Lett. B, 165:434{440, 1985. doi: 10.1016/0370-2693(85)91261-4.
- [234] P. O'Donnell, M. Frank, N. Isgur, and J.D. Weinstein, In 20th Rencontres de Moriond: QCD and Beyond, pages 497{502, 1985.
- [235] J.D. Weinstein. In Annual Meeting of the Division of Particle and Fields of the APS, page 8, 1985.
- [236] P.A. Zyla et al. Review of Particle Physics. Prog. Theor. and Exp. Phys., 2020(8), 2020. doi: 10.1093/ptep/ptaa104. URL https://pdg.lbl.gov/2020/hadronic-xsections/rpp2020-hadronicrpp_page1001.dat. 082C01.
- [237] J.A. Oller, E. Oset, and J.R. Pelaez. Phys. Rev. D, 59: 074001, 1999. doi: 10.1103/PhysRevD.59.074001.
- [238] J.R. Pelaez, Mod. Phys. Lett. A, 19(39):2879{2894, 2004. doi: 10.1142/S0217732304016160.
- [239] A. Dobado and J.R. Pelaez. Phys. Rev. D, 56(5):3057{3073, 1997. doi: 10.1103/PhysRevD.56.3057.
- [240] J.A. Oller. Nucl. Phys. A, 714(1-2):161{182, 2003. doi: 10.1016/S0375-9474(02)01360-X.
- [241] N. A. Tornqvist. Euro. Phys. J. C, 11(2):359{363, 1999. doi: 10.1007/s100529900192.
- [242] M. Napsuciale and S. Rodriguez, Phys. Lett. B, 603(3-4):195{202, 2004. doi:10.1016/j.physletb.2004.10.018.
- [243] M. Napsuciale and S. Rodriguez. Phys. Rev. D, 70(9):094043, 2004. doi:10.1103/PhysRevD.70.094043.
- [244] M. Ishida. Prog. of Theor. Phys., 101(3):661{669, 1999. doi: 10.1143/ptp.101.661.
- [245] M.D. Scadron. Euro. Phys. J. C, 6(1):141{145, 1999. doi: 10.1007/s100520050327.
- [246] A.H. Fariborz, J. Schechter, S. Zarepour, and S.M. Zebarjad. Phys. Rev. D, 90:033009, 2014. doi: 10.1103/PhysRevD.90.033009.
- [247] D. Black, A.H. Fariborz, F. Sannino, and J. Schechter. Phys. Rev. D, 59(7). doi:10.1103/PhysRevD.59.074026.
- [248] M. Gell-Mann and M. Levy. Il Nuovo Cimento, 16:705{726, 1960. doi:10.1007/BF02859738.
- [249] T. H. R. Skyrme. Proc. Roy. Soc. Lond. A, 260:127{138. doi: 10.1098/rspa.1961.0018.
- [250] T. H. R. Skyrme. A Unified Field Theory of Mesons and Baryons. Nucl. Phys., 31:556-569, 1962. doi: 10.1016/0029-5582(62)90775-7.
- [251] J. M. Speight. Phys. Lett. B, 781:455{458, 2018. doi: 10.1016/j.physletb.2018.04.026.
- [252] Y. Nambu and G. Jona-Lasinio. Phys. Rev., 122:345{358, 1961. doi: 10.1103/PhysRev.122.345.
- [253] I. M. Nugent. 2022. arXiv: 2202.02318 [hep-ph].
- [254] Richard Kokoski and Nathan Isgur. Phys. Rev. D, 35:907, 1987. doi: 10.1103/PhysRevD.35.907.
- [255] N. Isgur and J.E. Paton. Phys. Lett. B, 124:247-251, 1983. doi: 10.1016/0370-2693(83)91445-4.
- [256] N. Isgur and J.E. Paton. Phys. Rev. D, 31:2910, 1984. doi: 10.1103/PhysRevD.31.2910.
- [257] Nathan Isgur, Colin Morningstar, and Cathy Reader. Phys. Rev. D, 39:1357, 1989. doi: 10.1103/PhysRevD.39.1357.
- [258] M. Abramowitz and I. A. Stegun. Dover Publications Inc., New York, USA, 1964. ISBN 0-486-61272-4.
- [259] Wen Shen. World Scientific, 2016. ISBN 978-981-4730-06-08.
- [260] R.L. Libo. 3rd Ed. Addison-Wesely Publishing Company, Inc., 1997. Z. Phys. C, 69:243-252, 1996.
- [261] T. Barnes, N. Black, D.J. Dean, and E.S. Swanson, Phys. Rev. D, 60(2):045202. doi:10.1103/PhysRevD.60.045202.
- [262] S. Godfrey and Nathan Isgur. Phys. Rev. D, 32:189{231, 1985. doi: 10.1103/PhysRevD.32.189.
- [263] G.B. Arfken and H.J. Weber. 5th Ed. Harcourt/Academic Press, London, UK, 2001. ISBN 0-12-059825-6.
- [264] D. Scora and N. Isgur, Phys. Rev. D, 52:2783{2812, 1995. doi: 10.1103/PhysRevD.52.2783.
- [265] Mahiko Suzuki. Phys. Rev. D, 42:1252-1255, 1993. doi: 10.1103/PhysRevD.47.1252.
- [266] H.G. Bludell, S. Godfrey, and B. Phelps, Phys. Rev. D, 53:3712-3722, 1996. doi: 10.1103/PhysRevD.53.3712.
- [267] D.M. Asner et al., Phys. Rev. D, 62:072006, 2000. doi: 10.1103/PhysRevD.62.072006.
- [268] H. Sazdjian. Symmetry, 14(3):515, 2022. doi: 10.3390/sym14030515.
- [269] J.D. Walecka World Scientific, Singapore, 2008. ISBN 978-9812812247.
- [270] R.D. Woods and D.S. Saxon. Phys. Rev. D, 95:577, 1954. doi: 10.1103/PhysRevD.95.577.
- [271] L. Bergstrom, G. Hulth, and H. Snellman. Z. Phys. C, 16:263, 1983. doi: 10.1007/BF01571614.
- [272] J.R. Pelaez. Phys. Rept., 658:1, 2016. doi: 10.1016/j.physrep.2016.09.001.
- [273] B. Moussallam. Eur. Phys. J. C, 71:1814, 2011. doi: 10.1140/epjc/s10052-011-1814-z.
- [274] Y. Mao, X. Wang, O. Zhang, H.Q. Zheng, and Z.Y. Zhou. Phys. Rev. D, 79:116008, 2009. doi: 10.1103/PhysRevD.79.116008.
- [275] G.J. Gounaris and J.J. Sakurai. Phys. Rev. Lett., 21:244{247, 1968. doi: 10.1103/PhysRevLett.21.244.
- [276] J.P. Lees et al. Phys. Rev. D, 86:032013, 2012. doi: 10.1103/PhysRevD.86.032013.
- [277] I.M. Nugent, T. Przedzinski, P. Roig, O. Shekhovtsova, and Z. Was. Phys. rev. D, 88:093012, 2013. doi: 10.1103/PhysRevD.88.093012.
- [278] Bernard Aubert et al. Phys. Rev. Lett., 100:011801, 2008. doi: 10.1103/PhysRevLett.100.011801.
- [279] Thomas Williams, Colin Kelley, et al. Gnuplot 4.2: An Interactive Plotting Program. <http://gnuplot.sourceforge.net/>, 2007.
- [280] J. H. Kuhn and A. Santamaria. Z. Phys. C, 48:445-452, 1990. doi: 10.1007/BF01572024.
- [281] Markus Finkemeier and Erwin Mirkes.
- [282] T. Abe et al. Belle-II Technical Design Report, 2010.
- [283] E. Kou and other. The Belle II Physics Book. Progress of Theoretical and Experimental Physics, 2019(12), 2019. doi: 10.1093/ptep/ptz106.
- [284] D. M. Asner et al. Phys. Rev. D, 61:012002, Dec 1999. doi: 10.1103/PhysRevD.61.012002.
- [285] I.M. Nugent. Nucl. Phys. B - Proc. Suppl., 253-255:38{41, 2014. doi: 10.1016/j.nuclphysbps.2014.09.010.

Back-up Slides

Overview of Framework

The MC generator is a stand-alone object oriented C++ package containing the

i. Random Number Generators

- Mersenne Twister 32bit [79] and 64bit [80, 81]
- Marsaglia's xorshift64 and xorshift1064 generators [82]

ii. Phase-Space Generator based on the recursive mass formulation [84]

$$R_n(\sqrt{s}) = \int_{(m_1+\dots+m_n)^2}^{(\sqrt{s}-m_n)^2} dM_{n-1}^2 \int_{-1}^1 d\cos(\theta) \int_{-\pi}^{\pi} d\phi \frac{\sqrt{\lambda(s, M_{n-1}^2, m_n^2)}}{8s} \times R_{n-1}(M_{n-1}) \quad [\text{Eq. 3.84}]$$

Modified to include

- The Jacobian Normalization factors for computing the phase-space
- Embedded Importance Sampling [85,86] to optimize the simulation efficiency

iii. Physics Models

- Mathematic Routines
- Algebra, Tensor Notation & Integration
- Feynman Calculus (ie Spinor Algebra)
- QED & Electroweak Diagrams/Models
- Hadronic Physics Models

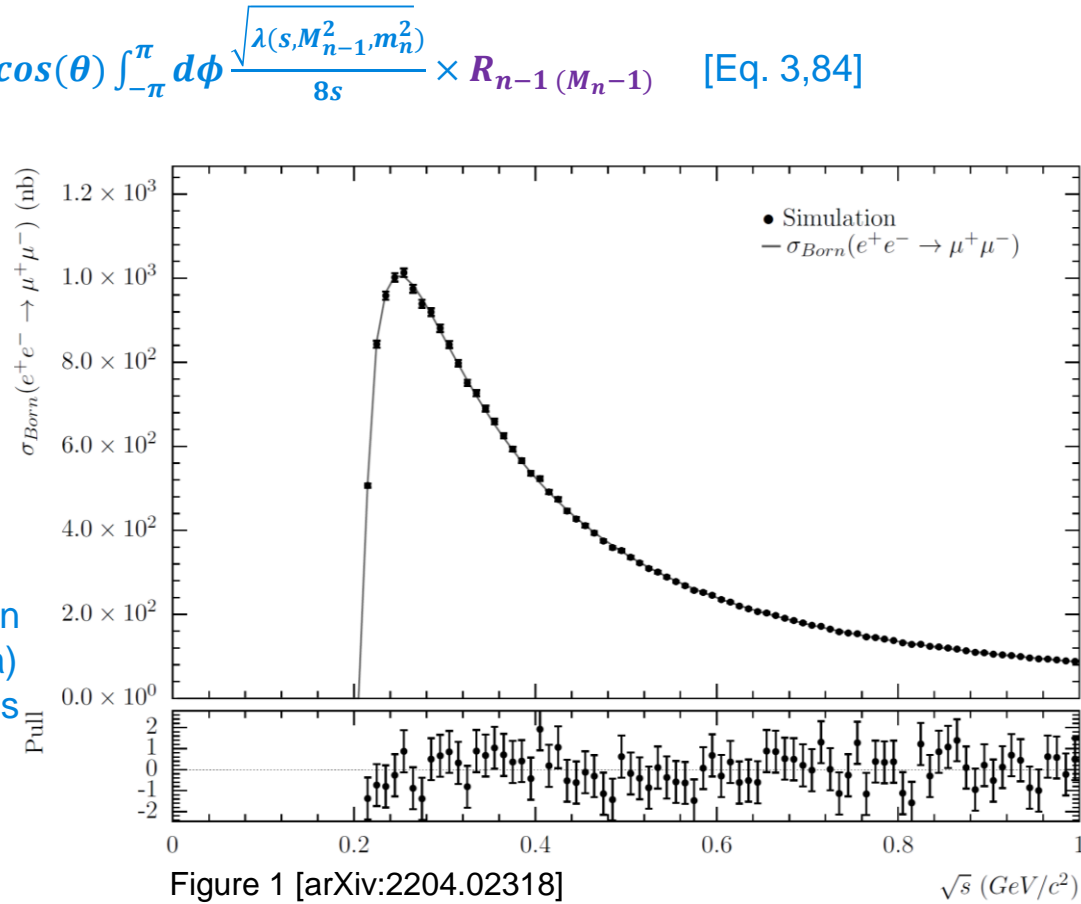


Figure 1 [arXiv:2204.02318]

Approach to QED Calculations

The cross-section is determined in terms of the **spin-averaged sum matrix element** $|\mathcal{M}_n^k|$ for n real photon emissions and k photon exchanges. The infra-red divergencies are removed through the multiplicative **Yennie-Frautschi-Suura Exponentiation procedure**, with the cut-off δM

$$d\sigma = \frac{\sum_{n=0}^{\infty} Y_i(Q_i^2) Y_f(Q_f^2) |\sum_{k=1}^{\infty} \bar{\mathcal{M}}_n^k|^2 dPS_n^{\delta M}}{4(|\vec{P}_{e^-}|E_{e^+} + |\vec{P}_{e^+}|E_{e^-})}$$

The matrix element, \mathcal{M}_n^k , is calculated directly from the individual Feynman Diagrams in terms of the Dirac Spinors, Polarization vectors, Proca propagators and γ matrices using an object orientated formalism, where all spin states are explicitly summed/averaged over.

$$\mathbf{u}(p) = \begin{pmatrix} \left[I \sqrt{\frac{E+M}{2}} - \vec{\sigma} \cdot \hat{\mathbf{P}} \sqrt{\frac{E-M}{2}} \right] \chi \\ \left[I \sqrt{\frac{E+M}{2}} + \vec{\sigma} \cdot \hat{\mathbf{P}} \sqrt{\frac{E-M}{2}} \right] \chi \end{pmatrix} \quad \chi(\uparrow) = \begin{pmatrix} \cos(\theta/2)e^{-i\phi/2} \\ \sin(\theta/2)e^{i\phi/2} \end{pmatrix}$$

$$\mathbf{v}(p) = \begin{pmatrix} \left[I \sqrt{\frac{E+M}{2}} - \vec{\sigma} \cdot \hat{\mathbf{P}} \sqrt{\frac{E-M}{2}} \right] \chi \\ -\left[I \sqrt{\frac{E+M}{2}} + \vec{\sigma} \cdot \hat{\mathbf{P}} \sqrt{\frac{E-M}{2}} \right] \chi \end{pmatrix} \quad \chi(\downarrow) = \begin{pmatrix} -\sin(\theta/2)e^{-i\phi/2} \\ \cos(\theta/2)e^{i\phi/2} \end{pmatrix}$$

Approach to QED Calculations

The cross-section is determined in terms of the **spin-averaged sum matrix element** $|\bar{\mathcal{M}}_n^k|$ for n hard-photon emissions and k photon exchanges. The infra-red subtraction are removed through the multiplicative **Yennie-Frautschi-Suura Exponentiation procedure**, with the cut-off δM

$$d\sigma = \frac{\sum_{n=0}^{\infty} Y_i(Q_i^2) Y_f(Q_f^2) |\sum_{k=1}^{\infty} \bar{\mathcal{M}}_n^k|^2 dPS_n}{4(\vec{P}_{e^-}|E_{e^+} + \vec{P}_{e^+}|E_{e^-})}$$

- Phase-space is based on the recursive mass formulation [84] modified with embedded Importance Sampling [85,86] to optimize the simulation efficiency and Jacobian Normalization factors

$$R_n(\sqrt{s}) = \int_{(m_1+\dots+m_n)^2}^{(\sqrt{s}-m_n)^2} dM_{n-1}^2 \int_{-1}^1 d\cos(\theta) \int_{-\pi}^{\pi} d\phi \frac{\sqrt{\lambda(s, M_{n-1}^2, m_n^2)}}{8s} \times R_{n-1}(M_{n-1}) \quad [\text{Eq. 3.84}]$$

- The matrix element, $\bar{\mathcal{M}}_n^k$, for n radiated hard-photons and k internal photon lines.
- $\bar{\mathcal{M}}_n^k$ is calculated directly from the individual Feynman Diagrams in terms of the Dirac Spinors, Polarization vectors, Proca propagators and γ matrices using an object orientated formalism, where all spin states are explicitly summed/averaged over.
- $Y_i(Q_i^2)$ and $Y_f(Q_f^2)$ are the multiplicative Yennie-Frautschi-Suura Exponentiation Form-Factors.

QED Simulation

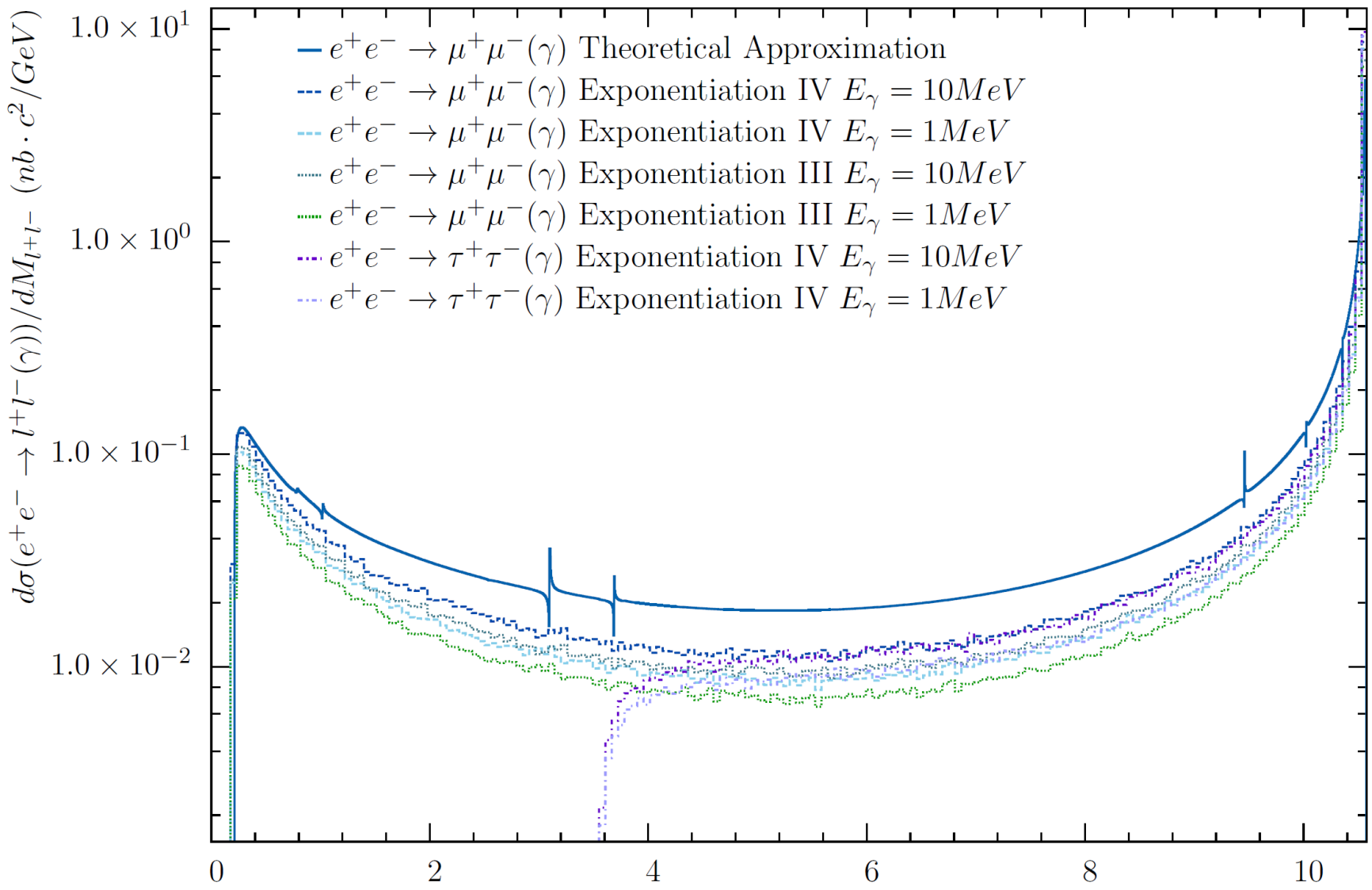


Figure 6 [arXiv:2204.02318]

YFS Exponentiation: Comparision

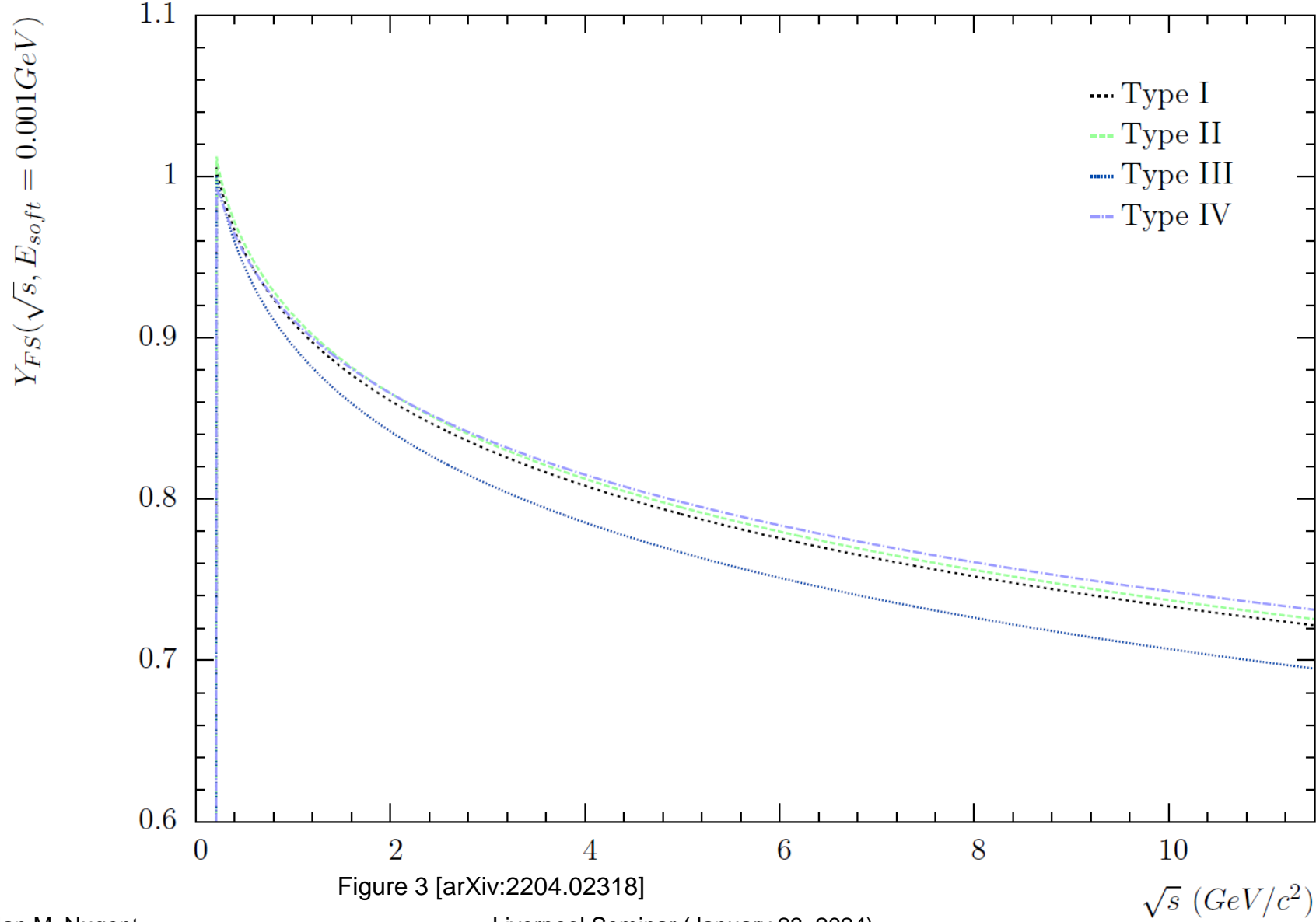


Figure 3 [arXiv:2204.02318]

Liverpool Seminar (January 23, 2024)

How Do We Use the MC Predictions?

In most physics analysis, MC is used to predict the theoretical distributions after applying the event selections criteria.

⇒ In general, this means that there are either explicit or implicit cuts on the number of photons and/or the kinematic of the photons... This applies to: basic selection cuts, kinematic fits, BDT, neural-networks,...

Feynman Fictitious Photon Mass Subtraction Method

- If these selection cuts have any bias between the selection efficient of the events with N_a and N_{a+1} photons then there will be a bias in the theoretical predictions using the Feynman Mass Method (bias from $\sum_{m=a+2}^{\infty} N_m$).
- No method to estimate the theoretical bias without comparing to an infrared safe calculation using YFS Exponentiation (ie. comparing to KK2F or eeMC).

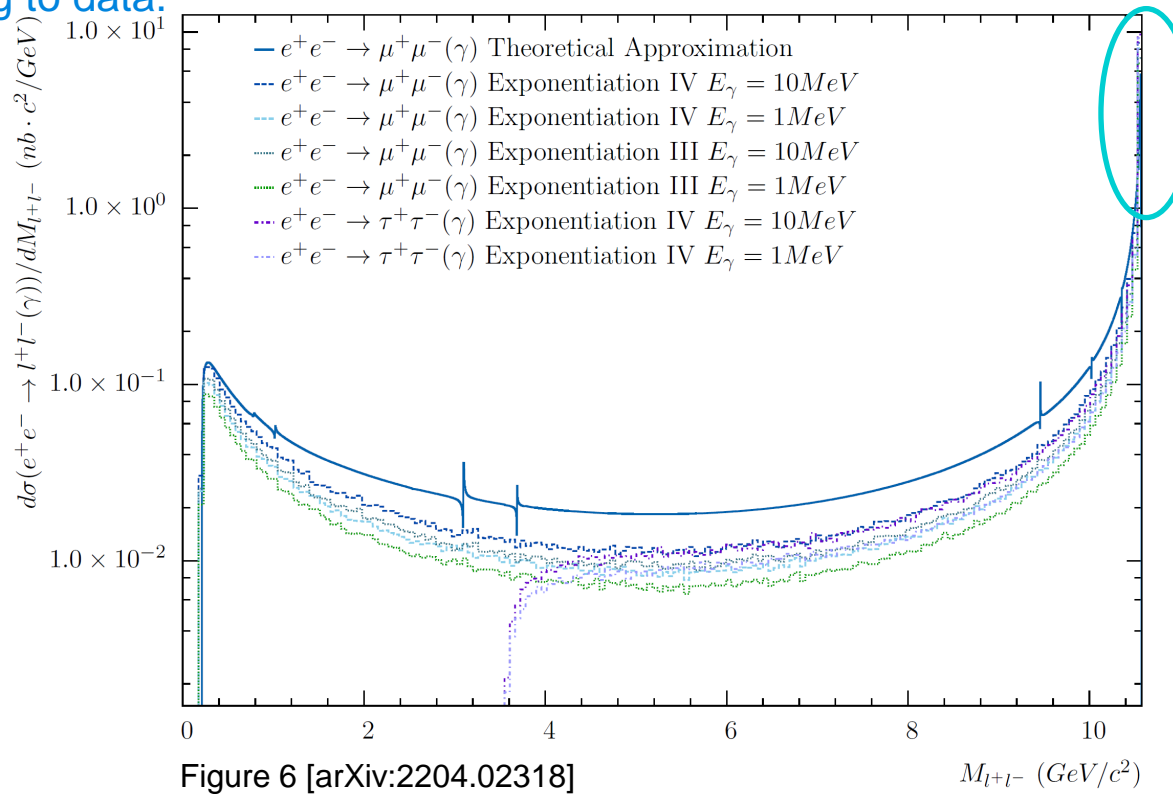
Yennie-Frautschi-Suura Exponentiation Procedure

- A theoretical uncertainty on the truncation error of the infinite perturbative Feynman series can be calculated for the given experimental observable [arXiv:2212.05388] (see paper for caveats) [after selection is applied].
- Within this uncertainty the theoretical prediction can be treated as infrared safe with or without cuts on the number of photons and their kinematics for the given observable.

Soft-Photon Cut-Off and the Mass Spectrum

An issue often overlooked in the comparison of the theoretical predictions to experimental data is the impact of the soft-photon cut-off on the mass-spectra of outgoing leptonic pair...

When applying a soft-photon cut-off, there is a discontinuity between the Born level outgoing lepton-pair mass and the lepton-pair mass from terms with LO or higher order radiative emission of hard-photons. When the experimental resolution $\sigma_M \leq \delta M$ or comparable to $\approx \delta M$ there will be a bias in the invariant mass spectrum of the outgoing leptonic pair mass near the Born level mass when comparing to data.



Approach to $e^+e^- \rightarrow Hadrons(n\gamma)$ Calculations

For a $e^+e^- \rightarrow V \rightarrow PP$ interactions the Born level matrix element may be written as

$$\mathcal{M}_a^b = (\bar{v}_2 i e \gamma^\mu u_1) \frac{g_{\mu\nu}}{q^2} i e Q_f N_c \frac{(g^{\nu\alpha} - q^\nu q^\alpha)}{P(s)} A(s) (\mathbf{p}_a - \mathbf{p}_b)_\alpha$$

Within the hadronic current formalism from which the hadronic τ decays are constructed this becomes:

$$\mathcal{M}_a^b \approx (\bar{v}_2 i e \gamma^\mu u_1) \frac{g_{\mu\nu}}{q^2} i e Q_f \times \mathbf{J}^\nu$$

Effective hadronic current

Where

$$\mathbf{J}^\nu = \mathbf{N} F(s) (g^{\nu\alpha} - q^\nu q^\alpha) (\mathbf{p}_a - \mathbf{p}_b)_\alpha$$

- $F(s)$ is the model dependent Form-Factor (Vector-Dominance, χRL , Flux-Tube Breaking, Quark-Pair-Creations Model, ...)
- $(g^{\nu\alpha} - q^\nu q^\alpha)$ is the tensor component of the spin 1 propagator
- $(\mathbf{p}_a - \mathbf{p}_b)_\alpha$ is the $V \rightarrow PP$ vertex coupling
- \mathbf{N} is the current amplitude calculated in the given hadronic model
 - Within the effective theories constructed from the SU(3) generator [12] \mathbf{N} implicitly includes the colour factor N_c [11]. Therefore we use the convention that N_c is implicitly included in \mathbf{N}

$e^+e^- \rightarrow \pi^+\pi^-(n\gamma)$ Interactions

Hadronic Model based on the Vector-Dominance Gounaris-Sakurai [25] using the formalism from [26]. The model parameters are tuned for an improved agreement with the PDG data [27].

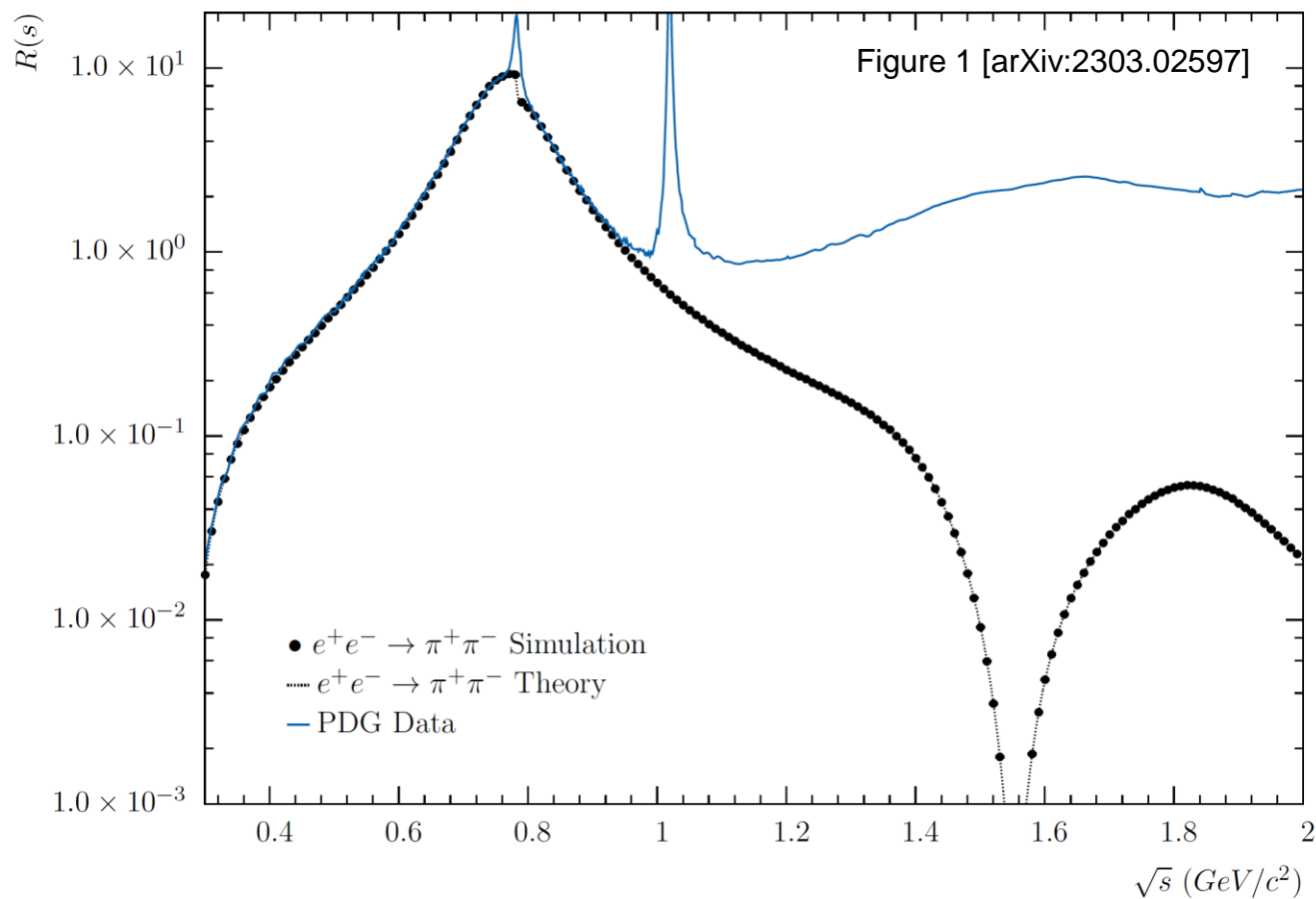
$$F(s) = \frac{\left(\frac{(BW_{GS}(s, m_{\rho(770)}, \Gamma_{\rho(770)}) + \alpha BW_{\omega}(s, m_{\omega(782)}, \Gamma_{\omega(782)}))}{1 + \alpha} + \beta BW_{GS}(s, m_{\rho'(1450)}, \Gamma_{\rho'(1450)}) + \gamma BW_{GS}(s, m_{\rho''(1700)}, \Gamma_{\rho''(1700)}) + \eta BW_{GS}(s, m_{\rho'''(2150)}, \Gamma_{\rho'''(2150)}) \right)}{(1 + \beta + \gamma + \eta)}$$

Where

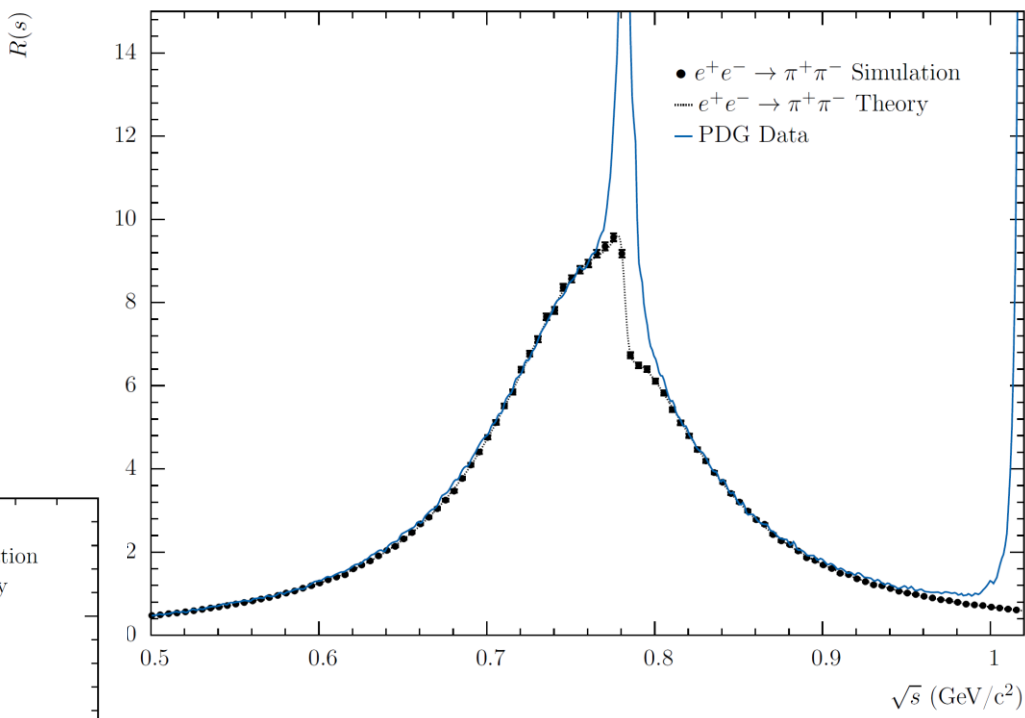
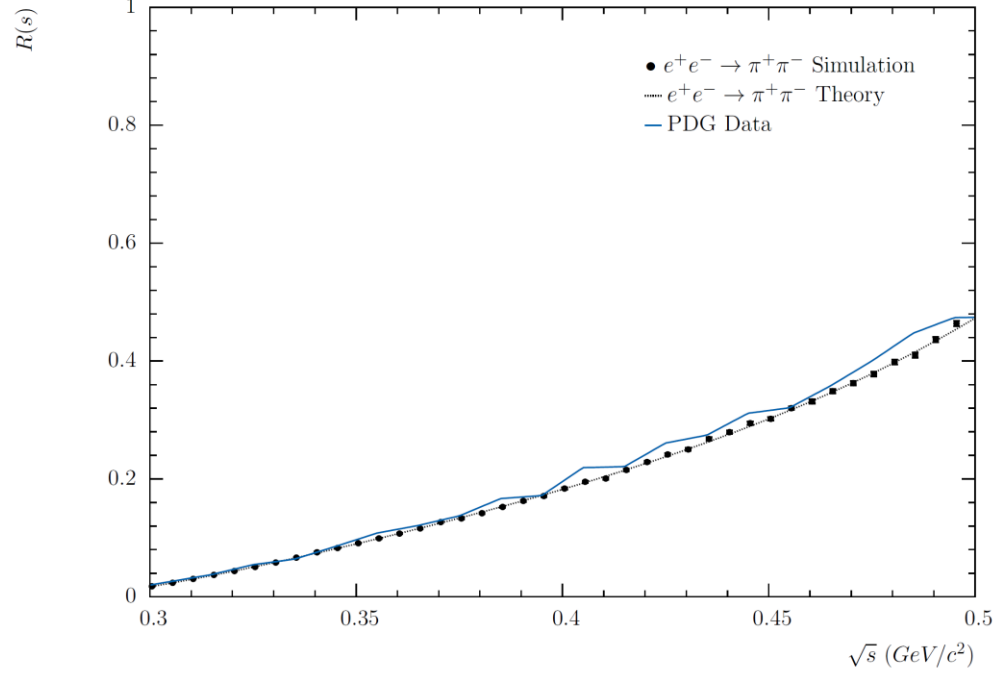
$$BW_{GS}(s, m, \Gamma) = \frac{m^2 \left(1 + \frac{d(m)\Gamma}{m} \right)}{m^2 - s + f(s, m, \Gamma) - im\Gamma(s, m, \Gamma)}$$

$f(s, m, \Gamma)$ and $d(m)$ are defined in [26].

$$BW_{\omega}(s, m, \Gamma) = \frac{m^2}{m^2 - s - im\Gamma}$$



$e^+e^- \rightarrow \pi^+\pi^-(n\gamma)$ Interactions

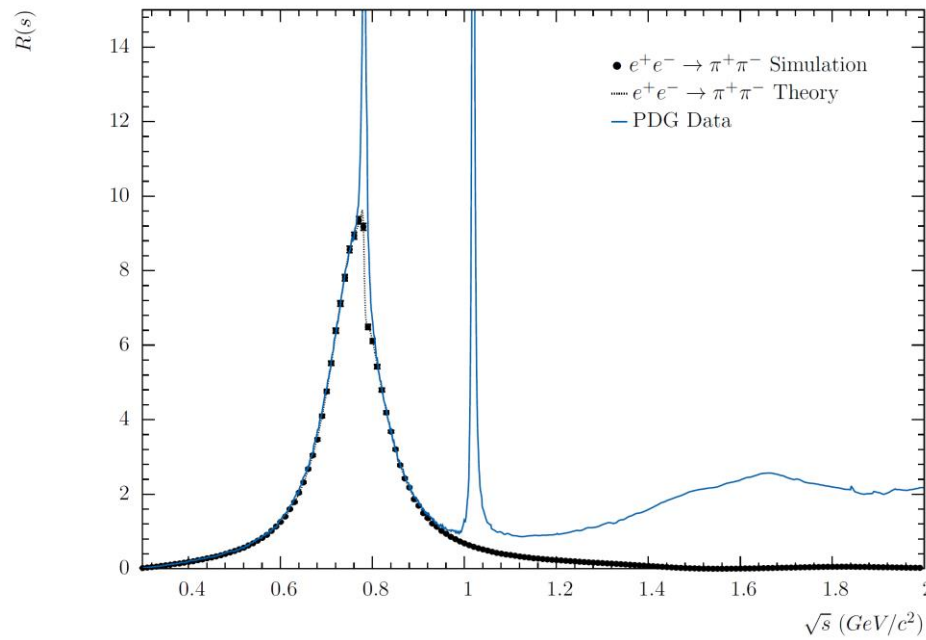


$e^+e^- \rightarrow \pi^+\pi^-(n\gamma)$ Interactions

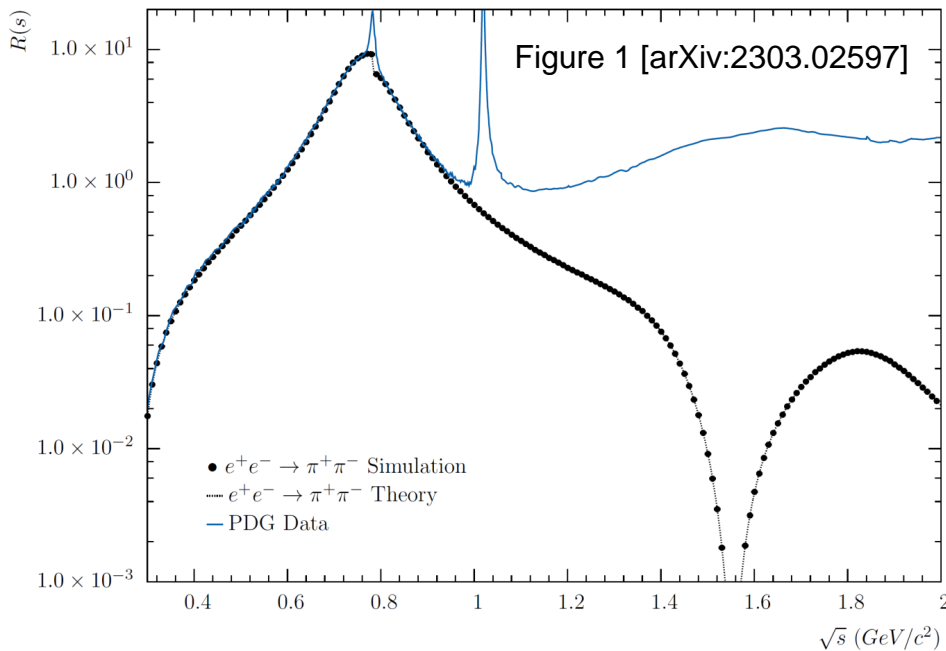
The most significant uncertainty from the truncation of the Feynman series with the YFS Exponentiation Formalism comes from the Initial-State-Radiation and is due to the small mass of the electron and positron similar to the $e^+e^- \rightarrow \mu^+\mu^-(n\gamma)$ process [$\mathcal{O}(2 - 3\%)$][28].

The uncertainty can be reduced to $< 1\%$ in the ratio of $\sigma(e^+e^- \rightarrow \pi^+\pi^-(n\gamma))$ to $\sigma(e^+e^- \rightarrow \mu^+\mu^-(n\gamma))$

- Final-State radiation will be the main source of the truncation uncertainty in the ratio - uncertainty can be calculated using method in [28].
- Low mass Initial-State tail converges slower than the total cross-section \Rightarrow Larger uncertainty
- Within the truncation uncertainty the observables are infra-red safe even with cuts on the number of γ
- Expect additional orders in $\bar{\mathcal{M}}_a^b$ before the theoretical error is sufficient for an analysis with the Initial-State Radiation Method [29].



Liverpool Seminar (January 23, 2024)



$SU(3)_f$ Suppression and the h_1 and K_1 State

Phenomenological Models for the $\tau^- \rightarrow K^-\pi^-\pi^0\pi^+\nu_\tau$ and $\tau^- \rightarrow K^-\pi^-K^+\pi^0\nu_\tau$ decays are constructed using a generalized vertex-propagator formalism using the Feindt [119] vertex.

$$J^\mu = \frac{4\sqrt{6}C_{g\otimes q}V_{ij}}{f_\pi^2} P_{1234}^{\mu\nu} A_{V \rightarrow AP}^{S/D} V_{v\alpha}^{Feindt,S/D} P_{123}^{\alpha\beta} A_{A \rightarrow VP}^{S/D} V_{\beta\gamma}^{Feindt,S/D} P_{12}^{\gamma\delta} (q_1 - q_2)_\delta$$

and for the $\tau^- \rightarrow K^-\omega(782)\nu_\tau$

$$J^\mu = \frac{4V_{us}}{f_\pi^2} P_{1234}^{\mu\nu} A_{V \rightarrow AP}^{S/D} V_{v\alpha}^{Feindt,S/D} P_{123}^{\alpha\beta} \epsilon_\beta^{\gamma mn} q_{12}^m q_3^n P_{12}^{\gamma\delta} (q_1 - q_2)_\delta {}^\dagger$$

The Form-Factors are based on the CHRL formalism [68,118,127].

$$F_\rho = BW_{\rho(770)}(s) + A_1 BW_{\rho'(1450)}(s) + A_2 BW_{\rho''(1700)}(s)$$

$$F_{K^*} = BW_{K^*(892)}(s) + B_1 BW_{K^{*\prime}(1410)}(s) + B_2 BW_{K^{*\prime\prime}(1680)}(s)$$

The intermediate resonances included in the model are:

- $\tau^- \rightarrow K^*\nu_\tau \rightarrow K^-\omega(782)\nu_\tau$
 - $\tau^- \rightarrow K^*\nu_\tau \rightarrow K_1^{-/0}(1270)\pi^{0/-}\nu_\tau$
 - $\tau^- \rightarrow K^*\nu_\tau \rightarrow K_1^{-/0}(1400)\pi^{0/-}\nu_\tau$
 - $\tau^- \rightarrow \rho\nu_\tau \rightarrow a_1^{-/0}(1260)\pi^{0/-}\nu_\tau$
 - $\tau^- \rightarrow \rho\nu_\tau \rightarrow h_1^0(1170)\pi^-\nu_\tau \rightarrow (\rho\pi)^0\pi^-\nu_\tau$
 - $\tau^- \rightarrow \rho\nu_\tau \rightarrow h_1^0(1415)\pi^-\nu_\tau \rightarrow (K^*(892)K)^0\pi^-\nu_\tau$
- } No $SU(3)_f$ suppression in hadronic decays
- } No $SU(3)_f$ suppression in hadronic decays

where the $h_1^0(1415)$ is suppressed by a factor $\delta_{h_1} = -0.175$

[†] Subscript indices in Levi-Civita indicate an odd number of contractions with the metric

$SU(3)_f$ Suppression and the h_1 State

The relative suppression of the $h_1^0(1415)$ to the $h_1^0(1170)$ state is consistent with ideal mixing

$$\frac{1}{\sqrt{2}}(u\bar{u} + d\bar{d}) \text{ and } s\bar{s}$$

where the $h_1^0(1415)$ or $s\bar{s}$ state is OZI [138, 139, 140] suppressed. The suppression factor

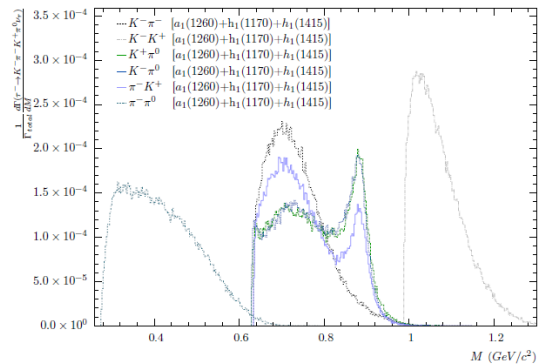
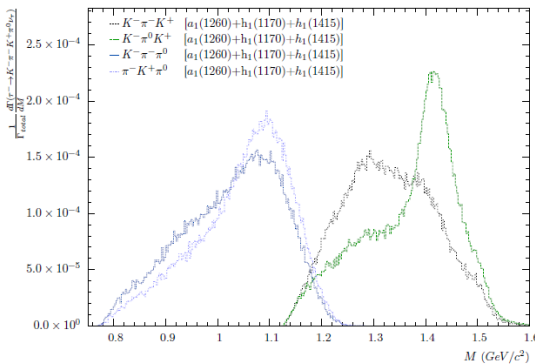
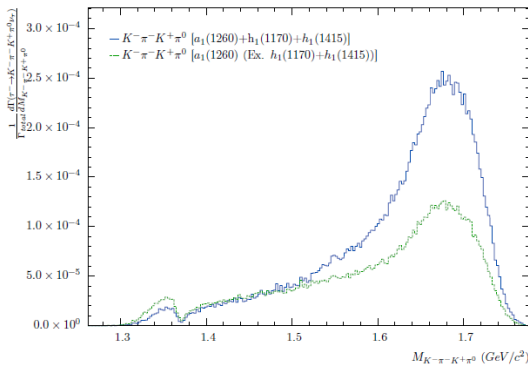
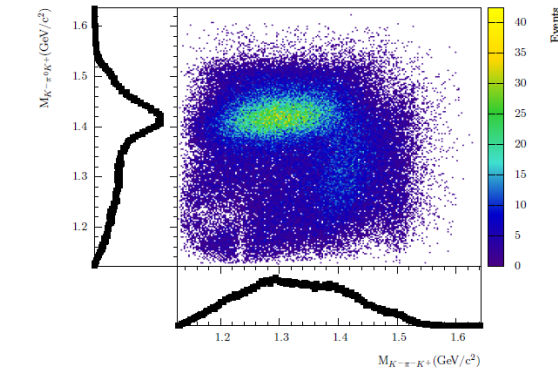
$$\delta_{h_1} = -0.175 \approx 33 \times$$

is consistent with the $20 - 100 \times$ expected by OZI suppressed modes. This prediction is consistent with BES measurement [141].

Expect sufficient statistics to measure both of the h_1 production modes

- $\tau^- \rightarrow \rho\nu_\tau \rightarrow h_1^0(1170)\pi^-\nu_\tau$
- $\tau^- \rightarrow \rho\nu_\tau \rightarrow h_1^0(1415)\pi^-\nu_\tau$

at Belle-II



Strange Singlet and Triplet Mixing

The mixing of the strange states is implemented using the full mixing relation instead of using the heavy quark approximation in [134]. This means the mixing angle is the same for both unsuppressed hadronic decays and $SU(3)_f$ suppressed decays.

$$\begin{bmatrix} |K_1(1270)\rangle \\ |K_1(1400)\rangle \end{bmatrix} = \begin{bmatrix} \delta_{K_1} \cos(\theta_{K_1}) & \sin(\theta_{K_1}) \\ -\delta_{K_1} \sin(\theta_{K_1}) & \cos(\theta_{K_1}) \end{bmatrix} \begin{bmatrix} |K_B(1^1P_1)\rangle \\ |K_A(1^3P_1)\rangle \end{bmatrix}$$

where the $SU(3)_f$ suppression factor, $|\delta_{K_1}| \sim \frac{m_s - m_u}{(m_s + m_u)} = 0.25$, is related to the effective quark masses in the QCD potential for a simple-harmonic oscillator wave-function in a Coulomb potential with a linear confining term within the non-relativistic static limit [134].

In general, the $SU(3)_f$ suppression factor is mass dependent, $\delta_{K_1} \rightarrow \delta_{K_1}(s)$, and provides complimentary information to the quark and gluon kinetic and potential energy tensor [156, 157, 158] which can be used to discriminate between various quark models.



Given the dependency of width and amplitudes of the individual modes on θ_{K_1} and δ_{K_1} and that within τ decays

$\tau^- \rightarrow K_1(1270/1400)\nu_\tau$ with $SU(3)_f$ suppression

$\tau^- \rightarrow K^{*''}(1680)\nu_\tau \rightarrow (K_1(1270/1400)\pi)^-\nu_\tau$ and $\tau^- \rightarrow K^{*'}(1410)\nu_\tau \rightarrow (K_1(1270/1400)\pi)^-\nu_\tau$ unsuppressed

There is the opportunity to simultaneously measure both θ_{K_1} and δ_{K_1}

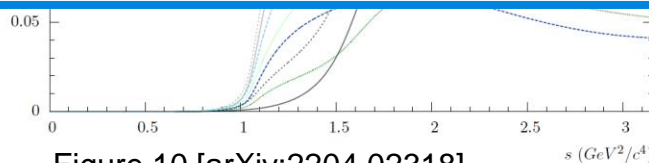
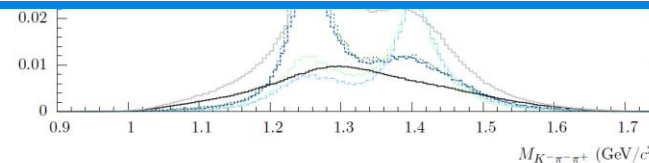


Figure 10 [arXiv:2204.02318]



QED Polarization: An Interface Approach

The spin dynamics of the QED interaction are by means of the modified Altrelli-Parsis Density Function [5,6,175]

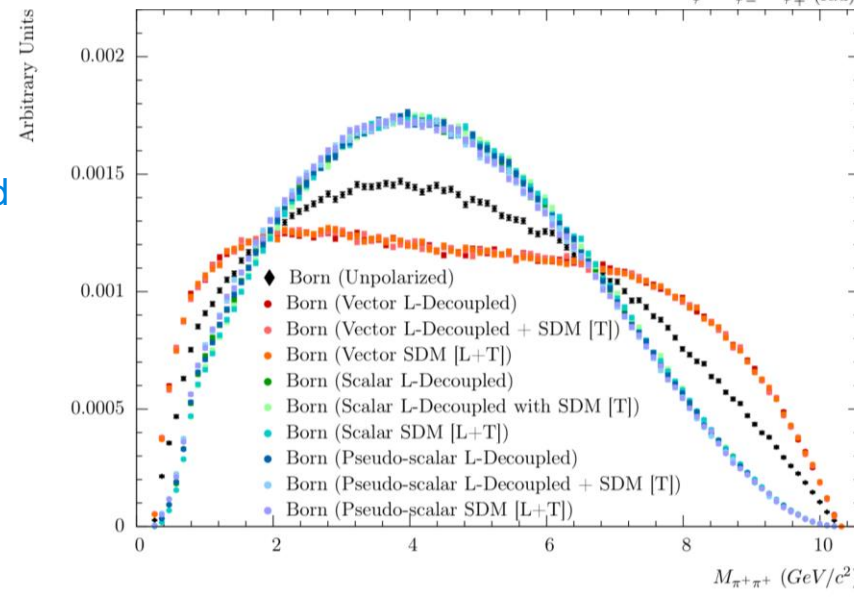
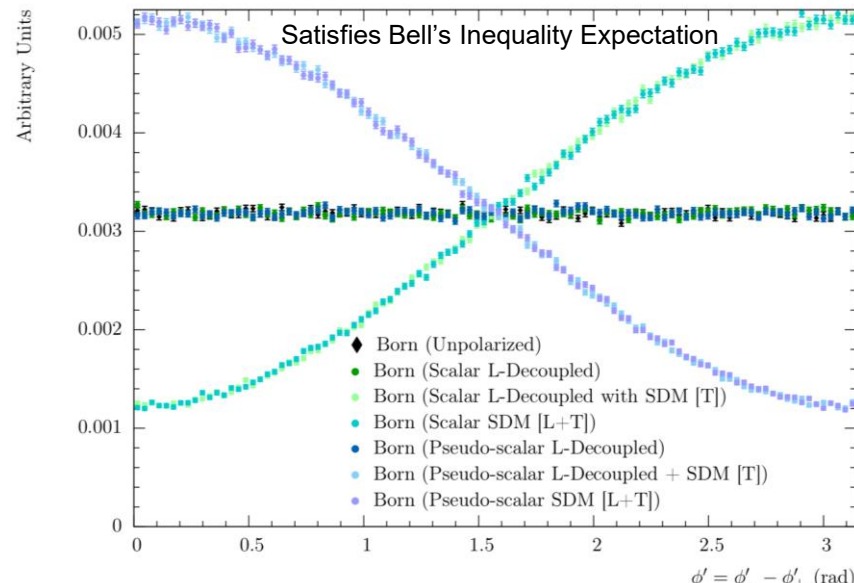
$$P = \frac{\rho_{\lambda_i, \lambda_j}}{|\mathcal{M}|^2} \times \mathcal{M}_{\lambda_i, \lambda_j, \lambda_k, \lambda_l, \dots, \lambda_n} \mathcal{M}_{\lambda_i, \lambda_j, \lambda'_k, \lambda'_l, \dots, \lambda'_n}^* \times \prod_{\alpha=k}^n D_{\lambda_\alpha, \lambda'_\alpha}$$

Where $D_{\lambda_\alpha, \lambda'_\alpha} = \frac{1}{|\mathcal{M}|^2} \mathcal{M}_{\lambda_\alpha, \lambda_\beta, \lambda_\gamma, \dots, \lambda_\nu}^{(D)} \mathcal{M}_{\lambda'_\alpha, \lambda'_\beta, \lambda'_\gamma, \dots, \lambda'_\nu}^{(D)*}$ for the τ leptons and $D_{\lambda_\alpha, \lambda'_\alpha} = \delta_{\lambda_\alpha, \lambda'_\alpha}$ for the photons [5,6].

To obtain a positive definite probability, an $SU(2) \rightarrow SO(3)$ transformation is applied using the completeness relation.

Accept/Reject Algorithm (SDM[L+T]):

- $e^+e^- \rightarrow \tau^+\tau^-(\gamma)$ events are simulated using the spin averaged matrix element with exponentiation.
- Both τ s are simulated as unpolarized.
- The decay products of the τ s are rotated longitudinally and transversely in their respective centre-of-mass frames before being boosted back to the e^+e^- centre-of-mass frame. After applying the $SU(2) \rightarrow SO(3)$ transformation, the acceptance/rejection is determined using the modified Altrelli-Parsis Density Function relative to a normalized random die.



QED Polarization: An Interface Approach

The spin dynamics of the QED interaction are by means of the modified Altrelli-Parsis Density Function [5,6,175]

$$P = \frac{\rho_{\lambda_i, \lambda_j}}{|\bar{\mathcal{M}}|^2} \times \mathcal{M}_{\lambda_i, \lambda_j, \lambda_k, \lambda_l, \dots, \lambda_n} \mathcal{M}_{\lambda_i, \lambda_j, \lambda'_k, \lambda'_l, \dots, \lambda'_n}^* \times \prod_{\alpha=k}^n D_{\lambda_\alpha, \lambda'_\alpha}$$

Where $D_{\lambda_\alpha, \lambda'_\alpha} = \frac{1}{|\bar{\mathcal{M}}|^2} \mathcal{M}_{\lambda_\alpha, \lambda_\beta, \lambda_\gamma, \dots, \lambda_\nu}^{(D)} \mathcal{M}_{\lambda'_\alpha, \lambda'_\beta, \lambda'_\gamma, \dots, \lambda'_\nu}^{(D)*}$ for the τ leptons and $D_{\lambda_\alpha, \lambda'_\alpha} = \delta_{\lambda_\alpha, \lambda'_\alpha}$ for the photons [5,6].

To obtain a positive definite probability, an $SU(2) \rightarrow SO(3)$ transformation is applied using the completeness relation.

Accept/Reject Algorithm (L-Decoupled+SDM[T]):

- $e^+e^- \rightarrow \tau^+\tau^-(\gamma)$ events are simulated using the spin averaged matrix element with exponentiation.
- Both τ s are simulated with longitudinal polarization using

$$P_{\lambda_k, \lambda_l} = \frac{\sum_i \sum_j \rho_{\lambda_i, \lambda_j} \sum_{m, \dots, n} |\mathcal{M}_{\lambda_i, \lambda_j, \lambda_m, \dots, \lambda_n}|}{|\bar{\mathcal{M}}|}$$

- The decay products of the τ s are rotated transversely. After applying the $SU(2) \rightarrow SO(3)$ transformation, the acceptance/rejection is determined using the modified Altrelli-Parsis Density Function relative to a normalized random die.

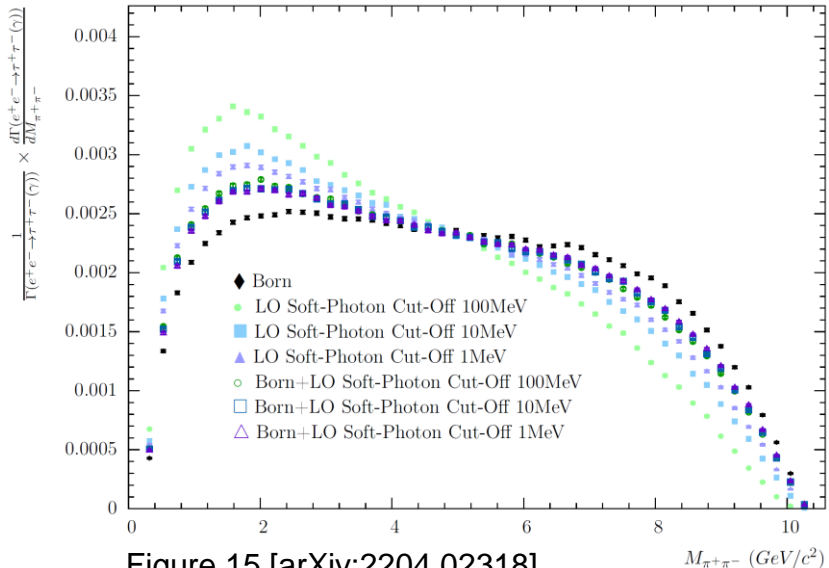


Figure 15 [arXiv:2204.02318]

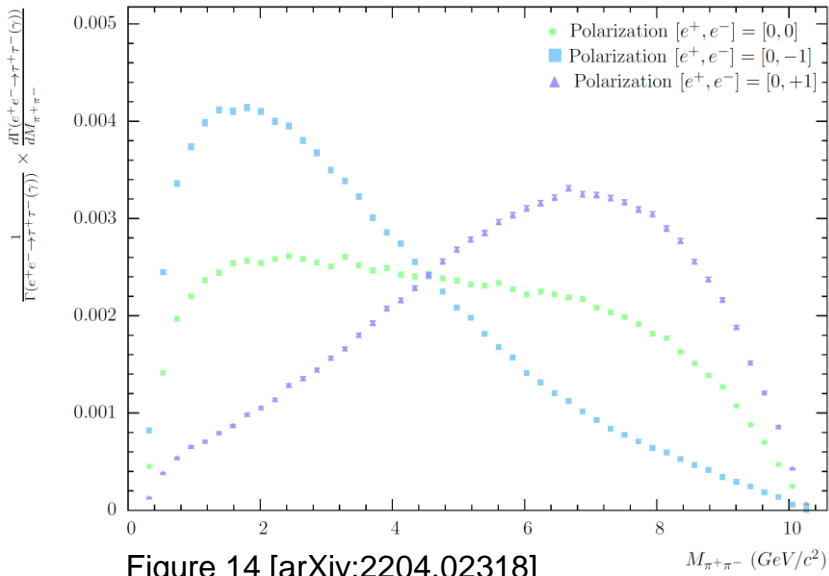


Figure 14 [arXiv:2204.02318]

QED Polarization: An Interface Approach

The spin dynamics of the QED interaction and subsequent τ decays are implemented by means of the **modified Altarelli-Parisi Density Function** [5,6,175]

$$\frac{\rho_{\lambda_i, \lambda_j}}{|\bar{\mathcal{M}}|^2} \times \mathcal{M}_{\lambda_i, \lambda_j, \lambda_k, \lambda_l, \dots, \lambda_n} \mathcal{M}_{\lambda_i, \lambda_j, \lambda_k', \lambda_l', \dots, \lambda_n'}^* \times \prod_{\alpha=k}^n D_{\lambda_\alpha, \lambda'_\alpha}$$

Where $D_{\lambda_\alpha, \lambda'_\alpha} = \frac{1}{|\bar{\mathcal{M}}|^2} \mathcal{M}_{\lambda_\alpha, \lambda_\beta, \lambda_\gamma, \dots, \lambda_\nu}^{(D)} \mathcal{M}_{\lambda'_\alpha, \lambda'_\beta, \lambda'_\gamma, \dots, \lambda'_\nu}^{(D)*}$ for the τ leptons and $D_{\lambda_\alpha, \lambda'_\alpha} = \delta_{\lambda_\alpha, \lambda'_\alpha}$ for the photons [5,6].

- The modified Altarelli-Parisi Density function allows for a partial factorization of the spin and matrix element algorithms, where the QED and τ decay processes can be computed separately.
- Both longitudinal and transverse spin correlations were included in the original algorithm from [arXiv:2204.02318], however, only longitudinal Initial-State polarization was included.

In [arXiv:2204.02318] two methods for calculating the Initial-State polarization are implemented

- i. A change of basis for the Initial-State electron and positron polarization by means of constructing the wave-function from a linear super-positioning of states.
- ii. An extension of the modified Altarelli-Parisi Density function to include an arbitrary Initial-State polarization.

$$\frac{\rho_{\lambda_i, \lambda_{i'}}^{e+} \times \rho_{\lambda_j, \lambda_{j'}}^{e-}}{|\bar{\mathcal{M}}|^2} \times \mathcal{M}_{\lambda_i, \lambda_j, \lambda_k, \lambda_l, \dots, \lambda_n} \mathcal{M}_{\lambda_{i'}, \lambda_{j'}, \lambda_{k'}, \lambda_{l'}, \dots, \lambda_{n'}}^* \times \prod_{\alpha=k}^n D_{\lambda_\alpha, \lambda'_\alpha}$$

Where $\rho_{\lambda_i, \lambda_{i'}}^{e+}$ and $\rho_{\lambda_j, \lambda_{j'}}^{e-}$ are the SU(2) representations of the polarimetric vectors and $\rho_{\lambda_i, \lambda_{i'=i}}^{e+} \times \rho_{\lambda_j, \lambda_{j'=j}}^{e-} = \rho_{\lambda_i, \lambda_j}$.

QED Polarization and the Spin Operator

The polarization of the electron and positron beams can be characterized in terms of an average polarimetric vector ($\vec{P} = |\vec{P}| \times \hat{n}$) in the CM frame of the collision. The direction of \vec{P} represents the average beam polarization direction and the magnitude $|\vec{P}|$ represents the average strength of the polarization.

Quantum-Mechanically, the expectation value of the spin along the polarization axis may be written in terms of the spin operator

$$\langle s_{\hat{n}} \rangle = \langle s_{1/2,m} | \hat{s}_{\hat{n}} | s_{1/2,m} \rangle = \left\langle s_{1/2,m} \left| \frac{\hbar}{2} [n_x \hat{\sigma}_x + n_y \hat{\sigma}_y + n_z \hat{\sigma}_z] \right| s_{1/2,m} \right\rangle$$

The eigen-vectors of this operator for the eigen-values $a_n(+1)$ and $b_n(-1)$ may be written as

$$a_n = \begin{pmatrix} \cos(\theta/2) \\ \sin(\theta/2)e^{i\phi} \end{pmatrix} \quad b_n = \begin{pmatrix} \sin(\theta/2) \\ -\cos(\theta/2)e^{i\phi} \end{pmatrix}$$

Taking the macroscopic polarimetric vector as the Quantum-Mechanical expectation value for an individual electron and positron the spin up and down wave-function can be constructed in terms of a super-positioning of the eigen-vectors.

Given that the QED matrix element and modified Altarelli-Parisi Density function are independent of a change of basis for the quantum states, the spin Dynamic can be computed using a similar method to before, where polarization is now along the \hat{n} axis instead of being the longitudinal polarization.

QED Polarization Algorithm

For consistency the convention with longitudinally polarized only beams, the polarization vector is defined in terms of three parameters:

P_l - The longitudinal polarization

F_p - The fraction of polarization

$\phi_{\hat{n}}$ - The angle in the x-y plane

$$\vec{P} = F_p \hat{n} = \begin{pmatrix} F_p \sqrt{1 - \left(\frac{p_l}{F_p}\right)^2} \cos(\phi_{\hat{n}}) \\ F_p \sqrt{1 - \left(\frac{p_l}{F_p}\right)^2} \sin(\phi_{\hat{n}}) \\ P_l \end{pmatrix}$$

The spin parameters can be updated on an event-by-event basis to allow for a distribution of spin states including tails caused by misalignment or spin relaxation distributions and to allow for the inclusion of changing detector conditions.

The **probability for a given spin configuration (P)** is determined using the modified Altarelli-Parisi Density function where a $SU(2) \rightarrow SO(3)$ transformation is applied using the **completeness relations and projection operators** to obtain a positive definite probability

$$P = \frac{\rho_{\lambda_i \lambda_{i'}}^{e^+} \times \rho_{\lambda_j \lambda_{j'}}^{e^-}}{|\mathcal{M}|^2} \times \mathcal{M}_{\lambda_i, \lambda_j, \lambda_k, \lambda_l, \dots, \lambda_n} \mathcal{M}_{\lambda_{i'}, \lambda_{j'}, \lambda_{k'}, \lambda_{l'}, \dots, \lambda_{n'}}^* \times \prod_{\alpha=k}^n D_{\lambda_\alpha, \lambda'_{\alpha}}$$

Where $D_{\lambda_\alpha, \lambda'_{\alpha}} = \frac{1}{|\mathcal{M}|^2} \mathcal{M}_{\lambda_\alpha, \lambda_\beta, \lambda_\gamma, \dots, \lambda_\nu}^{(D)} \mathcal{M}_{\lambda'_\alpha, \lambda'_\beta, \lambda'_\gamma, \dots, \lambda'_\nu}^{(D)*}$ for the τ leptons and $D_{\lambda_\alpha, \lambda'_{\alpha}} = \delta_{\lambda_\alpha, \lambda'_{\alpha}}$ for the photons [5,6].

Modified QED Polarization Algorithm

Accept/Reject Algorithm (SDM[L+T]):

- a. $e^+e^- \rightarrow \tau^+\tau^-(\gamma)$ events are simulated using the spin averaged matrix element with exponentiation.
- b. Both τ s are simulated as unpolarized.
- c. The decay products of the τ s are rotated longitudinally and transversely in their respective centre-of-mass frames before being boosted back to the e^+e^- centre-of-mass frame. After applying the $SU(2) \rightarrow SO(3)$ transformation, the acceptance/rejection is determined using the modified Altarelli-Parisi Density Function relative to a normalized random die.

Accept/Reject Algorithm (L-Decoupled+SDM[T]):

- a. $e^+e^- \rightarrow \tau^+\tau^-(\gamma)$ events are simulated using the spin averaged matrix element with exponentiation.
- b. Both τ s are simulated with longitudinal polarization using an accept/reject algorithm with probability
$$P_{\lambda_k, \lambda_l} = \frac{\sum_i \sum_j \rho_{\lambda_i, \lambda_j} \sum_{m, \dots, n} |\mathcal{M}_{\lambda_i, \lambda_j, \lambda_m, \dots, \lambda_n}|}{|\bar{\mathcal{M}}|}$$
- c. The decay products of the τ s are rotated transversely. After applying the $SU(2) \rightarrow SO(3)$ transformation, the acceptance/rejection is determined using the modified Altarelli-Parisi Density Function relative to a normalized random die.

* Transverse spin correlations related to Einstein-Padolsky-Rosen paradox and Bell's Inequality

QED Polarization: An Interface Approach

Reproduces the ultra-relativistic expectation for longitudinal and transverse polarization

- a. Longitudinal polarization observables are independent of transverse polarization in the Initial-State
- b. Transverse polarization does not impact the cross-section at ultra-relativistic energies

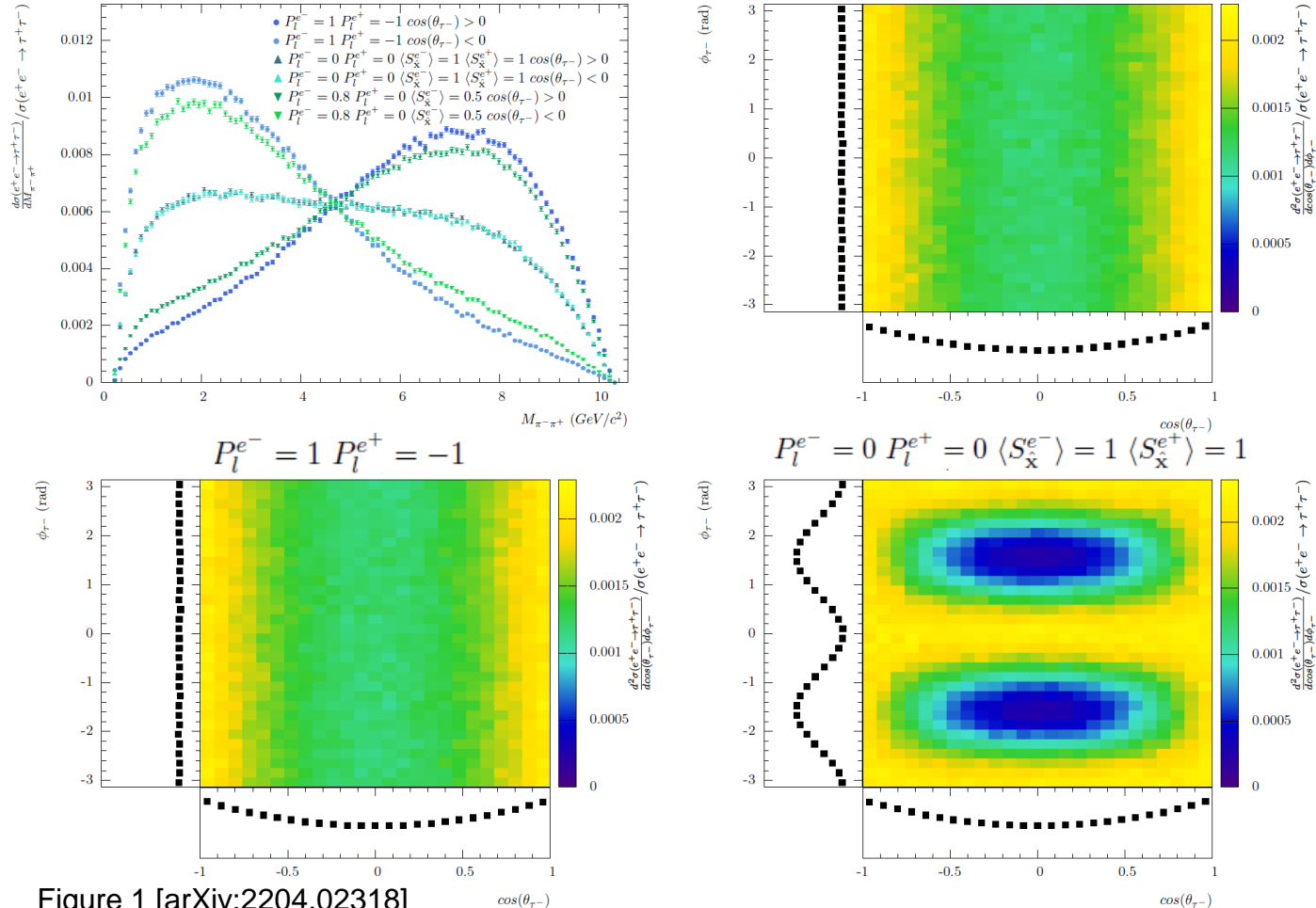


Figure 1 [arXiv:2204.02318]

QED Polarization: An Interface Approach

There transverse polarization in the Initial-State of the electron and positron can result in observable effects

- Oscillation in the transverse plane for the missing transverse energy (E_T^{Miss})
- Transverse polarization does not impact the cross-section at ultra-relativistic energies

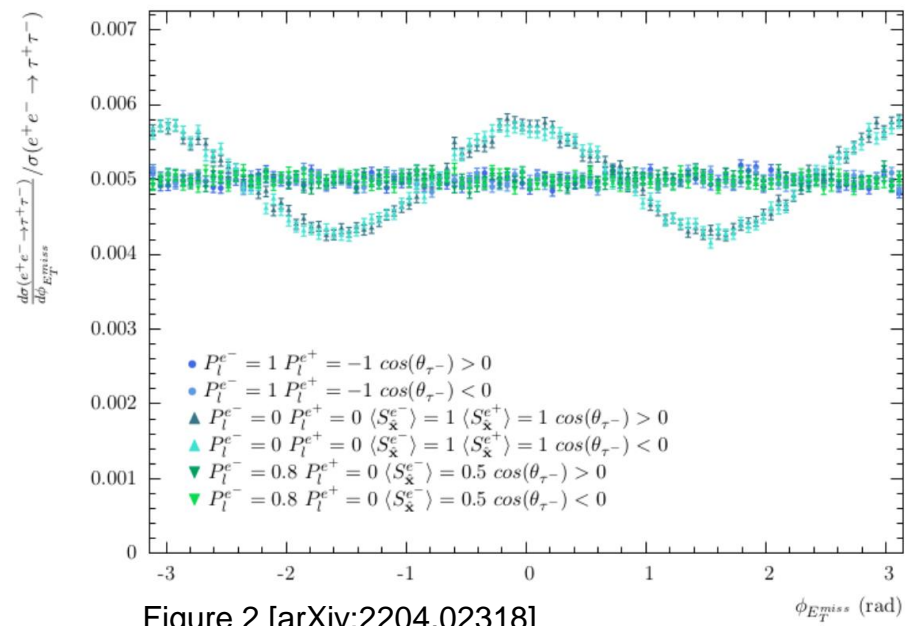
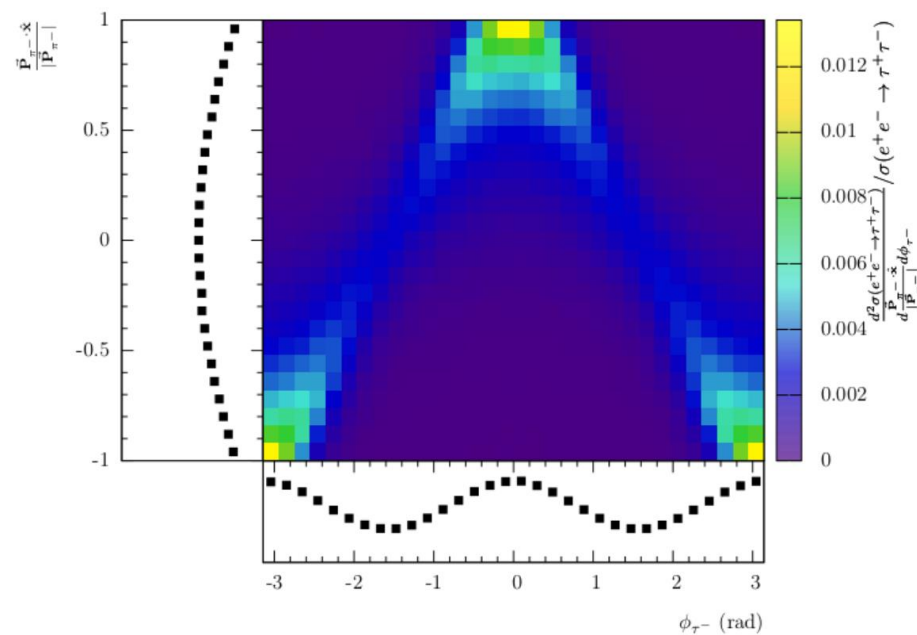
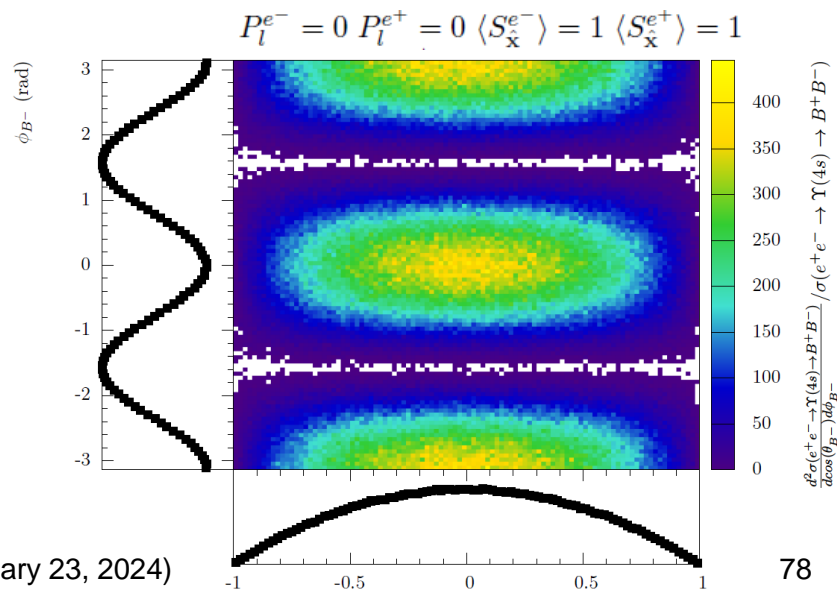
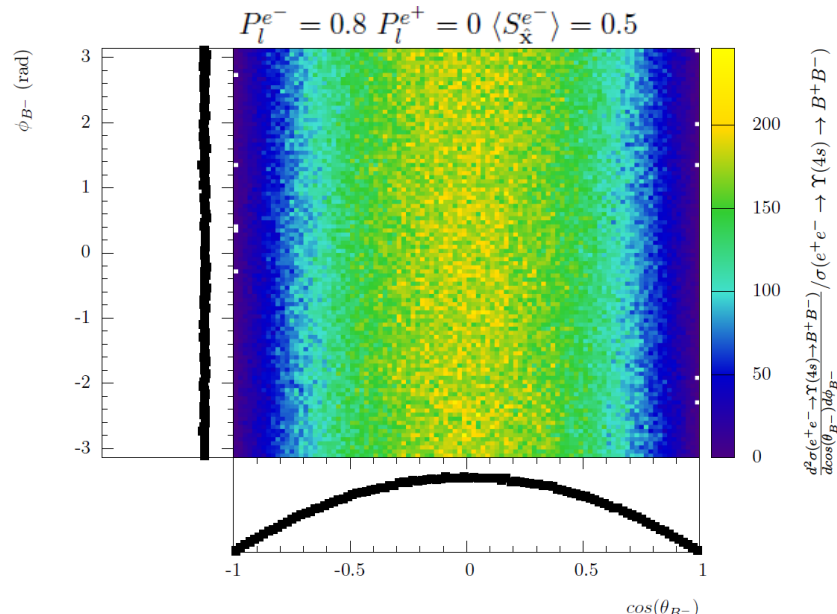
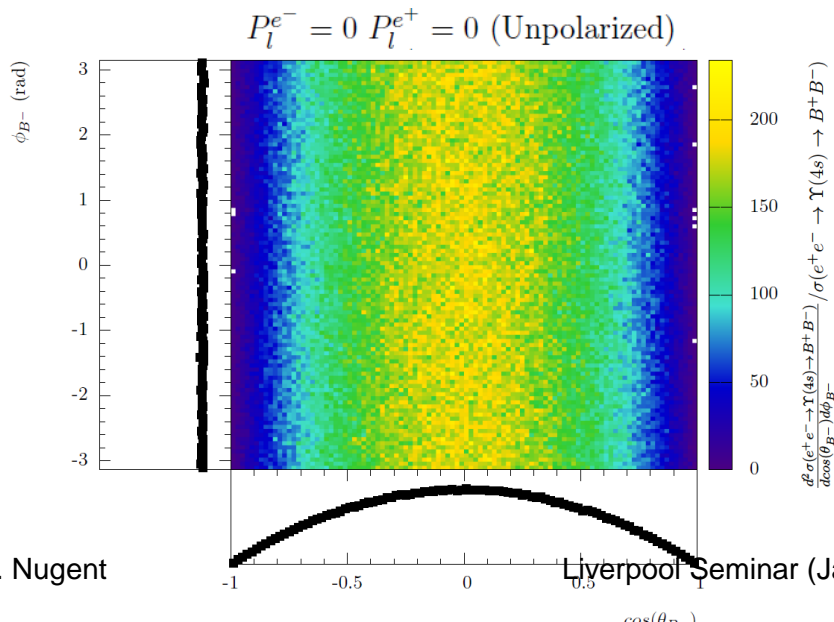
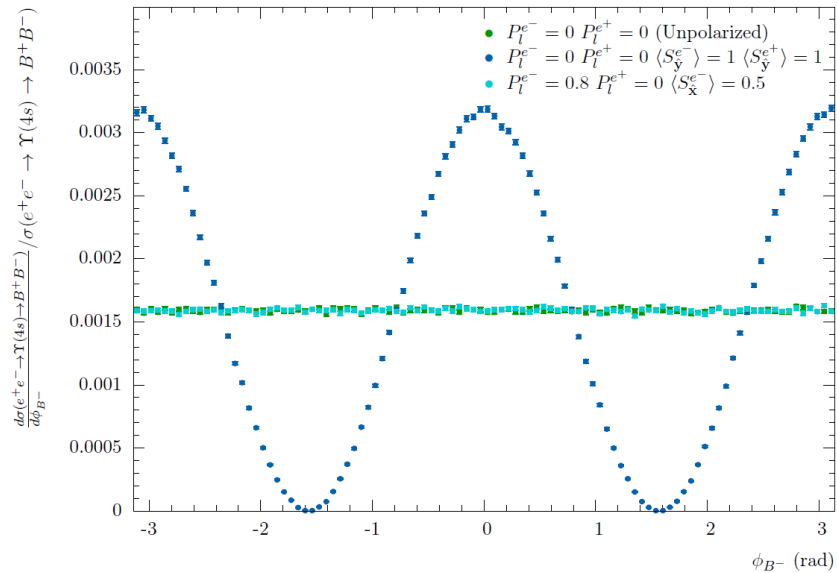


Figure 2 [arXiv:2204.02318]



$$e^+ e^- \rightarrow \Upsilon(4s)(m\gamma) \rightarrow B^+ B^- / B^0 \bar{B}^0 (n\gamma)$$

Figure 3 [arXiv:2303.02597]



Spin Dynamics in Hadronic τ Decays

Within the context of the hadronic models presented here, the covariant amplitudes are constructed using the Form-Factor approach for the formal structure of the vertex [33,89]

- Kuhn-Santamaria Model imposes current conservation $Q^\mu J_\mu = 0$ [119]
- G-2 leptonic Formal Vertex Structure imposes the Ward identity $q^\mu \Gamma_\mu = 0$ [89]
- Flux-Tube Model uses Transverse Vertices $p_\rho^\mu \Gamma_\mu = p_{a_1}^\mu \Gamma_{\mu\nu} = p_\rho^\nu \Gamma_{\mu\nu} = 0$ [33]
- Alternatively, for “on-shell” states only $\epsilon_{a_1} \cdot p_{a_1} = \epsilon_\rho \cdot p_\rho = 0$ [33]

This means that within the CHRL Models, the amplitudes are constructed under the assumption that the lowest dimensional Born terms are dominant [119,131]

An equally valid assumption is to construct the amplitudes corresponding to the lowest order angular momentum amplitudes [119]

When there is only one amplitude, these two methods correspond, however, where there is more than one amplitude the Born and angular momentum amplitudes do not necessarily correspond...

Both [33] and [119] relate the lowest energy Born terms to the helicity state...

$$\langle \rho(\mathbf{k} s_\rho) \pi(-\mathbf{k}) | H_{sb}(0) | a_1(\mathbf{0} s_{a_1}) \rangle = i f_{a_1 \rho \pi}^S \delta_{s_{a_1} s_\rho} Y_{00}(\Omega_k) + i f_{a_1 \rho \pi}^D \sum_{m_L} C(211; m_L s_\rho s_{a_1}) Y_{2m_L}(\Omega_k) \quad [\text{Eq. B11,33}]$$

Note: the CHRL Models assume the axial-vector decay is primarily through the lowest energy Born/S-wave state using the vertex $g^{\mu\nu}$. However, in [33] it was found this association is incorrect.

Spin Dynamics in Hadronic τ Decays

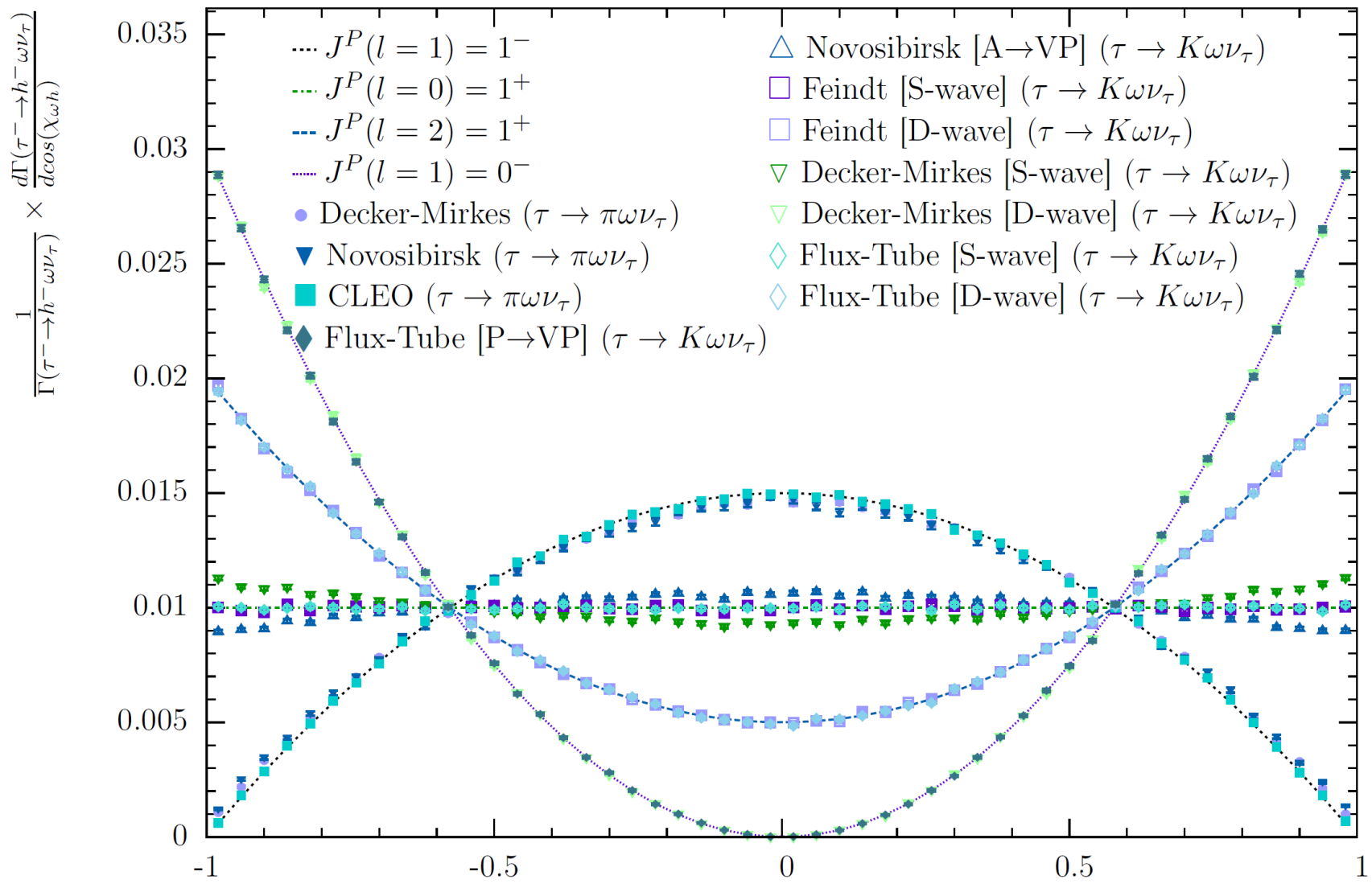


Figure 13 [arXiv:2204.02318]

Scalar States and Residual QCD Potential

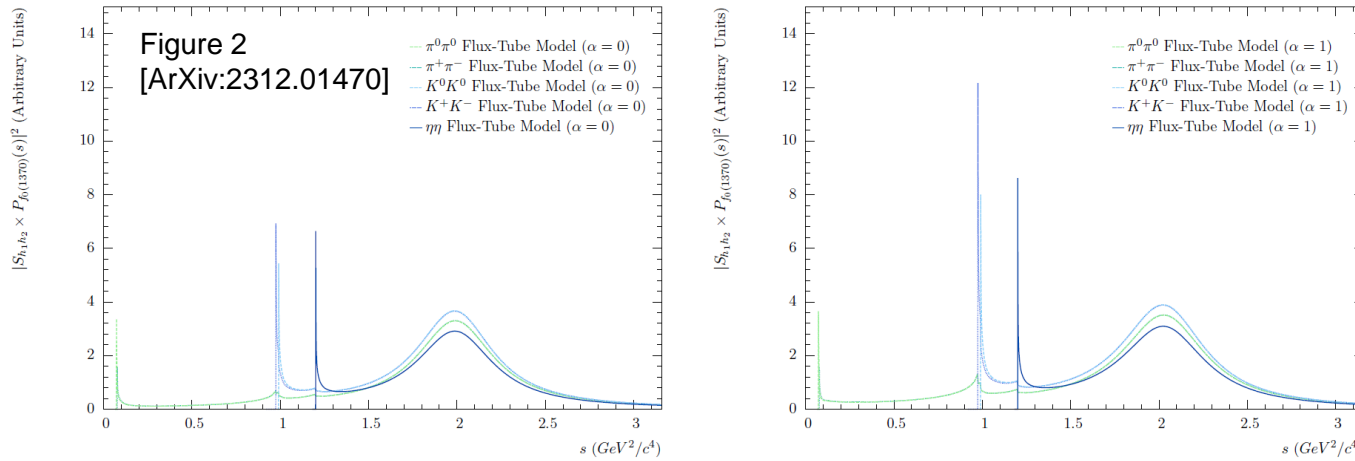
Although mesons are colour singlets, there is still a residual QCD potential between the mesons. This residual QCD potential modified the Final-state production through both a wave-function distortion and the modification of the propagator [228,229,230]. At low energies, only the wave function distortions play a significant role [230].

$$R_{h_1 h_2} = s_{h_1 h_2}^2 = \frac{\sigma(h_0 \rightarrow h_1 h_2 | V(r))}{\sigma(h_0 \rightarrow h_1 h_2)} \approx \frac{|\psi(r=0|V(r)|^2}{|\psi(r=0)|^2}$$

In the non-relativistic static limit, the wave-function amplitude distortion for potential $V(r)$ can be determined from the radial solution to the Schrodinger Equation.

$$R''(r) = -\frac{2}{r} R'(r) + 2\mu \left(\frac{l(l+1)}{2\mu r^2} + V(r) - E_{h_1 h_2} \right) R(r)$$

The relative amplitude is determined numerically [258,259] where the initial conditions are defined using the Spherical Bessel Functions [260] $J_0(x)$, $J_1(x)$ and $J_2(x)$ for the S, P and D waves respectively.



In the S states, the colour hyperfine spin-spin interaction produces a strong amplification near threshold [230]. This extension to the modified line-shape for scalar resonances presented in [228,229,230,231,232] can explain the strong KK contribution in the $f_0(980)$ [230,233,234,235], while explaining the $f_0(500)$ and $K_0^*(700)$. This provides another null hypothesis for Chiral-symmetry breaking being the origin of the composite-quark mass. Depending in the model for the strong annihilation there may or may not be an additional wave-function amplitude amplification of $f_0(1370) \rightarrow \eta \eta$ near the $\eta \eta$ threshold.

Residual Potential in Flux Tube Breaking Model

A ``chromoelectric flux-tube breaking model'' constructed in the context of the ``strong coupling lattice formulation'' [27,28,29,30] combined with a ``revitalized $[^3P_0]$ quark model'' [27,28,29,30].

Mesons are described by $q\bar{q}$ wave-function solutions for the Schrödinger equation with the potential

$$H_{ij}(\mathbf{p}, \mathbf{r}) = H_{ij}^{conf} + H_{ij}^{hyp} + H_{ij}^{so} + H_A \text{ where } H_{ij}^{conf} = \left(\frac{3}{4}c + \frac{3}{4}br - \frac{\alpha_s(r)}{r} \right) \frac{\lambda_i \cdot \lambda_j^*}{4} = \left(c + br - \frac{4\alpha_s(r)}{3r} \right).$$

Wave-function described in terms of harmonic oscillator $\psi \sim \text{polynomial} \times e^{-\beta^2 r^2}$, where β characterizes the wave-number and is constrained by the meson properties (ie charge radius)

Most significant residual QCD potential

Colour Hyperfine spin-spin interaction (H_{ij}^{hyp}) [27,34,35] \rightarrow only preserved in S-wave production [37]

$$\langle \psi_{ns} | H_{ij}^{hyp} | \psi_{ns} \rangle = \frac{32 \hat{S}_i \cdot \hat{S}_j \alpha_s \pi}{9 m_i m_j} |\psi_{ns}(0)|^2 \Rightarrow V_{hyp} = \frac{32 \hat{S}_i \cdot \hat{S}_j \alpha_s \beta^3}{9(2\pi)^{\frac{1}{2}} m_i m_j} e^{-\frac{(\beta r)^2}{2}}$$

Linear-Confining Potential ($H_{ij}^L = br$) [34]

$$V_L^{I=0}(r) = -C_I^2 \frac{b}{3\beta} \left(\beta r + 2 \sqrt{\frac{2}{\pi}} - \left(\beta r + \frac{2}{\beta r} \right) \text{erf}\left(\frac{\beta r}{2}\right) \right) e^{-\frac{(\beta r)^2}{2}} - \frac{2}{\sqrt{\pi}} e^{-\frac{3(\beta r)^2}{4}} \quad V_L^{I=0}(r) = -V_L^{I=1}(r)$$

Colour-Coulomb Potential ($H_{ij}^C = \frac{4\alpha_s(r)}{3r}$) [34]

$$V_C^{I=0}(r) = -C_I^2 \frac{4\alpha_s}{9r} \left(1 + \sqrt{\frac{2}{\pi}} \beta r - 4 \text{erf}\left(\frac{\beta r}{2}\right) \right) e^{-\frac{(\beta r)^2}{2}} \quad V_C^{I=0}(r) = -V_C^{I=1}(r)$$

Residual Potential in Shell Model

The Shell Model [42], describes the residual QCD potential both in the exterior and interior of the meson. Inside the meson the residual QCD potential it is effectively averaged over a colour charge density distribution. This produces a finite value of the colour Coulomb potential (and linear potential) in the meson.

The colour hyperfine spin-spin interaction is modeled empirically as Gaussian

$$V(r) = V_0 e^{-\frac{r^2}{2a_0^2}}$$

The remaining QCD potential is modeled using the Shell Model for Parabolic Shell Model Distribution [42]

$$V(r) = \begin{cases} 0, & r > a_0\sqrt{2} \\ V_0 \left(1 - \left(\frac{r}{a_0\sqrt{2}} \right)^2 \right), & r < a_0\sqrt{2} \end{cases}$$

Woods-Saxon Shell Model Distribution [43]

$$V(r) = V_0 \left(\frac{1 + e^{\frac{r_0}{a_0}}}{1 + e^{r - \frac{r_0}{a_0}}} \right)$$

Parabolic Shell Model with Yukawa Distribution outside of the meson

$$V(r) = \begin{cases} V_0 \left(\frac{e}{2} \right) \frac{a_0}{r} e^{-\frac{r}{a_0}}, & r > a_0 \\ V_0 \frac{1}{2} \left(1 + \left(1 - \left(\frac{r}{a_0\sqrt{2}} \right)^2 \right) \right), & r < a_0 \end{cases}$$

These distributions are normalized to the Flux-Tube Breaking colour Coulomb and linear confining potentials. This results in potential energies of $\sim 20\text{-}100\text{MeV}$ which is consistent with nuclear models.